UNIVERSIDADE D
COIMBRA

Iolanda Beatriz Albuquerque Rodrigues

SYNTHESIS OPTIMISATION OF HIGH SPECIFIC ACTIVITY CARBON-11 RADIOPHARMACEUTICALS FOR BRAIN PET STUDIES

Dissertation to obtain a Master's degree in Biomedical Engineering, specialization in Image and Radiation, supervised by Prof. Antero José Pena Afonso de Abrunhosa, co-supervised by Prof. Francisco José Cerqueira Alves, and presented to the Physics Department of Faculty of Sciences and Technology of the University of Coimbra.

February 2020

FACULDADE DE CIÊNCIAS E TECNOLOGIA
UNIVERSIDADE D COIMBRA

Synthesis Optimisation of High Specific Activity Carbon-11 Radiopharmaceuticals for Brain PET Studies

Dissertation presented to the University of Coimbra in fulfilment of the requirements necessary to obtain a Master degree in Biomedical Engineering, specialization in Image and Radiation

Iolanda Beatriz Albuquerque Rodrigues

Supervisor:
Antero José Pena Afonso de Abrunhosa (ICNAS, University of Coimbra)

Co-supervisor:
Francisco José Cerqueira Alves (ESTeSC, Polytechnic Institute of Coimbra)

February, 2020

This project was developed in collaboration with

ICNAS-Produção Unipessoal Lda.

ICNAS
PRODUÇÃO
UNIPESSOAL
LDA

Instituto de Ciências Nucleares Aplicadas à Saúde

1 2  9 0

INSTITUTO DE
CIÊNCIAS NUCLEARES
APLICADAS À SAÚDE
UNIVERSIDADE D
COIMBRA

Aos meus pais,

Pelo apoio incondicional.

Acknowledgements

Em primeiro, quero agradecer ao Professor Antero pela orientação, pela oportunidade e pela tamanha confiança em mim depositada para levar a cabo este trabalho, numa área que tanto me apaixona. Obrigada por acreditar em mim desde o primeiro momento.

Ao Professor Francisco, pelo jeito tão característico de conseguir juntar ciência com humor. Obrigada pelas gargalhadas e boa disposição! Agradeço à Ângela e ao Vítor por todos os ensinamentos sobre carbono-11.

Obrigada Mariana, my girl, por estares presente por todo e qualquer motivo! Pelas parvoíces, pelas conversas sérias, pelas risadas, pelos conselhos, pelo spam quase diário, por viveres todas as minhas alegrias e tristezas comigo. És linda, minha pirralha! Contigo, nunca estou sozinha!

A ti Carla, um obrigada do tamanho do mundo. Obrigada por me trazeres clareza quando mais preciso dela e por me mostrares como a generosidade pode trazer coisas tão bonitas, a nós e aos outros. Muito do que sou hoje, a ti devo.

Obrigada Zé, meu querido amigo, pelos longos anos de genuína amizade. Pode passar-se o tempo que passar, colocarem-se mil quilómetros pelo meio, que nada muda. Obrigada àquele tão simples, mas tão impactante trabalho de física sobre radiocenas com os míticos gatos 'radioativos' que me fez pensar "opá isto é muita giro!!". Dez anos depois e cá estou eu, feliz a fazer radiocenas! No momento em que agora encerro este capítulo, não podia fazer mais sentido reviver esta nossa memória, porque foi aí que tudo começou. Obrigada por teres estado sempre presente!

Obrigada Sara, por todas as partilhas ao longo destes anos e por toda a amizade que fomos construindo. Obrigada pelo teu apoio e pela tua capacidade única de conseguires sempre fazer-me rir nos piores momentos, tudo fica mais fácil com a tua boa energia e sensatez!

Obrigada Rui, por toda a tua preocupação e por teres sempre uma palavra amiga para dar, principalmente nesta fase. Obrigada Ritinha, Andreia, Olivs, Filipa, João e Filipe, vocês são muito especiais e levo-vos convosco para a vida!

Obrigada ao meu irmão e a toda a minha família, por desejarem sempre o melhor para mim e por se preocuparem tanto comigo.

Aos meus pais, as pessoas mais importantes da minha vida e a quem dedico esta tese. Sem vocês, nada disto seria possível. Obrigada pelo apoio incondicional, por me ampararem sempre que precisei, por fazerem os possíveis e impossíveis por mim, por sempre acreditarem em mim. Tudo o que sou, a vós devo. Todas as minhas vitórias são vossas também.

Abstract

Radiochemistry and engineering applied to synthesis are the foundations of radiopharmaceutical production and its further use in diagnostic imaging techniques such as positron emission tomography. The introduction of [^{11}C]methyl iodide and [^{11}C]methyl triflate as labelling molecules of biologically active compounds motivated not only the development of carbon-11 labelled radiopharmaceuticals but also of automated solutions for the synthesis of these radiolabelling agents.

In this work, we studied the automated production of [^{11}C]methyl triflate, starting from [^{11}C]CO_2 produced in a cyclotron by the nuclear reaction $^{14}N(p,\alpha)^{11}C$, by two different synthetic routes: the so-called "wet" method and the gas phase approach. From this radioactive precursor, state-of-the-art radiopharmaceuticals such as [^{11}C]PiB and [^{11}C]β-CITFE can be produced, using the captive solvent method, to study important neurodegenerative diseases such as Alzheimer's and Parkinson's. After purification using high performance liquid chromatography, these products were reformulated and sterilized to obtain an injectable solution ready for human use after the appropriate quality control tests. It was our goal to evaluate which of the synthesis techniques was more suitable in the routine context as well as to optimise the gas phase approach and establish maintenance procedures in order to have a functional and reliable equipment.

Molar activities of 128.65 ± 56.73 GBq/µmol and 93.39 ± 48.83 GBq/µmol, and 81.24 ± 29.83 mCi and 90.66 ± 41.47 mCi activities were obtained in the end of synthesis for [^{11}C]PiB and [^{11}C]β-CITFE, respectively. High molar activities attained make the gas phase the technique of choice for [^{11}C]PiB and [^{11}C]β-CITFE synthesis and these results should be applicable to other ^{11}C-radiopharmaceuticals. Additionally, this process proved to be very suitable in a busy production schedule due to the possibility of performing multiple synthesis per day following a very simple daily maintenance routine. The established preventive maintenance procedures have resulted in a highly reproducible and reliable process with a very high synthesis success rate (approximately 100%).

Keywords: Carbon-11, gas phase method, radiochemistry, molar activity, [^{11}C]PiB, [^{11}C]β-CITFE, Alzheimer's disease, Parkinson's disease, positron emission tomography.

Resumo

A radioquímica e a engenharia aplicada à síntese são as fundações da produção radiofarmacêutica e o seu posterior uso em técnicas de diagnóstico por imagem como a tomografia por emissão de positrões. A introdução do [^{11}C]iodeto de metilo e do [^{11}C]metil triflato como moléculas marcadoras de compostos biologicamente ativos impulsionou não só o desenvolvimento de radiofármacos marcados com carbono-11 como também de soluções automatizadas para a produção destes agentes de radiomarcação.

Neste trabalho, estudámos a produção automatizada de [^{11}C]metil triflato, partindo de [^{11}C]CO_2 produzido em ciclotrão através da reação nuclear ^{14}N(p,α)^{11}C, através de duas vias de síntese: o tão chamado método de fase líquida e a processo em fase gasosa. A partir deste precursor radioativo, radiofármacos no estado da arte como [^{11}C]PiB e [^{11}C]β-CITFE podem ser produzidos, usando o método de captura de solvente, para o estudo de doenças neurodegenerativas como Alzheimer e Parkinson. Após purificação por cromatografia líquida de alta performance, estes produtos foram reformulados e esterilizados para se obter uma solução injetável pronta para uso humano, após apropriados testes de controlo de qualidade. Foi nosso objetivo avaliar qual das técnicas de síntese era mais apropriada num contexto de rotina ativa bem como otimizar o método de fase gasosa e estabelecer procedimentos de manutenção de modo a ter um equipamento funcional e fiável.

Foram obtidas atividades molares de 128.65 ± 56.73 GBq/µmol e 93.39 ± 48.83 GBq/µmol e atividades de 81.24 ± 29.83 mCi e 90.66 ± 41.47 mCi no fim de síntese para [^{11}C]PiB e [^{11}C]β-CITFE, respetivamente. As altas atividades molares alcançadas tornam a fase gasosa a técnica de eleição para a síntese de para [^{11}C]PiB e [^{11}C]β-CITFE, sendo que estes resultados devem ser aplicados a outros radiofármacos marcados com carbono-11. Além disso, este processo provou ser-se muito adequado numa ativa rotina de produção pela possibilidade da realização de várias sínteses sucessivas por dia, seguindo uma simples rotina diária de manutenção. As manutenções preventivas adotadas refletiram-se num processo altamente reprodutível e fiável com uma taxa de sucesso de sínteses muito elevada (aproximadamente 100%).

Palavras-chave: Carbono-11, método de fase gasosa, radioquímica, atividade molar, [^{11}C]PiB, [^{11}C]β-CITFE, Doença de Alzheimer, Doença de Parkinson, tomografia por emissão de positrões.

Table of contents

List of figures

List of tables

List of acronyms and abbreviations

6-OH-BTA-0	2-(4'-Aminophenyl)-6-hydroxybenzothiazole
6-OH-BTA-1	2-[4'-(Methylamino)phenyl]-6-hydroxybenzothiazole
ACN	Acetonitrile
AD	Alzheimer's Disease
AgOTf	Silver Triflate
A_i	Activity
ALARA	As Low As Reasonably Achievable
AMF	Ammonium Formate
ApoE ε4	Apoliprotein E ε4 allele
APP	Amyloid Precursor Protein
Aβ	Beta-amyloid
BBB	Blood-brain-barrier
BTA-1	2-(4' methylamoniphenyl)-benzothiazole
CSF	Cerebrospinal fluid
CH_3OTf	Methyl triflate
CITFE	N-2-fluoroethyl-3-β-(4-iodophenyl)nortropane-2-β-carboxylic acid methyl ester
CITFES	N-2-fluoroethyl-3-β-(4-iodophenyl)nortropane-2-β-carboxylic acid
CT	Computed Tomography
DA	Dopamine
DAT	Dopamine Transporter
DOPA	6-fluoro-L-DOPA
DTBZ	Dihydrotetrabenzine
EMA	European Medicines Agency
EOB	End of bombardment
EOS	End of synthesis
FDA	Food and Drug Administration

FDG	Fluorodeoxyglucose
FPV	Final Product Vial
FP-β-CIT	N-(3-fluoropropyl)-2β-carbomethoxy-3β-(4-iodophenyl)-nortropane
GLP	Good Laboratory Practices
GMP	Good Manufacturing Practices
HPLC	High performance liquid chromatography
HT-oven	High temperature oven
ICNAS	Institute for Nuclear Sciences Applied to Health
ICNAS-P	ICNAS-Produção Unipessoal Lda.
LAL	*Limulus* Amebocyte Lysate
MCI	Mild Cognitive Impairment
min	Minute
MRI	Magnetic Resonance Imaging
MRS	Magnetic Resonance Spectroscopy
ND	Neurodegenerative Disease
NFTs	Neurofibrillary Tangles
n_i	Total molar mass
PD	Parkinson's Disease
PET	Positron Emission Tomography
Ph. Eur.	European Pharmacopoeia
PiB	Pittsburgh Compound B
QC	Quality Control
SPE	Solid Phase Extraction
SPECT	Single Photon Emission Computed Tomography
TBAOH	Tetrabutylammonium hydroxide solution
THF	Tetrahydrofuran
US	Ultrasound
UV	Ultraviolet
VMAT2	Vesicular Monoamine Transporter 2

V/V	Volume to volume
WFI	Water For Injection
β-CIT	2β-carbomethoxy-3β-(4-iodophenyl)tropane
β-CITFE	N-(2-fluoroethyl)-2β-carbomethoxy-3β-(4-iodophenyl)nortropane
β-CFT	2β-carbomethoxy3β-(4-fluorophenyl)tropane)

Chapter I - Introduction

This work was developed at the Institute for Nuclear Sciences Applied to Health (ICNAS), specifically at the Radiochemistry and Cyclotron Laboratory. ICNAS is an organic unit of the University of Coimbra, with a multidisciplinary character and it is devoted to clinical research of biomedical use of radiation. The Radiochemistry and Cyclotron Laboratory, managed by the University of Coimbra owned company ICNAS-Produção Unipessoal Lda (ICNAS-P), is responsible for the production, commercialization and research of Positron Emission Tomography (PET) radiopharmaceuticals. As ^{11}C-radiopharmaceuticals are dependent on an in-house cyclotron, they are intended for internal use at ICNAS to support on-going pre-clinical and clinical research studies. For that reason, the proposed project was actively included in the company's routine.

Since 2011 until May of 2017, synthesis of the methylation precursors, [^{11}C]CH_3I and [^{11}C]methyl triflate ([^{11}C]CH_3OTf), was carried out by the classical "wet" chemistry method. However, in June of 2017, the more recent gas phase synthesis approach was installed in the laboratory, rising the critical need of optimising this synthesis process and establish maintenance procedures in order to keep the new equipment working at full potential to fulfil the radiopharmaceutical production schedule.

Beyond this first objective, we also evaluate which synthesis technique is more suitable in the routine context of ICNAS-P, considering not only specific activities and radiochemical yields obtained for the final products, in the end of synthesis (EOS), but also the practical advantages and drawbacks of both modules on a daily basis, mainly on preparation and maintenance concerns.

Apart from the focus on [^{11}C]CH_3I and [^{11}C]CH_3OTf gas phase synthesis, we further optimised some specific processes regarding [^{11}C]PiB and [^{11}C]β-CITFE production, state of the art radiopharmaceuticals for Alzheimer's (AD) and Parkinson's (PD) disease diagnosis, respectively, in order to produce in a sterile and injectable solution for preclinical and clinical PET studies, with high radiochemical yields, high radiochemical and chemical purity, with the highest specific activity possible.

Considering the daily requests for [^{11}C]PiB and [^{11}C]β-CITFE PET scans at ICNAS, optimisation of the whole radiosynthesis process is of the utmost importance to ensure the reproducibility and reliability of several successive synthesis per day. Amongst the various ^{11}C-radiopharmaceuticals produced in ICNAS-P, [^{11}C]PiB and [^{11}C]β-CITFE are actually the most frequently requested and produced radiotracers.

Accordingly, the optimisation of the whole radiosynthesis process is achieved considering the following aspects:

- The process must be performed in the shortest amount of time as ^{11}C is a short-lived radioisotope;

- Establishment of maintenance procedures for the gas phase module;
- Optimisation of the specific activity of the final product;
- Optimisation of the radiochemical yield obtained in the EOS;
- Quality control (QC) of the final product;
- The rate of synthesis success must be as high as possible, avoiding failures, unnecessary costs and inconveniences for patients.

In this context, this project is pertinent as it assists with actually relevant radiopharmaceuticals that meet the need of preclinical and clinical molecular imaging in ICNAS. Besides this fact, and bearing in mind that ICNAS-P is the only facility in Portugal that produces ^{11}C-radiopharmaceuticals, and thus [^{11}C]PiB and [^{11}C]β-CITFE, this work is expected to make an impact on the diagnosis and clinical management of AD and PD in our country and provide an important tool for basic and clinical research and development in this area. Additionally, [^{11}C]CH_3I gas phase synthesis optimisation is also applicable to other ^{11}C-radiopharmaceuticals produced in ICNAS-P, such as [^{11}C]Flumazenil, [^{11}C]PK11195, [^{11}C]Methionine and [^{11}C]Raclopride.

1 – Molecular Imaging

Molecular imaging is defined as a discipline at the intersection of molecular biology and *in vivo* imaging that provides real time visualisation of pathophysiological and physiological processes noninvasively in living species, at the cellular and molecular levels. By imaging particular targets or pathways, this technique enables the study of the underlying mechanisms of several diseases, early detection and staging of disease as well as the assessment of therapeutic response or investigation of potential treatment strategies in the case of incurable diseases [1, 2].

Ultrasound (US), optical imaging, magnetic resonance imaging (MRI), computed tomography (CT) and nuclear imaging are different modalities of molecular imaging where each of them presents different strengths and weaknesses meaning that some might be more appropriate to image certain pathologies than others. US, MRI and CT provide valuable anatomical/structural information. On the other hand, nuclear imaging techniques such as PET and single photon emission computed tomography (SPECT) have the ability to monitor molecular events occurring at the nanomolar level with high sensitivity and specificity in living patients (see Figure 1). For this reason, these technologies have been in the frontline of molecular imaging and are widely used in the clinical setting for application in oncology, cardiology and neurology [3]. Moreover, using basic scientific findings, nuclear imaging can facilitate translational research to solve problems related to clinical practice [4].

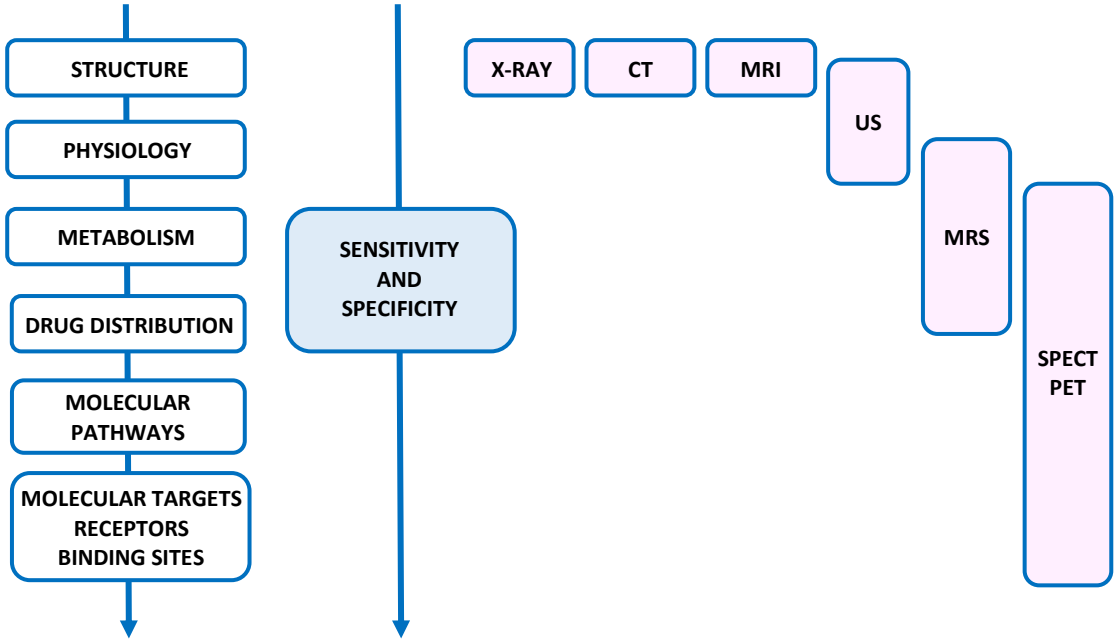

Figure 1. Spectrum of medical imaging. The range covers from millimolar (top) to nanomolar (bottom). X-ray, CT and MRI give accurate structural information with high resolution. Nuclear imaging techniques (SPECT and PET) provide functional information with lower resolution. MRS: magnetic resonance spectroscopy. Adapted from [5].

1.1 – Principles of Positron Emission Tomography

PET is one of the most sensitive and specific techniques to image non-invasively specific targets and molecular pathways *in vivo*. Imaging in PET is obtained by the administration into an animal/human of a compound labelled with a short-lived positron-emitting radionuclide, i.e., a radiopharmaceutical (or radiotracer), in order to create a three-dimensional map of distribution and functional process [1]. Fluorine-18 (^{18}F), carbon-11 (^{11}C), nitrogen-13 (^{13}N) and oxygen-15 (^{15}O) are the most typically short-lived radionuclides used in PET, in part because of their favourable physical characteristics as they decay almost exclusively by positron (β^+) emission, but, most importantly, due to the fact that they are low atomic mass elements highly present in biomolecules (see Table 1). Therefore, these radionuclides can be incorporated into any biologically active molecule that has a specific function in the organism, without significantly change its physicochemical properties [6].

Table 1. Physical characteristics of the most commonly used PET radionuclides. EC: electronic capture. [7]

Radionuclide	Half-life (minutes)	Decay mode Decay product	Max. energy (MeV)	Mean energy (MeV)	Max. range (mm)
^{18}F	109.80	97% β^+ 3% EC Oxygen-18	0.69	0.202	2.4
^{11}C	20.40	99.8% β^+ 0.2% EC Boron-11	0.96	0.326	4.1
^{13}N	9.98	100% β^+ Carbon-13	1.19	0.432	5.4
^{15}O	2.03	100% β^+ Nitrogen-15	1.70	0.650	8.0

In β^+ decay, due to the excess of positive charges in its nucleus, the unstable atom decays towards a stable state by the transformation of a proton into a neutron, along with the emission of a neutrino and a positron. As a consequence of the energy released by the spontaneous decay, the emitted positron travels a few millimetres through the tissue until it annihilates with one electron of a surrounding atom, resulting in the simultaneous emission of two gamma photons of 511 keV each, projected in opposite directions. When a tracer labelled with a positron emitter is administered to a patient, these two high-energy gamma photons escape from the body and are simultaneously detected along a "line of coincidence" by the PET scanner. PET detection systems consist of a circular ring of detectors surrounding the patient, in which each detector is located on the opposite side of the ring so that coincident events are detected over all angles around the body axis. The location in which millions of individual annihilations take place correlates with the distribution of the radiotracer in the patient, making it possible to reconstruct a PET image (see Figure 2) [8, 9].

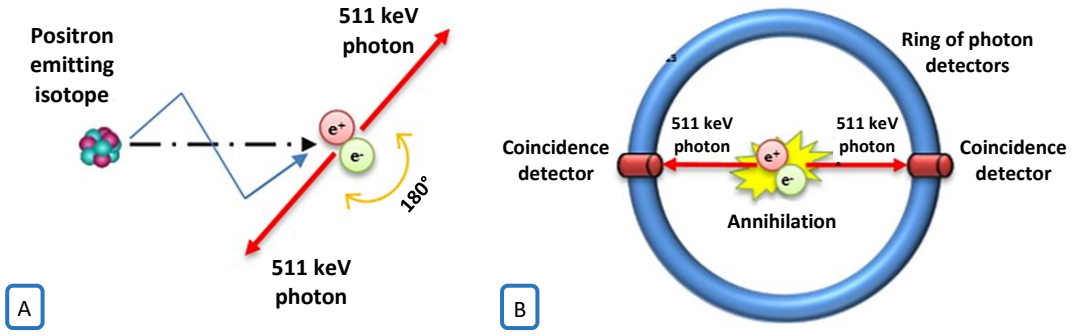

Figure 2. Principle of PET detection. (A) The unstable nucleus decays spontaneously by the emission of a positron whose energy is lost until it annihilates with an electron of a surrounding atom. As a result, two photons of 511 keV are emitted, 180º to each other. (B) The two gamma ray photons escape from the body of the patient due to their high penetrating power and are detected by an external ring of detectors as coincident events. By timing the detection of these photons, the position of the molecule in time and space can be determined, allowing in vivo quantitative 3D imaging acquisition. Obtained from [10].

By monitoring the radiotracer distribution and concentration in the body, valuable information and quantitative assessment of physiological and/or biochemical function can be made, making PET imaging a quantitative technique. However, due to some physical restrictions, three-dimensional reconstructed images must include corrections for scattering, accidental coincidences, attenuation, detector dead-time and normalization, which limits the spatial resolution of PET when comparing to that obtained with anatomical imaging techniques like MRI or CT [11]. Combining the potentiality of PET functional imaging and CT anatomical information, hybrid clinical PET/CT scanners were developed having the first commercial PET/CT appeared in 2001. Other than allowing a single diagnostic scan session per patient, CT offers an extremely accurate attenuation correction for the PET data simultaneously [12].

The production of radionuclides used for further labelling requires the use of a cyclotron - a high energy particle accelerator. Administration of short-lived positron emitting radioisotopes like ^{11}C, ^{13}N and ^{15}O labelled compounds is limited to centres equipped with an on-site medical cyclotron and radiochemistry laboratories because of their short half-life, while ^{18}F-radiopharmaceuticals are possible to be commercially distributed to facilities that do not possess such equipment.

1.2 – Cyclotron: the production of PET radioisotopes

A cyclotron is a particle accelerator in which charged particles are accelerated to a sufficiently high energy so that, when they collide with a target, nuclear reactions occur causing the atoms in the target to transform into other elements. A cyclotron differs from a linear accelerator by the expanding spiral trajectory made by the accelerated particles rather than a straight line trajectory, respectively.

The first cyclotron was developed and patented by Ernest Lawrence in 1932. This and other machines constructed later were mainly used in physics research until 1941, year when the first medical cyclotron was installed, at Washington University [13]. Currently, most of the radionuclides used for labelling PET tracers are produced by cyclotron bombardment while a smaller portion is produced in radionuclide generators [8].

A cyclotron operates using an electric field to accelerate ions, such as H^- (protons) or D^- (deuterons), and a magnetic field that bends the moving charges trajectory into a circular path. Structurally, this machine has two hollow electrodes (dees) under vacuum. The two dees are connected to a high frequency power supply (radiofrequency oscillator) to create an electric field between the two electrodes. During an irradiation, the polarity of the dees change, meaning that when one dee is positively charged, the other dee (counter-dee) is negatively charged. By placing both dees and vacuum chamber between the poles of a strong magnet, an approximately uniform magnetic field is produced perpendicularly to the plane of the motion.

Negative ions are generated in an ion source placed at the centre of the cyclotron by application of a high voltage to hydrogen or deuterium gas. Once extracted from the ion source, they are accelerated out towards the positively charged dee by the application of an electric field. When ions enter the dee, they only experience the magnetic field which causes the particles to move along a circular path. As soon as they leave that dee, the polarity of the dees

is reversed so that the ions are accelerated again as they pass to the counter dee through a gap between them. Since the rotational frequency of the ions remains constant as the energy of the particles increase, the diameter of the orbit increases, moving in a spiral outward from the centre, until the particles reach the border of the magnetic field (see Figure 3). At this point, the negative ions hit a stripping foil (usually graphite) which removes the electrons. The magnetic field reverses the path curvature of the resulting positively charged ions causing them leave the magnetic field and move straight towards an external target, where collision with the target material takes place and radioisotopes are generated. It is required that the irradiating beam of particles have sufficient energy to generate this nuclear reaction, and there must also be sufficient beam current to give practical yields, in a context of biomedical applications [13]. The type of radionuclide produced depends on the irradiating particle, its energy and the target material nucleus.

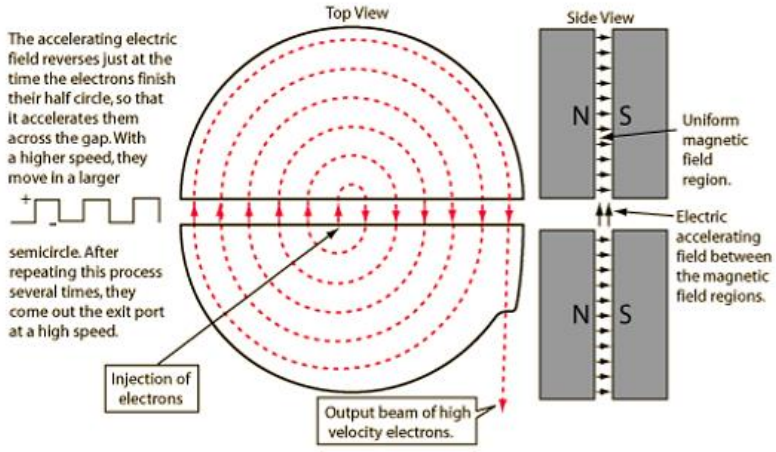

Figure 3. Schematic representation of the acceleration of a particle in the cyclotron. Obtained from [10].

The target consists of a container (target chamber) made from different materials, such as silver or aluminium, that must be chemically and physically inert and resistant to high pressures and temperatures, since its irradiation by the beam of accelerated particles produces a lot of heat. For this reason, cyclotrons are equipped with target cooling systems of water and helium. Target material to be irradiated is composed of a stable isotope usually in gaseous or liquid state and it is crucial that the material is in its most pure form to avoid side reactions caused by any impurity present.

Targets designed for the production of the most used PET radionuclides, ^{11}C, ^{13}N, ^{15}O and ^{18}F, are currently available in all commercial cyclotrons.

1.3 – PET Radiopharmaceuticals

A radiopharmaceutical, also commonly called radiotracer, is a radiolabelled molecule designed for *in vivo* application and should be sterile, pyrogen-free, safe for human use and effective for a specific indication. In nuclear medicine, approximately 95% of the

radiopharmaceuticals are used for diagnostic purposes and evaluation of response to specific therapies using SPECT or PET, while the rest is used for therapy [14]. Beyond these major clinical applications, relevant research on the field of radiotracers has been carried on towards drug development, pharmacokinetics, preclinical and clinical investigations.

Usually, a PET radiopharmaceutical consists of two linked components: a molecular compound (ligand/tracer) that determines the biochemical interactions in the living organism and so determining the radiopharmaceutical *in vivo* distribution; and a positron emitting radionuclide that provides an external detectable signal (see Figure 4). Radiolabelling is the chemical reaction in which a radionuclide is incorporated into the molecule of interest.

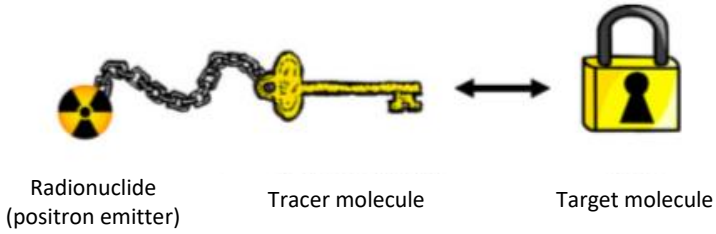

Figure 4. Schematic design of a PET radiopharmaceutical and its interaction with the target binding site. Adapted from [15].

The development and selection of a PET radiotracer must take into consideration several important characteristics regarding its biological aspect as well as the choice of the radionuclide. An appropriate ligand for molecular imaging should have high affinity and high specificity for its target so that the concentration and interaction of the radiotracer with the target is maximized, allowing high contrast PET images. Also important is the lipophilicity of the radiotracers as it determines the ability of the molecule to cross cell membranes and the blood-brain-barrier (BBB), indispensable characteristic regarding radiotracers for neuronal studies for example. Pharmacokinetic properties and clearance should be favourable according to the intended study along with the metabolism of the radiotracer, since the presence of labelled metabolites can disturb the quality of the image and invalidate the study [16]. Due to the fact that radiopharmaceuticals are used in tracer quantities, they usually do not present any pharmacologic effects [14].

Considering the time domain of each biological process, it is pertinent to choose a radioisotope with a suitable half-life for the study. Those used in PET are short-lived. This way patients receive a really small dose of radiation. This time limitation though puts some concerns regarding the synthesis of PET radiotracers, as they must be synthesized as fast as possible. This process should ideally not take longer than two half-lives in order to maintain high radiochemical yield and specific activity of the final product [17].

Specific activity is defined as the radioactivity per unit mass of a radiolabeled compound or, in other words, the ratio between the labelled and non-labelled compound. It is usually measured in GBq/mg. This property is often a critical parameter for PET studies since the competition between the labelled and non-labelled compound may cause target molecules

saturation in circumstances where these are limited. Thereby, administration of a low specific activity radiopharmaceutical eventually provides poor contrast between the target tissue and its surroundings (target-to-background activity ratio is low), resulting in an unreliable imaging study where details from the target molecules might be obscured [2]. Since in chemistry, the mass of material is frequently denoted in moles, related chemical properties are indicated in "molar" units as well. So, it has been recently and widely standardized in radiopharmaceutical chemistry that the correspondent property that measures the radioactivity per mole of compound is defined as molar activity (GBq/μmol) [18].

The development of a new radiopharmaceutical is a process in which firstly it is necessary to identify the target molecule intended to study, then develop a compound with high affinity for that molecule, and lastly label the compound with a positron emitting radionuclide. The successful application of the resulting PET radiotracer relies on the interaction of three major disciplines: medical physics, clinical imaging and radiopharmaceutical sciences [15].

2 – Radiochemistry

In the last century, radioactivity has revolutionized biomedical sciences in a way that today radiopharmaceuticals are the gold standard in nuclear medicine as they have an increasing impact both in diagnostic and therapeutic applications, where radionuclides must be used with respect to their decay modes and half-lives according to the demanded application. The use of radiopharmaceuticals in PET provides valuable knowledge about disease physiopathology, progression and diagnosis in living organisms and also contributes to the development of new drugs and therapies.

The practice of radiopharmacy, a concept firstly described in 1960 by William H. Briner at the National Institutes of Health, demands a deep understanding of pharmaceutical, chemical, physical, biochemical and biological characteristics of radiopharmaceuticals so that this extensive know-how is ultimately applied to the design, radiosynthesis and QC of radiopharmaceuticals for clinical application. Having the appropriate skills to handle radioactive substances, which include their management, storage, dispensing and use, is also of great importance in this context [14, 19, 20].

The production of positron emitting radionuclides in the cyclotron requires extensive knowledge of nuclear physics and production techniques, whereas the production of radiolabelled compounds relies mainly on applied chemistry, in order to synthesise a radiopharmaceutical that meets the high standard requirements for medical applications. The synthesis of these radiotracers forms the basis of radiochemistry [21].

Advances in radiochemistry and automatic and remotely controlled instrumentation for synthesis as well as handling radiotracers is crucial to ensure maximum radiological protection and to optimise synthesis processes, especially in clinical applications where these procedures are routinely performed. It can be said that radiochemistry is a hybrid science between organic chemistry and engineering, as these work hand-in-hand (see Figure 5).

Figure 5. From molecule to man: the process of a PET radiotracer production begins in the cyclotron and ends at the PET/CT scanner, with the patient. From top left: a commercially available cyclotron; an automated radiosynthesis system controlled from outside the hot cell; QC laboratory; a combined PET/CT scanner; a processed PET image.

Considering that carbon atoms are present in all organic molecules hence virtually allowing the synthesis of radiolabelled versions of any biomolecule of interest without significantly changing its biochemical characteristics, ^{11}C is one of the most attractive and used radionuclides for PET radiotracers.

2.1 – Carbon-11

Due to the already mentioned ubiquity of carbon in biological molecules and ^{11}C-labelled molecules having the same chemical and biological activity as their unlabelled equivalents, another reason for which ^{11}C is frequently utilised in PET is the half-life of 20.4 minutes that allows repeated low radiation dose injections in the same patient on the same day. ^{11}C decays 99.8% by positron emission to stable boron-11 (^{11}B) that can be disregarded with respect to any biological relevance, an important issue when using ^{11}C in research and clinical applications. The physical properties of ^{11}C were investigated when Crane and Lauritsen made the first production of this radioisotope in 1934 [22]. The main physical characteristics of this radionuclide are summarized in Table 2.

Table 2. Characteristics of ^{11}C as a PET radionuclide.

Carbon-11
Half-life: **20.4 minutes**
Decay equation: $^{11}_{6}\mathbf{C} \rightarrow {}^{11}_{5}\mathbf{B} + {}^{0}_{+1}\boldsymbol{\beta} + \boldsymbol{\nu}$
Decay mode: **99.8% β^+, 0.2% electronic capture**
Maximum energy: **0.96 MeV**
Most probable energy: **0.326 MeV**
Maximum range: **4.1 mm**

Since the first published use of ^{11}C in biological experiments in 1939 and the first human study in 1945, along with the development of cyclotrons and PET scanners, a wide range of ^{11}C-radiotracers have been created and are currently being applied in several medical applications where pathophysiological processes are studied non-invasively and *in vivo* [23].

However, the short half-life brings considerable challenges regarding the radiosynthesis of compounds meaning that the preparation, purification and formulation of ^{11}C-labelled molecules should be executed as fast as possible. After this whole process, the resulting ^{11}C-radiotracer still has to go through a strict QC to assure its high chemical and radiochemical purity, adequate pH and organic volatile solvents concentration, to ultimately be intravenously administrated. The total time required to the synthesis production and QC should not exceed one hour or three ^{11}C half-lives (see Figure 6). This factor limits the application of ^{11}C-radiopharmaceuticals exclusively to centres equipped with a cyclotron, radiochemistry and QC laboratories and PET scanners [24].

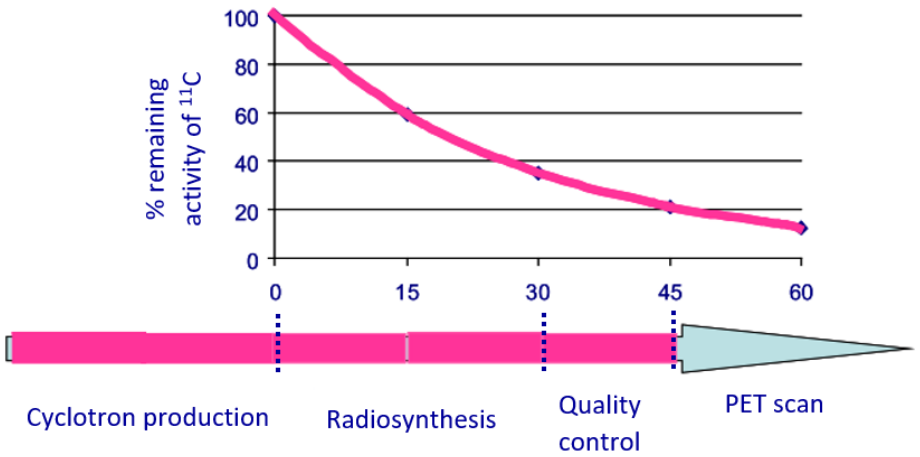

Figure 6. Loss of activity of ^{11}C as a function of time since end of bombardment in the cyclotron production until the beginning of the PET scan. Adapted from [25].

In addition to the short half-life, another concern in ^{11}C radiochemistry is related to competing side reactions with atmospheric $[^{12}C]CO_2$ as they make the synthesis of high molar activity ^{11}C-radiopharmaceuticals one of the most challenging to prepare [26].

2.2– Production of Carbon-11

Along with the greater number of publications and research regarding ^{11}C, this radionuclide started to receive increasing attention in the clinical setting in the sixties, when medical cyclotrons and PET scanners begun to be installed in the same facility [27].

Among several available nuclear reactions, ^{11}C can be obtained by cyclotron bombardment of a nitrogen gaseous target with high-energy protons according to the $^{14}N(p,\alpha)^{11}C$ nuclear reaction, being this the most convenient and most commonly used method to produce ^{11}C. Depending on whether the irradiated target contains O_2 (0.05-2%) or H_2 (5-10%), ^{11}C is stabilized in the chemical form of $[^{11}C]CO_2$ or $[^{11}C]CH_4$, respectively. Even though $[^{11}C]CO_2$ can be used as a primary precursor to directly label some organic molecules, both $[^{11}C]CO_2$ and $[^{11}C]CH_4$ are species with low chemical reactivity, which means that their conversion to more reactive secondary precursors is required so that a wider spectrum of ^{11}C-labelled molecules can be prepared [24].

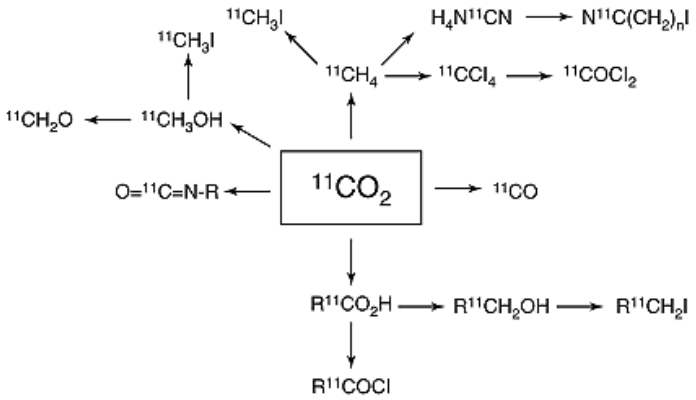

Figure 7. Secondary precursors obtained from $[^{11}C]CO_2$.

2.3 – $[^{11}C]CH_3I$ production

$[^{11}C]CH_3I$ has been the most widely used secondary precursor to introduce the radioactive ^{11}C isotope into the molecule of interest.

After cyclotron irradiation, the obtained radioactive $[^{11}C]CO_2$ obtained is transferred to a lead-shielded radiation containment chamber (hot cell) and concentrated on a trap. From this point on, a sophisticated array of automated reactions is carried out using a fully automated and programmed synthesis module in order to produce $[^{11}C]CH_3I$. This labelling agent can synthesised via two distinct methods: the "wet" method and the "gas phase" method.

2.3.1 – "Wet" method and gas phase method

The "wet" method was developed and published in 1976 by Langstrom and Lundqvist and is a classic method of organic synthesis in which the labelling agent $[^{11}C]CH_3I$ is produced in the following steps: (i) trap and release of the cyclotron produced $[^{11}C]CO_2$ using molecular

sieves; (ii) reduction of $[^{11}C]CO_2$ to $[^{11}C]CH_3OH$ in the presence of $LiAlH_4$ in tetrahydrofuran (THF); (iii) THF solvent evaporation; (iv) iodination with hydriodic acid (HI); (v) distillation of $[^{11}C]CH_3I$ under continuous flow of inert gas through an ascarite column.

This method is very reliable in terms of radiochemical yields, however it presents various drawbacks, mainly the contamination of $LiAlH_4$ with atmospheric $[^{12}C]CO_2$ which causes a decrease in the molar activity of $[^{11}C]CH_3I$ and, consequently, in the final labelled product [28]. Besides its radioactive specie, $LiAlH_4$ is also reduced with $[^{12}C]CO_2$, hence meticulous care when preparing and/or handling $LiAlH_4$ reagent solution is essential. Plus, in order to avoid the presence of carrier ^{12}C in the reaction environment, the whole synthesis procedure should be carried out in an inert atmosphere and under anhydrous inert gas flow.

Low molar activity obtained using the "wet" method as well as the use of corrosive chemicals that deteriorate the system thus implying intense and time-consuming cleaning and drying procedures have promoted the development of alternative production methods, such as the "gas phase" method [29].

The gas phase synthesis method was developed in the nineties and it exploits the conversion of $[^{11}C]CH_4$ to $[^{11}C]CH_3I$. $[^{11}C]CH_4$ can be obtained either directly from the cyclotron or by reducing $[^{11}C]CO_2$ with hydrogen on a nickel catalyst. $[^{11}C]CH_4$ is finally iodinated to $[^{11}C]CH_3I$ in the presence of molecular iodine vapours at high temperature (700-750°C), using a gas pump that promotes gas recirculation though the iodine reactor to maximize the conversion of the molecules. As this circulation happens, recently formed $[^{11}C]CH_3I$ is trapped in a porapak column, which is later heated to release the $[^{11}C]CH_3I$.

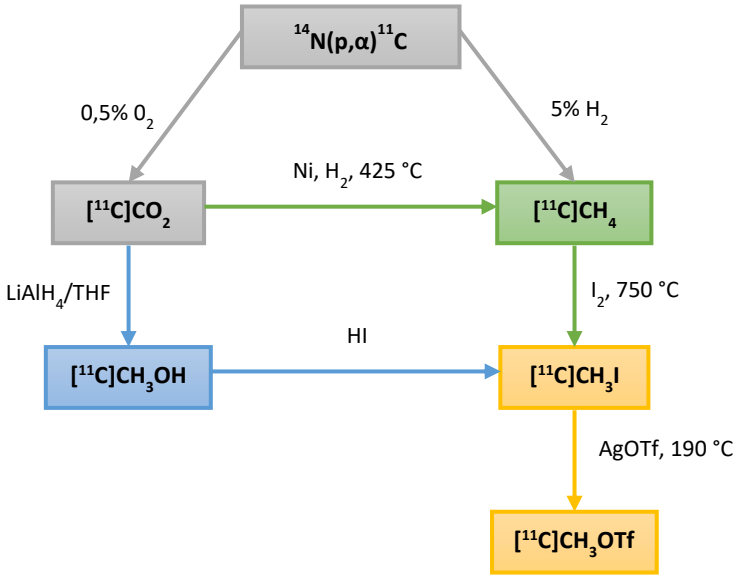

Figure 8. Routes to produce ^{11}C-labelling precursors. $[^{11}C]CH_3I$, the mostly used secondary precursor, can be produced using the "wet" chemistry (blue pathway) or the gas phase (green pathway) approach. The grey pathway represents the two possible primary precursors' production on cyclotron, and the yellow represents the $[^{11}C]CH_3OTf$ production.

Although at the expense of a lower radiochemical yield, this newer and simpler methodology enables the production of $[^{11}C]CH_3I$ with higher molar activity when compared to the "wet" chemistry method due to the low presence of $[^{12}C]CO_2$ in the system and mainly due to the disuse of the $LiAlH_4$/THF solution. Moreover, a longer longevity of the system apparatus is predicted because it does not use damaging chemical reagents which brings practical advantages in a way that it dispenses any cleaning procedure, allowing short recovery time for subsequent synthesis on a daily basis [28].

Gas phase method systems are more indicated for brain imaging studies with receptor-interacting ^{11}C-radiopharmaceuticals since high molar activity in these cases is quite significant. High molar activity means that the ratio between the labelled and the non-labelled compound is high, so receptors are likely to be saturated with ^{11}C-radiotracer providing PET images with high contrast and high quality while undesirable pharmacological effects are not expected [24].

2.3.2 – $[^{11}C]CH_3OTf$ production

Some radiotracers show low radiochemical yields when labelled with $[^{11}C]CH_3I$. In these cases, the more reactive methylation agent $[^{11}C]CH_3OTf$ can be instantaneously produced by passing $[^{11}C]CH_3I$ in a nitrogen or helium flow through a column filled with graphite and silver triflate preheated at 180-200°C.

Since $[^{11}C]CH_3OTf$ is less volatile, it is more easily trapped in smaller amounts of desmethyl-precursor and smaller volumes of solvent. It is also favourable when comparing to reactions using the less reactive $[^{11}C]CH_3I$ as methylation reactions can proceed at room temperature, with lower reaction times which results in higher radiochemical yields [30]. Actually, due to the higher efficacy of $[^{11}C]CH_3OTf$ in ^{11}C-methylations, all commercial modules dedicated to the synthesis of $[^{11}C]CH_3I$ are equipped with an additional heating unit for its conversion to $[^{11}C]CH_3OTf$.

Over the years, other ^{11}C-labelling precursors, like [^{11}C]ethyl iodide, [^{11}C]propyl iodide and [^{11}C]formaldehyde, have been developed for methylation reactions, but $[^{11}C]CH_3I$ and $[^{11}C]CH_3OTf$ remain the most frequently used [28].

2.3.3 – ^{11}C-methylation

The most commonly used route to incorporate the ^{11}C radionuclide into a target compound is by *N*-, *O*- and *S*-methylation reactions using $[^{11}C]CH_3I$ and $[^{11}C]CH_3OTf$ as labelling agents. Such simple and fast reactions are a form of alkylation, more precisely a nucleophilic substitution, where a radioactive methyl group ($[^{11}C]CH_3$) (from $[^{11}C]CH_3I$ or $[^{11}C]CH_3OTf$) replaces an hydrogen atom of an appropriate demethylated precursor compound that typically contains amine, thiol or hydroxyl groups.

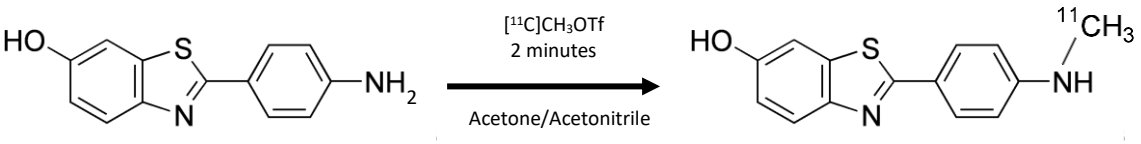

Figure 9. N-methylation reaction for the synthesis of [^{11}C]PiB using [^{11}C]CH_3OTf. An hydrogen atom from the amine group of the PiB precursor is replaced by a radioactive methyl group.

The widespread use of ^{11}C-methylations is justified by the favourable stoichiometric ratio between the cold precursor for future labelling and the methylation agent that can reach a factor higher than 10000. As a consequence, the radioactive precursor is rapidly consumed in a first order reaction kinetics resulting in good radiochemical yield within a very short reaction time [24].

^{11}C-methylation reactions can be carried out using a traditional vial-based approach or alternatively using solid support (on-cartridge or in-loop methods). Using the loop method, [^{11}C]CH_3I or [^{11}C]CH_3OTf is trapped in a stainless steel standard high performance liquid chromatography (HPLC) injection loop which has been internally pre-coated with the non-methylated precursor dissolved, usually, in an organic solvent. These solvents do not participate in the reaction neither cause chemical reaction or chemical configuration changes in the precursor reagent as they only trap the methylation agent and stabilize the leaving group. Methylation by this captive solvent method is really fast (typically < 5 minutes) and is done using a minimum amount of non-methylated precursor in a minimum volume of solvent (< 100 µl). Since the loop is fully integrated as part of a HPLC system, after the reaction the products are directly transferred to the HPLC purification column and the fraction of interest is then collected [6, 31].

The introduction of the loop method, in 2000, has proved a remarkable advance in the automated labelling of ^{11}C-compounds, becoming a technique characterized by its simplicity, versatility, reproducibility and ease of use and automation. In-loop ^{11}C-methylations require neither heating or cooling nor any additional solid support and the system is very efficient as it provides labelling reactions with high radiochemical yield, high specific activity and a high purity final product. Additionally, it requires minimal clean up and there are no activity transfer losses to the loop and to the chromatographic system. All these advantages have made the loop method the ideal technique for most ^{11}C-radiotracers prepared using [^{11}C]CH_3I or [^{11}C]CH_3OTf which motivated the adaptation of many commercial modules by simply adding a transfer line to carry the stream of the ^{11}C-methylation agent to the clean and dry HPLC injection loop and, likewise, the modernization of the whole incorporated HPLC system in which the cold precursor can be loaded, labelled, and the product separated and collected with real time activity and chromatogram monitoring [32].

2.4 – Molar activity

As previously mentioned in chapter 1.3, medical imaging studies using

radiopharmaceuticals labelled with short-lived positron emitters require good radiochemical yield, high radiochemical and chemical purity but also high molar activity. This property can be expressed using equation (1) and is usually defined as the activity of a radionuclide (A_i) divided by the mass of a compound (n_i), i.e., GBq/µmol, where this mass represents the combined mass of radioactive species and the non-radioactive counterpart present in the same chemical and physical form [33].

$$Molar\ activity = \frac{A_i}{n_i} \quad (1)$$

In practice, molar activity is a measure of the number of radioactive tracers that are bound to the target, and it is particularly significant when molecular targets are present in a limited number in the organism and when they are easily saturable, such as receptors, enzymes, antigens and antibodies. As a result of the competition between cold and radioactive compounds for the target binding sites, target saturation with non-radioactive species can occur affecting the quality of the PET image obtained, and undesired pharmacodynamics or toxicological effects can also take place.

Besides its importance in clinical brain imaging studies, the concept of molar activity becomes even more relevant in ^{11}C preclinical studies using small animals such as mice. Due to the tiny size of these animals and the limited number of receptors available, the volume and mass of injected radiopharmaceutical are important factors in preclinical imaging. The injection of too much mass can change the binding kinetics, thus affecting the results of the PET study due to a decrease in the molar activity. On the other hand, the maximum injectable volume of 200 µl for mice up to 25 grams and the radioactivity lost in the inner walls of the syringe and also due to physical decay, demand for a high radiopharmaceutical solution concentration. For these reasons, it is essential to work high molar activity radiotracers and have very high radiochemical yields in the final product [34].

One of the major challenges in ^{11}C radiochemistry lies in the development and production of ^{11}C-radiopharmaceuticals with high molar activity, that, from equation (1), it is clear that it can be increased by either increasing the amount of radioactivity and/or decreasing the amount of stable isotopes. Even though the theoretical specific activity for ^{11}C is 341140 GBq/µmol (9220 Ci/µmol), this value is far from the real value obtained in the EOS as the number of factors contributing to its decrease is high and normally difficult to be controlled.

Due to the incorporation of stable carbon during the preparation and/or production of the radiotracer, there is a critical need to eliminate possible sources of ^{12}C, as these are the main causes to the serious reduction of the molar activity of the radiotracer. Accordingly, highly pure inert gases (He or N_2) as well as good quality reagents used in the synthesis should be used to minimize contaminations with undesired chemicals. In addition to this, the physical decay of ^{11}C not only reduces the activity of the final product but also reduces its molar activity by a factor of 2 for every 20.4 minutes (half-life of ^{11}C), meaning that the whole radiosynthesis process must be optimized so that this process is executed in the shortest time possible [17].

In the automated synthesis of $[^{11}C]CH_3I$ and $[^{11}C]CH_3OTf$ by the gas phase method, higher molar activity of these species are generally achieved when using cyclotron produced $[^{11}C]CH_4$ since $[^{11}C]CO_2$ is completely eliminated from the reaction system and the production system

becomes more simplified as the $[^{11}C]CH_3I$ is produced right after in a single step iodination. Thus, starting with $[^{11}C]CO_2$ gives lower molar activity as it still requires its posterior reduction to $[^{11}C]CH_4$ [35].

Another topic of great importance that strongly influences the final molar activity of ^{11}C-radiopharmaceuticals is related to the very beginning of the whole process: the ^{11}C production in the cyclotron. The main factors on which the ^{11}C molar activity depends are: the purity of the nitrogen gas (highest possible purity to minimize side reaction products); target chamber tightness (to prevent leaks and also stable isotopes and carrier carbon contamination); chemical constitution of the target window and the inner walls of the target chamber (the interaction of the beam and the target can lead to the release of contaminants and stable carbon into the target gas mixture), and the transfer lines to the synthesis module; total time of bombardment and, therefore, the amount of radioactivity produced during the irradiation [17, 33]. However, higher amounts of radioactive precursor produced in the cyclotron not always result in higher molar activity since the molar activity decreases by a factor of 2 for every half-life passed.

Even though there are currently several automated options for the synthesis of ^{11}C-radiotracers, this process is far from being linear and competing side reactions with atmospheric carbon is a permanent threat. Bearing in mind that ^{11}C is a short-lived radionuclide, the whole synthesis procedure must be optimized according to the particular equipment configuration used in order to obtain a final product with high molar activity, a critical requirement for the successful use of ^{11}C-radiopharmaceuticals.

3 – PET Radiopharmaceuticals for Neurodegenerative Diseases

Neurodegenerative Diseases (NDs) include a group of disorders that are characterized by the progressive degeneration of the structure and function of the central nervous system which leads to a gradual restriction of normal daily activities. Currently, the two most prevalent NDs are AD and PD. The extension of lifespan due to improvements in health care in the past century contributes to an increasing prevalence of NDs, disorders that not only affect emotional and socially patients themselves but also places significant burdens on their caregivers. Given these concerns, considerable scientific research has been carried on to understand the pathophysiology of the different NDs, leading to the identification and design of new specific and sensitive biomarkers that allow an early diagnosis of the disease prior to the onset of symptoms. As a consequence, these developments will also provide treatment strategies to prevent or slow disease progression through early interventions when the neurodegeneration process may still be partially reversible [9, 36]. In this context, the development of specific biomarkers combined with molecular imaging studies represents the ultimate tool to address these important concerns.

Due to its high sensitivity, quantification capacity and low invasiveness, PET has established itself as the leading technique in the clinical diagnosis of NDs by allowing *in vivo* measurement of different molecular processes characteristic of the pathophysiology of these conditions even before symptoms are manifested.

Since glucose is the primary source of energy for the brain, its metabolism reflects the neuronal integrity of underlying brain pathology. Degeneration of specific brain regions followed by loss of neurons in these conditions hence results in decreased local glucose consumption, which can be evaluated using the well establish [^{18}F]fluorodeoxyglucose (FDG), an analogue of glucose. PET scans using this radiotracer allow the identification of disease-specific cerebral metabolic patters in various ND at an early disease stage. However, there is some overlap among some NDs patterns which can difficult diagnosis and demand for complementary clinical information. In addition to this, interpretation of the images alone can be misleading as traumas, seizures and vascular disorders can change glucose metabolism [37]. These challenges have motivated the development of more specific tracers capable of probe intra and extra-cellular proteins and receptors that are intimately related to the underlying mechanisms of brain diseases thus providing a much closer knowledge and comprehension of the pathophysiology essence of ND rather than general metabolic brain changes.

In the first place, PET tracers for imaging neurodegenerative diseases must penetrate the highly selective BBB, meaning that they have to be lipophilic molecules. Additionally, in general, they should be neutral or have a weak ionization at physiological pH, present low molecular weight and low percentage of plasma protein binding [2]. In many disorders, receptors are present in extremely low concentrations which requires the synthesis of radiopharmaceuticals with high molar activity and high affinity.

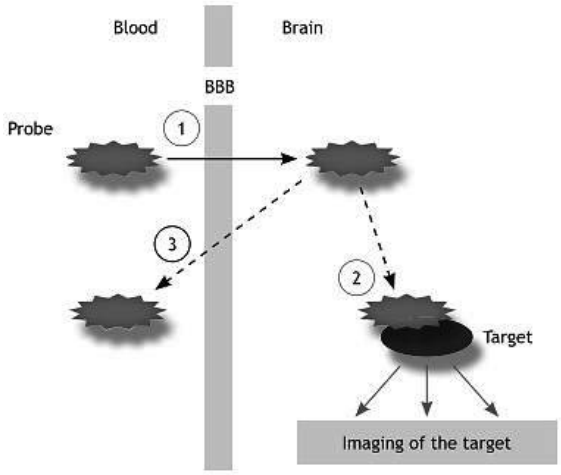

Figure 10. The basic requirements for suitable brain target-imaging tracers include: (1) prompt crossing the BBB; (2) selective binding to the target molecules; (3) clear and contrasting signals between target molecules and the background. Obtained from [38]

3.1 – Alzheimer's Disease

AD, the most common type of dementia, leads to an irreversible and gradual deterioration of cognitive functions, and is clinically characterized by memory loss, behavioural changes and thinking, speaking and reasoning problems. These symptoms usually develop slowly but worsen progressively over time due to an ongoing neurodegenerative process that ultimately leads to synaptic failure and neuronal death to an extent that it interferes with a person's daily tasks and even its ability to live independently [39].

This ND, that is the cause of approximately two thirds of cases of dementia, was first described in 1906 by the German psychiatrist Alois Alzheimer and was named after him [40]. In 2019, the Alzheimer's Disease International estimates that over 50 million people live with dementia worldwide, corresponding to an estimated annual cost of one trillion US dollars, a figure set to double by 2030. In 2050 the number of patients suffering from dementia is expected to increase to 152 million. According to a research from 2015, it was estimated that 160.000 people aged more than 60 years old suffered from dementia in Portugal, of which approximately 96.000 have AD [41, 42].

3.1.1 – Molecular mechanisms of Alzheimer's Disease

Dementia is a general term that includes a wide range of specific diseases caused by gradual and irreversible abnormal brain changes that trigger a more severe decline in cognitive functioning and behavioural abilities. Many types of dementias such as vascular dementia, dementia with Lewy Bodies and frontotemporal lobar degeneration, as well as other syndromes of cognitive impairment can mimic several symptoms and share some neuropathological features of AD, which can make it difficult to differentiate between the onset of AD, the above mentioned dementias and even normal aging cognitive decline [40]. A definitive diagnosis of AD was effectively possible when a histopathological examination of post-mortem brain tissue allowed Alois Alzheimer to identify extracellular beta-amyloid (Aβ) plaques and intraneuronal neurofibrillary tangles (NFT) in the cerebral cortex. These two hallmarks of AD are directly related to the widespread synaptic degeneration and neuronal loss, with resultant gross cortical atrophy that can be observed macroscopically [43–46].

Although the exact cause and underlying mechanisms behind AD are not fully understood, some concepts have been proposed to explain the AD pathogenesis. Nevertheless, scientific evidence available up to date has made the amyloid cascade hypothesis the most prevalent model to describe it. The latter assumes that the accumulation of Aβ in the brain is the primary event in a cascade of effects; posterior formation of NFTs and clinical manifestation of AD is proposed to result from an imbalance between Aβ production and Aβ clearance (see Figure 11) [47, 48].

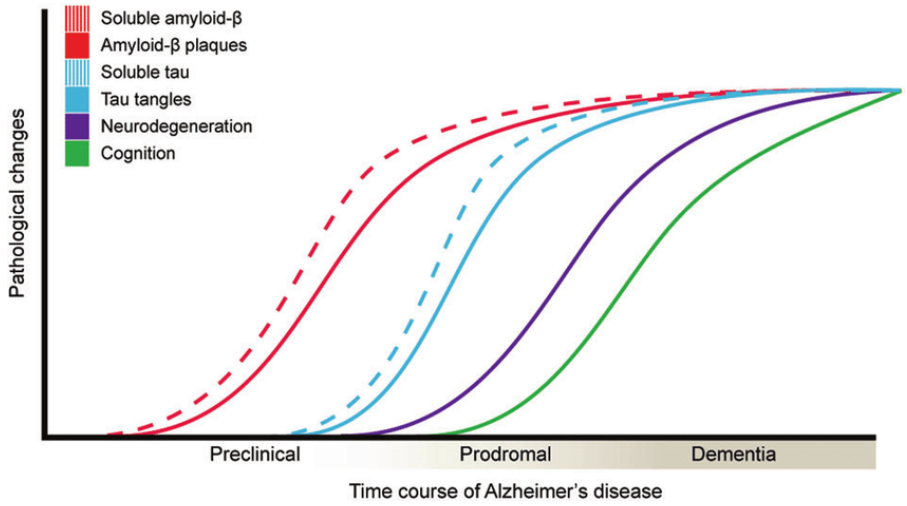

Figure 11. Possible time course of pathological changes in AD. The deposition of Aβ plaques takes place many years prior to the detection of cognitive symptoms. It is believed that these Aβ aggregates are responsible for setting in motion a series of neuronal damaging processes that lead to cognitive impairment in AD patients. Obtained from [49].

Aβ peptides (mostly 40 or 42 amino acids in length) are cleaved by specific enzymes (β- and γ-secretases) from the amyloid precursor protein (APP), a transmembrane protein implicated in neuronal plasticity and in the adherence of neurons to the extracellular space. In healthy conditions, these soluble Aβ peptides are released to the space outside the neuron and are removed through specific Aβ clearance pathways [50]. However, in the harmful pathway, when these Aβ peptides released to the extracellular space reach a critical concentration due to impaired clearance mechanism, they become insoluble and aggregate in the form of Aβ fibrils and plaques, with $A\beta_{42}$ oligomers being the most abundant component due its higher rate of fibrillization and insolubility comparing to $A\beta_{40}$ (see Figure 11) [51]. These oligomers and Aβ-containing fibrils and plaques are likely to be the key pathological substrates that set in motion a series of neuronal damaging processes in AD, such as inflammation, oxidative stress, excitotoxicity or accumulation of hyperphosphorylated tau (τ) protein, that ultimately culminate in loss of synaptic connections and cell death [40, 52].

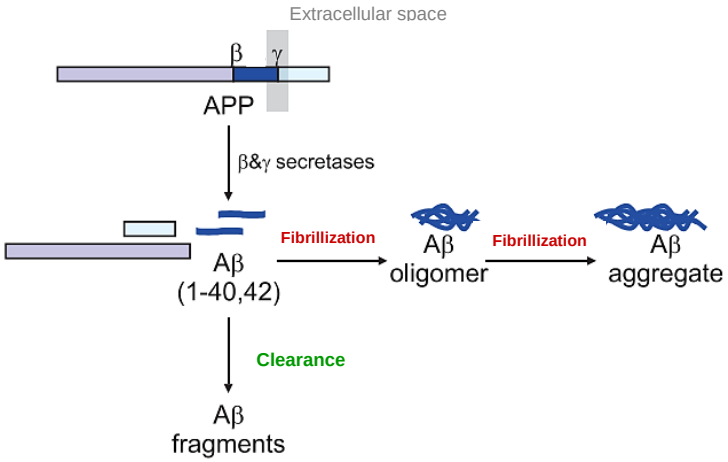

Figure 12. Schematic diagram of the production of Aβ peptides from APP via sequential β- and γ-secretases cleavages, and anabolic and catabolic pathways of Aβ peptides. $Aβ_{40}$ and $Aβ_{42}$ monomers, the most abundant, are believed to aggregate in the extracellular space to form soluble Aβ oligomers. Some Aβ oligomers are believed to form slightly soluble Aβ fibrils and plaques. These Aβ aggregates are likely to set in motion subsequent damaging processes in AD. Obtained from [50].

Besides the formation of Aβ plaques during the amyloid cascade, extensive intracellular NFTs deposits are produced, the second histologic lesion of AD, even though the Aβ component far outweighs the latter on a total mass basis in most brain regions [53]. τ proteins are intraneuronal highly-soluble proteins abundant in the neurons of the central nervous system and are responsible for the binding and stabilization of microtubules, providing mechanical support to the cytoskeleton. However, during AD pathogenesis, there is a continuous abnormal accumulation of insoluble hyperphosphorylated τ protein that aggregate structurally in the form of paired helical filaments, constituting NFT. As a consequence of this process, τ protein's affinity to microtubules decreases and these become unstable, causing cytoskeleton rupture, inappropriate protein metabolism, synaptic malfunction, and impaired signalling. Decline in these functions may contribute significantly to the death of the afflicted neurons and neuronal degeneration [40, 51, 54]. The precise mechanism of the formation of NFTs is still not entirely understood, but it is believed that the deposition of Aβ oligomers might alter the function of GSK3β kinase, promoting the abnormal phosphorylation of τ proteins [55].

The vast majority of all AD cases (99%) are sporadic, i.e., they have no specific family inheritance, and can be caused by a complex combination of several factors, such as the individual's lifestyle, environment, and age, being the latter the most recognised and influential risk factor for developing AD. Actually, more than 90% of cases have an onset between 60 to 65 years of age [56]. Meanwhile, genetic background is another strong known risk factor for AD because of the inheritance of the apoliprotein E ε4 (ApoE ε4) allele. Even though its mechanisms of action is unknown, between 40% and 80% of AD patients possess at least one ApoE ε4 alelle [57].

On the other hand, familial AD has a positive family history in at least three generations and is entirely passed down through genetics as these patients carry mutations in at least one

the following genes: presenilin 1, presenilin 2 and APP. These mutations increase the production of $A\beta_{42}$ resulting on a much earlier onset of AD. Familial AD accounts for less than 1% of all AD cases [56, 58].

The cascade of pathogenic events proposed by the cascade hypothesis to explain the AD pathogenesis is summarized in Figure 13.

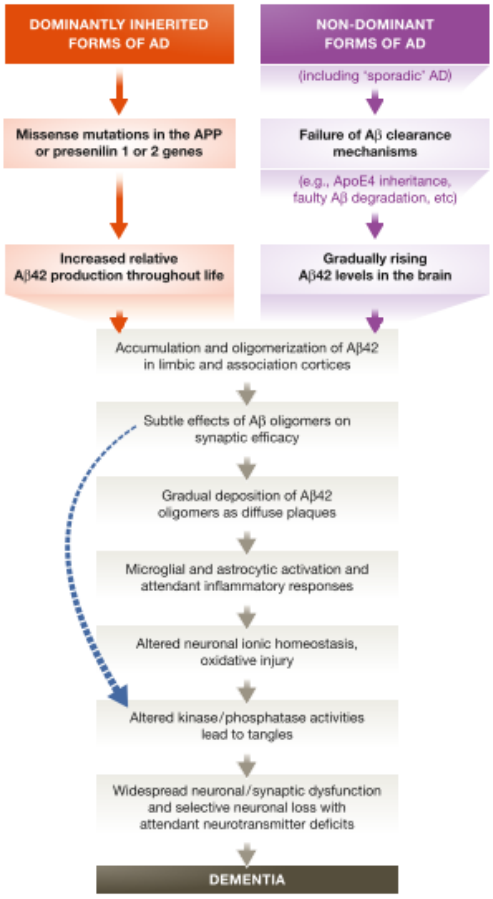

Figure 13. Possible causes of AD and further sequence of major pathogenic events leading to AD proposed by the cascade hypothesis. The curved blue arrow indicates that Aβ oligomers may directly injure the synapses and brain neuronal processes, in addition to activating microglia and astrocytes. Obtained from [47].

There is currently no cure for AD neither a single medical test that can unequivocally diagnose AD in life, meaning that clinically, only probable diagnosis of AD is possible. AD is usually diagnosed from a detailed history of the type and progression of symptoms from the patient, and by excluding other diseases that may also present with dementia, whereas assessment of intellectual functions and neuropsychological tests can additionally characterize the stage of the disease. Since the pathologic process begins years before symptoms are evident, diagnosing AD at a pre-symptomatic stage is of high priority because it not only allows patients and their families to plan their future to have the best possible quality of life but, more importantly, because those patients may strongly benefit from potential early medicinal

intervention aimed at reducing/eliminating Aβ deposition in the brain before extensive synaptic and irreversible neuronal loss occurs [46, 55].

Mild cognitive impairment (MCI) is a diagnosis given to subjects who present cognitive decline, frequently memory loss, beyond that expected for their age and education but to an extent that does not interfere with normal daily activities. As such, it can be interpreted as a prodromal stage of AD or, as often conceptualized, a transitional stage between normal aging and dementia [36]. Indeed, the development of specific biomarkers able to clarify this prognostic would be of great value. Cerebrospinal fluid (CSF) biomarkers for Aβ or τ have been used for this purpose, as $A\beta_{42}$ levels are typically decreased while τ levels are increased [59]. There is evidence of changes of these CSF biomarkers in prodromal AD meaning that this analysis can predict progression to AD in individuals suffering from MCI with fairly high accuracy [60].

MRI has become a reference in neuronal imaging studies to evaluate whole brain volume, hippocampal and entorhinal cortical volume in individuals with MCI or genetic risks for AD as these measures are, on average, smaller in AD patients than in normal older people [61]. Since MRI is a powerful technique to detect brain atrophy, one of the downstream effects of AD, it can be used to assess disease progression [46].

Besides its application in oncology, [^{18}F]FDG has been extensively used to support the diagnosis of ND, especially in AD as it reflects resting cerebral glucose metabolism, which is an indicator of neuronal activity, a pathological feature severely affected in AD due to the synaptic dysfunction and functional impairment of neurons. Hypometabolism of temporal, parietal, frontal as well as the posterior cingulate cortices have been widely associated with AD, a pattern closely similar to the distribution of Aβ plaques found at autopsy, with functional studies showing a sensitivity of 91% and specificity of 86%. Another valuable clinical use [^{18}F]FDG relies in its potential to help differentiate AD from other causes of dementia [62]. Since Aβ deposition occurs significantly earlier than cerebral metabolic perturbation, [^{18}F]FDG has diagnostic value once the stage of established AD is reached. In this phase of the disease, while amyloid deposition in most regions has plateaued, [^{18}F]FDG uptake continues to decline along with cognitive function, and correlates well with disease progression [63, 64].

3.1.2 – Molecular imaging of Alzheimer's Disease

Having Aβ plaques as one of the hallmarks of AD, vast research has been done focusing on the development of ^{11}C and ^{18}F-PET radiotracers for imaging these plaques *in vivo*. The first *in vivo* imaging of Aβ plaques in AD patients and healthy controls took place in the University of California, in 2002, using [^{18}F]FDDNP, a radiotracer developed in 1999. However, this radiopharmaceutical showed to be not specific to senile plaques as it also bound to NFT, at the same time that non-specific binding was reported with a relatively low target-to-background ratio [40].

Based on the thioflavin-T histologic staining dye, used for decades for its high affinity for most amyloid deposits, an uncharged and lipophilic thioflavin-T derivative 2-(4' methylamoniphenyl) benzothiazole (BTA-1) was developed in 2001, in the University of Pittsburgh Medical Centre. Studies with AD brain tissue using this compound demonstrated a

much higher binding in Aβ-containing areas, where most of it appeared to be specific, suggesting that the binding of BTA-1 to the AD brain tissue is dominated by specific interaction with aggregated, fibrillar Aβ deposits, a conclusion that ultimately supported the use of BTA-1 as an *in vivo* tracer for AD diagnosis and treatment evaluation [65]. However, these studies showed that this compound did not bind to the amorphous Aβ deposits, such as those that predominate in the cerebellum.

Afterwards, in 2004, a hydroxylated BTA-1 derivative compound emerged and was chosen for the first human trial of benzothiazole Aβ imaging PET tracers, using ^{11}C as the labelling radionuclide (see Figure 14). This small, neutral and lipophilic compound, *N*-methyl-[^{11}C]2-(4' methylamoniphenyl)-6-hydroxybenzothiazole or [^{11}C]6-OH-BTA-1, more simply referred as "Pittsburgh Compound-B" or PiB, displays high binding affinity and specificity for fibrillar Aβ plaques plus excellent *in vivo* kinetics since it enters the brain rapidly, and also shows good clearance properties, typical of many PET radiotracers [66]. Besides the mentioned binding, [^{11}C]PiB additionally binds to Aβ oligomers, albeit with lower affinity, and to other Aβ containing lesions, which made this compound the first selective tracer that allowed the non-invasive assessment and quantification of Aβ pathology *in vivo*, presenting a sensitivity of 90% for AD [67].

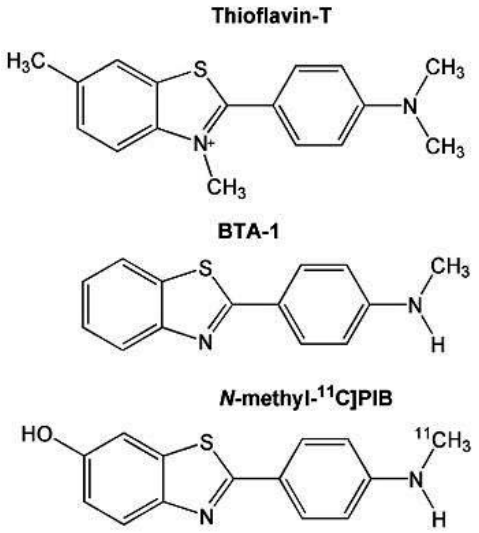

Figure 14. Chemical structures of the thioflavin-T histologic staining dye and its analogues, BTA-1 and [^{11}C]PiB.

In healthy subjects, some [^{11}C]PiB non-specific binding might be observed mainly in the white matter due to the lipophilicity of this tracers. In contrast, in patients with AD a specific binding in the parietal, temporal and frontal association cortex is seen. This binding pattern revealed a positive correlation with the distribution of Aβ plaques found in post mortem studies as well as with $A\beta_{1-42}$ in CSF.

In numerous studies with [^{11}C]PiB, almost all patients clinically diagnosed with AD exhibited positive Aβ uptake. Yet, some follow-up studies noticed that there was no significant increase in [^{11}C]PiB during the progression of AD, suggesting that Aβ deposition plateaus when clinical dementia is already established. At this stage, symptoms are visible at the same time

that brain atrophy and hypometabolism accelerate, correlating more strongly with disease severity and clinical progression. Moreover, at least 50% of subjects with MCI show increased levels of [^{11}C]PiB uptake similar to those in AD patients, which is highly predictive of subsequent conversion to AD [9, 45].

Due to [^{11}C]PiB specificity to study Aβ deposition both in pre-symptomatic stages of AD and in other ND, it has been the most successful and widely PET tracer used for this purpose. Nonetheless, because of the short ^{11}C half-life, ^{18}F-labelled analogue tracers have been developed which can be transported and commercialized from radiopharmaceutical production sites to hospitals equipped with PET scanners. [^{18}F]flutemetamol, [^{18}F]florbetapir and [^{18}F]florbetaben have already been approved in the United States and Europe by the Food and Drug Administration (FDA) and European Medicines Agency (EMA), respectively, for clinical application. Despite providing a good discrimination between healthy individuals and AD patients, these tracers present though some technical limitations specially a lower degree of specific binding *in vivo* and a high uptake in healthy controls which reduces the contrast between the target and background imaging [38].

3.2 – Parkinson's Disease

PD was firstly described in 1817 by James Parkinon and, despite being currently the second most prevalent ND, its pathophysiology is not entirely understood neither there is a certain test for its diagnosis during life. A study from 2016 estimated that, potentially due to the increasing life expectancy as well as longer disease duration and environmental and social risk factors, the global burden of PD in that year is of 6.1 million patients, a tendency expected to rise to 12 million patients by 2050 [68].

PD is a very complex chronic disorder primarily recognized by four cardinal motor manifestations: bradykinesia (slowness of movement), tremor at rest, muscular rigidity and postural instability. Besides these symptoms, patients often exhibit freezing phenomenon, mainly during gait, which combined with postural instability can be devastating as the risk of falling is higher. The progressive nature of PD is disabling, reducing gradually the quality of life of the patient and its independence on normal daily activities.

In addition to these motor features, PD is also characterized by several non-motor symptoms such as autonomic disturbances (sexual and urinary dysfunction, constipation, orthostatic hypotension), sensory dysfunction (pain, hyposmia), sleep disorders (restless legs syndrome, rapid eye movement sleep behaviour disorder); cognitive impairment that typically progresses to dementia; and neuropsychiatric features like depression, anxiety and apathy. Epidemiological studies have revealed that some non-motor and psychiatric symptoms develop in a prodromal stage of PD, years before clinical manifestations of motor symptoms [69].

Even though most cases of PD appear with increasing age and/or sporadically, a genetic contribution may have a role to the overall risk of PD, which justifies that a medical history is usually done when diagnosing PD [70]. Besides this evaluation, and more importantly, physical and neurological examinations are also performed. However, diagnosis of PD is far from being straightforward as other movement disorders such as essential and dystonic tremor, and other

parkinsonian syndromes (multiple system atrophy, progressive supranuclear palsy, corticobasal degeneration, Lewy body disease, encephalopathy, and so forth), present overlap symptoms, especially in an early stage. In this regard, several clinicopathological studies have shown that approximately 25% of patients diagnosed with PD during life are confirmed to have an alternative diagnosis on autopsy. This difficult diagnosis, sometimes wrong or even inconclusive, have been motivating, during the last thirty years, the creation of various criteria and guidelines to improve and facilitate PD diagnosis and its therapeutic approach [69]. In Portugal, the clinical diagnosis of PD is nowadays done using the Movement Disorder Society Clinical Diagnostic for PD, from 2015. The Movement Disorder Society criteria considers both motor and non-motor features, as the latter often dominate the clinical presentation, and the diagnosis of PD is performed in two steps. Firstly, the parkinsonism is diagnosed; afterwards the criteria defines whether this parkinsonism is attributed to PD [71].

Considering that PD is a disease with high clinical heterogeneity, its diagnostic accuracy varies significantly according to the stage and progression of the disease, age, expertise of the physician and response to Parkinson medication. Therefore, it becomes important to understand the underlying mechanisms of this disease as well as other neurodegenerative diseases that happen to also cause parkinsonian symptoms in order to minimize diagnostic errors and direct patients to more accurate therapeutic management and follow-up.

3.2.1 – Molecular mechanisms of Parkinson's Disease

PD is pathologically characterized by the inclusion of Lewy bodies, aggregations containing α-synuclein proteins, inside neuronal cells. It is thought that these α-synuclein inclusions lead to synaptic dysfunction and interfere with axonal transport which eventually causes a selective loss of dopamine (DA) neurons in the basal ganglia, mainly in the substantia nigra pars compacta – a hallmark pathological feature of PD. Considering that the most prominent function of the latter structure is related to motor control, the death of those neurons, whose cause remains unknown, damages the nigrostriatal transmission system, triggering the core motor features of PD [72].

Due to the uncertain nature of the neurodegeneration in PD, the actual onset of this condition is difficult to define. At the time of diagnosis, when motor symptoms are evident, about 50-60% of DA neurons have already been lost in certain parts of the basal ganglia. Regarding this issue, imaging and pathological studies suggests that PD patients experience a prodromal phase (incidence of non-motor symptoms) which duration is still unclear, but likely to last at least for 5 years, and up to 20 years (see Figure 15) [73, 74].

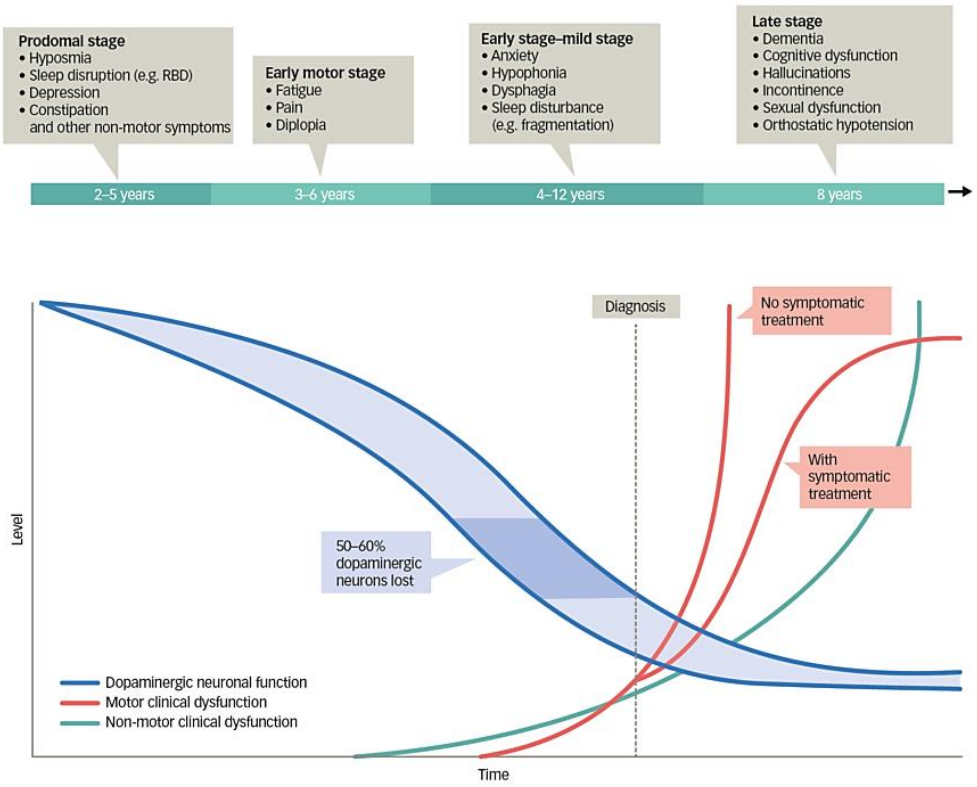

Figure 15. Time courses of the onset of motor and non-motor features of PD. Non-motor symptoms often manifest early when DA neurons have begun to decline, but before motor symptoms have appeared. Pharmacologic treatment can help controlling the motor symptom. RBD: rapid eye movement sleep behaviour disorder. Obtained from [74].

As previously mentioned, accurate clinical diagnosis to know whether a person has PD or another condition with parkinsonism symptoms (essential tremor, for example) may be challenging, especially in the early course of disease, owing to largely overlapping symptomatology. This earlier and reliable diagnosis, and consequently earlier intervention, is hence desirable as it improves disease management which may lead to superior outcome.

There is currently no cure for PD, however symptoms can be relieved by physical and speech therapy, occupational therapy, pharmacologic and surgical treatment. Physical and speech therapies aim to improve and maintain motor and communicational skills while occupational therapy utilizes adaptive equipment to optimize the patients' everyday routines despite the limitations.

Amongst all the pharmacologic treatment options available for PD, dopamine replacement therapy, i.e. the use of levodopa (DA precursor) and/or DA agonists, is the most widely used treatment for controlling PD symptoms. Neuropsychiatric features present in PD patients can be controlled using antipsychotic, antidepressants and other medications, all options that must be individualized and tailored to the clinical presentation of the patient.

Surgery is used generally to treat the most advanced cases of PD when pharmacologic treatment is insufficient to relieve the symptoms. The most promising surgical method available nowadays is deep brain stimulation. This technique involves the implantation of a pacemaker-like device, usually in the patient's chest, that generates electrical impulses to stimulate certain

locations in the basal ganglia. This stimulation can be adjusted to the need of each individual patient and it has proven to block the brain activity that causes PD symptoms [75].

3.2.2 – Molecular imaging of Parkinson's Disease

The presynaptic nerve terminals of the DA neurons in the nigrostriatal pathway express dopamine transporters responsible for the reuptake of DA released into the synaptic cleft. With the damage of the nigrostriatal transmission system comes the loss of DA neurons, thus leading to a decrease in DA production and release, which eventually results in parkinsonism when the deficiency becomes too severe [76].

SPECT and PET imaging of dopaminergic neuronal integrity and function has markedly advanced allowing earlier and more accurate diagnosis of PD of high risk patients, contributing to make a better differential diagnosis between PD and other forms of parkinsonism, as well as helping monitor disease progression and drug treatment. Molecular imaging techniques also support investigation in the identification of potential disease-modifying agents or interventions, greatly needed advances in such a vast field where no definite cure exists.

Presynaptic imaging and, specifically, dopamine transporter (DAT) imaging, the most widely used technique for *in vivo* measurement of striatal DA functional integrity, have shown high accuracy in differentiating between PD and non-degenerative mimicking disorders (see Table 3).

Table 3. Differential diagnosis between degenerative and non-degenerative parkinsonism in patients with tremor [77].

Degenerative Disorders
Parkinson's disease
Multiple system atrophy parkinsonian type
Progressive supranuclear palsy
Corticobasal degeneration
Dementia with Lewy bodies
Non-degenerative Disorders
Essential tremor
Dystonic tremor
Vascular parkinsonism
Drug-induced parkinsonism
Tremor related to metabolic or functional causes

In a normal DAT imaging scan, when DA neurons are intact and functioning normally, plenty of DAT are available for binding of high affinity DAT molecules, so high radiotracer uptake is expected to be seen. However, low uptake of a DAT tracer normally suggests underlying neurodegeneration, supporting a diagnosis of PD or other parkinsonian syndrome which thus identifies patients in whom dopaminergic replacement therapy may be beneficial. However,

DAT imaging is not helpful differentiating between PD and other parkinsonian syndromes as the loss of presynaptic DA neurons is a common feature in these conditions [1]. In these cases, postsynaptic dopaminergic imaging may be helpful, but this distinction does not often provide any different disease-modifying therapy [78].

Beyond these applications, DAT imaging might also help differentiate between PD dementia and Alzheimer's disease since the dopaminergic pathway integrity is preserved in the latter [78].

Many of the compounds used for presynaptic DAT imaging are tropane derivative tracers that have a chemical structure similar to that of cocaine since they compete for the same binding sites in the brain. Tropane derivatives show excellent binding affinity to DAT, but also some affinity to serotonin and norepinephrine receptors. However, this fact does not represent a concern regarding DAT imaging because the total number of DAT binding sites in the basal ganglia and substantia nigra is way higher than that of serotonin and norepinephrine transporters in these locations [1].

The iodine-123 (^{123}I) labelled compound N-(3-fluoropropyl)-2βcarbomethoxy-3β-(4-iodophenyl)-nortropane, [^{123}I]FP-β-CIT, has become the radiotracer of choice for SPECT imaging of DA neuronal degeneration, demonstrating high sensitivity and specificity in the differentiation of PD from non-degenerative forms of parkinsonism along with its rapid binding kinetics. Commercialized by the trade name of DaTSCAN™, this radiotracer became available in the United States and Europe for routine clinical use for diagnosing and monitoring the treatment response in PD patients. However, due to the challenging logistics of ^{123}I cyclotron production and distribution, and having that technitium-99m (^{99m}Tc) can be readily available from a generator, the tracer [^{99m}Tc]TRODAT-1 has been developed [1, 77].

With the development of ^{11}C radiochemistry, very appropriate for brain studies as mentioned before in this work, and considering the better resolution provided by PET scanners, a wide variety of ^{11}C-cocaine analogues for DAT integrity measurement have also been designed for PET studies. In the early 1990's, studies using [^{11}C]2β-carbomethoxy-3β-(4-iodophenyl)tropane (β-CIT) and its fluorinated analogue 2β-carbomethoxy-3β-(4-fluorophenyl)tropane (β-CFT) either labelled with ^{11}C or ^{18}F have proved their high affinity to DAT. However, these radiotracers have later shown not to be ideal for quantification due to their *in vivo* slow distribution kinetics as the binding equilibrium takes much longer than the reasonable time to perform the PET scan [79].

To overcome these weaknesses, more PET tropane derivatives have been developed over the years including [^{11}C]PE2I, [^{11}C]RTI-32, [^{18}F]FP-β-CIT, [^{11}C]N-(2-fluoroethyl)-2β-carbomethoxy-3β-(4-iodophenyl)nortropane (β-CITFE), and more recently, in 2019, the radiotracer [^{18}F]LBT-999 which is currently in the stage of clinical studies [80].

The β-CITFE molecule, a N-fluoroethyl analogue of β-CIT, was firstly introduced in 1994. One year later, in 1995, the first living human brain study using ^{123}I-labelled β-CITFE takes place revealing a very fast uptake of the radiotracer allowing the completion of the study within 1 hour after intravenous injection. This represents a greater advantage when comparing the more than 8 hour DAT binding peak equilibrium in the basal ganglia achieved with [^{123}I]β-CIT and the 3-4 hour peak uptake of [^{123}I]FP-β-CIT in the same location, kinetics not convenient for daily

clinical use [81]. Taking into account these results and the suitable ^{11}C radiochemistry, in 2000, a PET study using [^{11}C]β-CITFE in humans supported that this radiopharmaceutical provides high brain uptake and confirmed that it reaches peak equilibrium within less than 1 hour after intravenous injection (36-45 minutes), satisfying the condition for peak equilibrium during a suitable time period for the PET data acquisition. [^{11}C]β-CITFE is hence admitted as a very suitable radiotracer for clinical studies for DA functional integrity assessment, additionally when repeated PET scans are needed on the same day [79].

Presynaptic imaging for the evaluation of nigrostriatal neuronal integrity and function can also be done by the uptake measurement of 6-[^{18}F]-fluoro-L-dopa ([^{18}F]DOPA), the first approach introduced in the clinical setting for this purpose. This radiotracer is an analogue of L-DOPA and a false substrate for the enzyme L-aromatic amino-acid decarboxylase responsible for the conversion of L-DOPA to DA. Its uptake reflects the *in situ* enzymatic synthesis of endogenous DA within the presynaptic terminal and provides information about dopaminergic neuronal activity. However, [^{18}F]DOPA images can underestimate the degree of DA depletion due to compensatory changes that result in an up-regulation of the enzymatic activity. In addition to this, some [^{18}F]DOPA O-methylated derivatives can be taken up in the brain, contributing to a high background noise [1, 82].

Another strategy for assessment of dopaminergic system integrity consists on imaging the vesicular monoamine transporter 2 (VMAT2) using mainly [^{11}C]dihydrotetrabenzine (DTBZ) or its more recently commercially available ^{18}F analogue. VMAT2 are responsible for storing and taking up DA, and other neurotransmitters as well, from the synaptic cleft into presynaptic vesicles, thus regulating synaptic concentration of neurotransmitters in the brain. Since the expression level of VMAT2 reflects the density of DA terminals, [^{11}C]DTBZ uptake shows the degree of degeneration of DA neurons [82].

In summary, the possibilities for imaging presynaptic dopaminergic function are represented in Figure 16 whereas Figure 17 shows examples of healthy and abnormal SPECT/PET images resultant from DA neurons imaging.

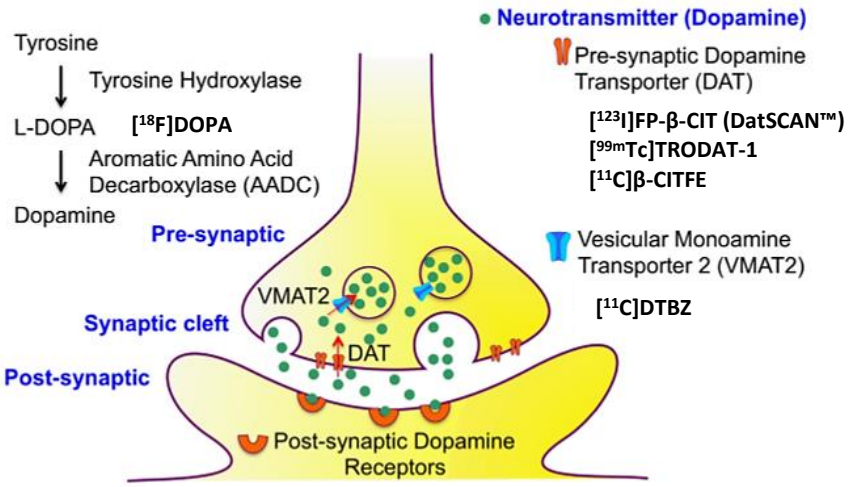

Figure 16. Schematic representation of DA dynamics between two neurons and examples of SPECT and PET imaging radiotracers for mapping DA neurons. Adapted from [1].

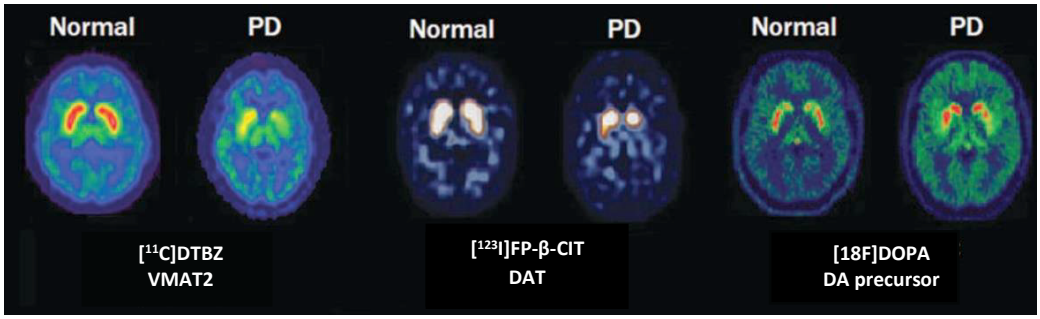

Figure 17. Molecular imaging of dopaminergic dysfunction in PD. Example of PET ([^{11}C]DTBZ and [^{18}F]DOPA) and SPECT ([^{123}I]FP-β-CIT) imaging in a PD patient that show decreased VMAT2 activity, DAT availability and synthesis of DA (low uptake in all cases resultant from neuronal loss) compared with a healthy control. Adapted from [77].

Chapter II – Materials and Methods

1 - General

Irradiations were performed on a IBA Cyclone 18/9 cyclotron (IBA, Louvain-La-Neuve, Belgium) by the $^{14}N(p,\alpha)^{11}C$ nuclear reaction in order to produce $[^{11}C]CO_2$. $[^{11}C]CO_2$ was then converted to $[^{11}C]CH_3I$ and $[^{11}C]CH_3OTf$ methylation precursors by the "wet" chemistry approach, using the MeI-Plus™ module (Bioscan Inc., Washington DC, USA), and gas phase approach, using the Synthra [11C]Choline commercial module (Synthra GmbH, Hamburg, Germany). ^{11}C-methylation reaction occurred at room temperature in a specially designed loop system, the AutoLoop™ (Bioscan Inc., Washington DC, USA), whose inner surface was pre-coated with cold precursor. Afterwards, using a semi-preparative HPLC system composed by an ASI Isocratic 521 HPLC Pump (ASI, Richmond, USA), a Phenomenex Luna® C18(2) 5 μm, 10x250 nm (Phenomenex®, Torrance, USA) reverse-phase HPLC column, a K-200 WellChrom fixed ultraviolet wavelength (254 nm) detector (Knauer GmbH, Berlin, Germany) and a Bioscan Hot Cell HC-003 radiation detector, the crude reaction products are separated and purified. After collection of the fraction of interest, reformulation of the product was done using a Synthera Extension module (IBA) and a specially designed cassette support (manufactured in-house) compatible with a disposable kit for ^{11}C-radiopharmaceuticals reformulation (Fluidomica Lda., Coimbra, Portugal). With this last step, a sterile injectable solution was obtained, ready for QC and posterior preclinical or clinical use.

The whole radiosynthesis process was carried out in a shielded MIP1-1P hot cell (Comecer SPA, Castel Bolognese, Italy) with all the equipment previously described being remotely controlled. The operator visually monitors the process through a leaded-glass window and by making use of specific software programs that displays real-time graphical view of each procedure and associated physicochemical information (activity, temperature, flow, pressure, volume).

N-2-fluoroethyl-3-β-(4-iodophenyl)nortropane-2-β-carboxylic acid (CITFES) cold precursor for $[^{11}C]$β-CITFE was purchased from ABX (Advanced Biochemical Compounds GmbH, Radeberg, Germany) while 2-(4'-aminophenyl)-6-hydroxybenzothiazole (6-OH-BTA-0) cold precursor for $[^{11}C]$PiB was purchased from Huayi (Huayi Isotopes Co., Changshu City, China). Liquid nitrogen required for the Synthra module was obtained from Air Liquide (Air Liquide Portugal, Miraflores, Portugal). For the $[^{11}C]CH_3I$ "wet" method production, $LiAlH_4$, THF and HI reagents were acquired from Sigma-Aldrich (Sigma-Aldrich, St. Louis, USA). Chemicals required for the gas phase system included NaOH beads, carboxen, iodine anhydrous beads and porapak, all purchased from Sigma-Aldrich as well as nickel powder catalyst (Alfa Aesar, Heysham, United Kingdom). Silver triflate with trace metals upper than 99.95% and Carboxen adsorbent, both from Sigma-Aldrich, were used to prepare the silver triflate (AgOTf) column in which $[^{11}C]CH_3I$ is

converted to [^{11}C]CH_3OTf. Consumable NaOH iodine trap cartridges were purchased from Synthra.

Acetonitrile (ACN), water (Fisher Scientific, Hampton, USA) and ammonium formate (AMF) (Honeywell, New Jersey, USA) were used to prepare the mobile phases for the semi-preparative HPLC purification. Solvent delivery module required water, ether (Fisher Scientific), ethanol and acetone (VWR International Ltd, Leicestershire, United Kingdom).

Reformulation of the final product was done by solid phase extraction (SPE) method using a C18 light SPE cartridge (Waters, Milford, USA) that was eluted with ethanol (Rotem Industries Ltd, Arava, Israel). Sterile water for injections (WFI) and 0.9% NaCl were purchased from B. Braun (B. Braun Melsungen AG, Melsungen, Germany). Sterilization of the final product was guaranteed by the use of Sterile 0.22 μm SLGV004SL Millex-GV Millipore (Merck Millipore, Molshmei, France) filters, and Minisart NML 0.2 μm, 25 mm Syringe μm (Sartorius, Goettingen, Germany) sterilization filters.

Process gases such as H_2, He and N_2 were of scientific grade (99.999%) and were obtained from Praxair Portugal Gases S.A. (Praxair Portugal Gases S.A., Maia, Portugal) taking in consideration the purity and composition described in the European Pharmacopoeia (Ph. Eur.) and also the specifications of the equipment's manufacturers.

All reagents and solvents used in the radiosynthesis were obtained from commercial suppliers of Ph. Eur. or HPLC grade, as appropriate.

QC is a fundamental requirement to assess if a radiopharmaceutical is of pharmaceutical quality and safe for injection. For that reason, chemical and radiochemical impurities of [^{11}C]PiB and [^{11}C]β-CITFE were detected and quantified by a Agilent 1200 Series HPLC system (Agilent Technologies, Santa Clara, USA) that is controlled via GINAstar™ Software, from Elysia-Raytest (Elysia-Raytest GmbH, Straubenhardt, Germany). The system is equipped with a Elysia-Raytest Gabi Star 1207 radiometric detector, a Rheodyne model 7125i syringe-loading sample injector valve (IDEX H&S, Wertheim-Mondfeld, Germany) with a 20 μl loop, and an analytical Agilent Zorbax Eclipse XDB-C18 HPLC column, 5 μm, 4.6x150 mm where the chromatographic separation was performed. On the other hand, using an Agilent 6850 Series II gas chromatography system, organic volatile solvents concentration was analysed. The pH was measured using a Jenway 3510 pH meter (Bibby Scientific Limited, Staffordshire, United Kingdom) and the isotope half-life, radioactivity and concentration of the final product were measured using an ISOMED 1010 dose calibrator (Nuklear-Medizintechnik Dresden GmbH, Dresden, Germany). Bacterial endotoxins analysis was performed using Endosafe® PTS™ cartridges 0.05 EU/ml (Charles River Laboratories, Massachusetts, USA).

2 - Experimental Procedures

Since this work involved the use and manipulation of radioactive substances, standard requirements regarding radiological protection and safety were satisfied whereas the ALARA principle ("As Low As Reasonably Achievable") was always applied to prevent unnecessary exposure. Accordingly, use of personal protective equipment and lead barriers was transversal

to all experimental procedures, and control of radiation exposure was performed with approved personal dosimeters, which were regularly checked and their readings recorded. All this work was conducted under Good Laboratory Practices (GLP) and Good Manufacturing Practices (GMP).

The process of radiosynthesis of a radiopharmaceutical labelled with ^{11}C suitable for animal and human injection, such as [^{11}C]PiB and [^{11}C]β-CITFE in this project, comprises several interdependent components that work sequentially throughout the following processes (see Figure 18):

1. Irradiation of a gaseous N_2 + 0.5% O_2 target in the cyclotron to produce [^{11}C]CO_2;

2. Conversion of the [^{11}C]CO_2 to [^{11}C]CH_3I and then [^{11}C]CH_3OTf in the commercial synthesis module;

3. ^{11}C-methylation of the cold precursor by captive solvent method;

4. Purification in reverse-phase HPLC system;

5. Reformulation of the compound into an injectable and sterile solution of ethanol and NaCl.

[^{11}C]CO_2 production
IBA Cyclone 18/9

[^{11}C]CH_3I production

Synthra [11C]Choline module (gas phase)
- Trapping of [**^{11}C**]CO2
- Conversion to [**^{11}C**]CH3I
- Conversion to [**^{11}C**]CH3OTf
- Optional by-passing

Labelling reaction

AutoLoop™ system
- ^{11}C -methylayion reaction
- Room temperature reaction
- Cleaning system

Purification

Phenomenex Luna® C18(2)
5 µm, 10x250 nm
- Reverse phase HPLC
- UV and radiation detector
- Fraction collection

Reformulation

IBA Synthera Extension
- SPE purification
- Final product formulation (ethanol and NaCl)
- Sterile filtration

Connected system through valves and tubing lines

Figure 18. Overview of the five necessary procedures for a successful 11C-radiosynthesis.

After the synthesis, the final product was transferred to the QC laboratory to assess if the radiopharmaceutical fulfilled quality standards to be intravenously administered. QC procedures included physicochemical tests and biological tests.

2.1 - Production of $[^{11}C]CO_2$

^{11}C was initially obtained in the chemical form of $[^{11}C]CO_2$ via the $^{14}N(p,\alpha)^{11}C$ nuclear reaction, in the IBA Cyclone 18/9 cyclotron. The target consists of an aluminium body that is covered with an aluminium window foil through which the proton beam hits the target. The target was loaded with gaseous mixture of N_2 + 0.5% O_2 and was irradiated with protons that had an effective beam energy on target of 18 MeV and an integrated current between 14 and 20 μAh. All irradiations had a time of bombardment of 45 to 55 minutes, which corresponded to a sufficient activity level for the synthesis of $[^{11}C]$PiB and $[^{11}C]$β-ClTFE. ^{14}N target gas was of scientific grade purity (99.9999%).

When the irradiation stopped, $[^{11}C]CO_2$ was transferred by spontaneous expansion through a stainless steel tube that established a direct connection between the target, in the cyclotron, and the synthesis module placed inside a hot cell, in the radiochemistry laboratory. The hot cell must be correctly pressurized, otherwise the transfer of the radioactive gas would not be possible.

2.2 - Production of $[^{11}C]CH_3I$ and $[^{11}C]CH_3OTf$

2.2.1 – "Wet" method

$[^{11}C]CH_3I$ and $[^{11}C]CH_3OTf$ were synthesised by "wet" method using the MeI-Plus™ automated module. In the beginning of the day, before any synthesis, tubing and valve systems were fully cleaned with ethanol, acetone and diethyl ether, provided from the solvent delivery module, and then dried under a continuous flow of N_2 (see Figure 19). The prepared $LiAlH_4$/THF solution and HI reagent vials were therefore placed in their corresponding positions in the module, loaded onto the system and pressurized to avoid external contamination, followed by another full system cleaning.

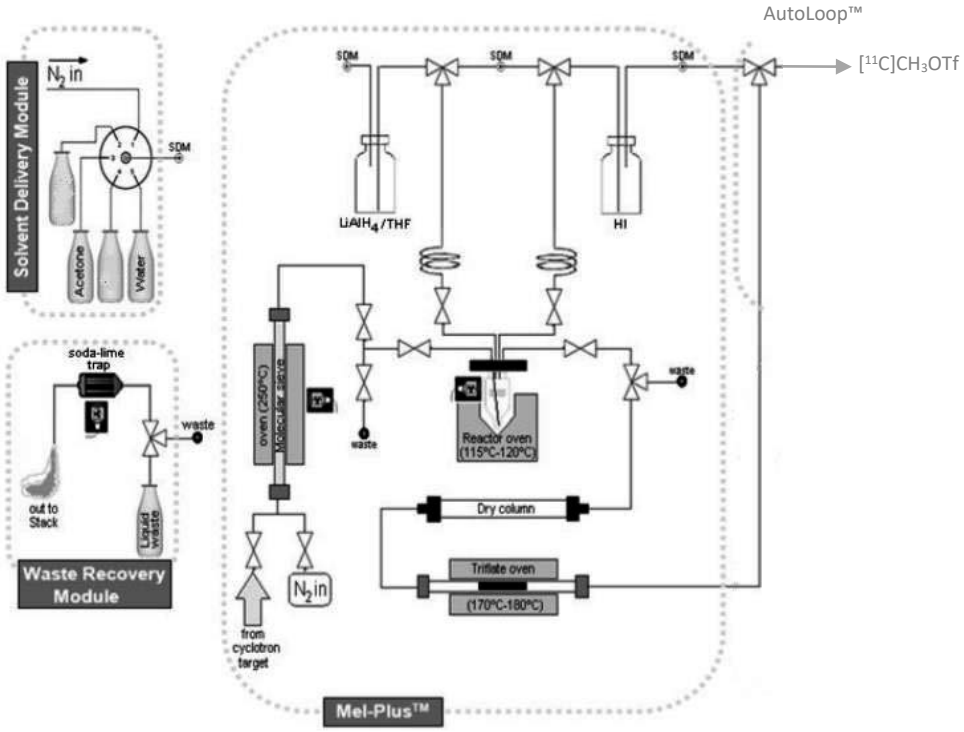

Figure 19. Schematic representation of the MeI-Plus™ automated module and its connection with the solvent delivery module and waste recovery module. Adapted from [83].

Several flow tests should also be performed to ensure that there were no obstructions between the module and the loop and that all the valves were working properly. Before the synthesis it was also required to condition a copper column filled with molecular sieves by heating it at 250°C, for at least 20 minutes, to remove traces of stable CO_2 and hence increase the molar activity. Once all these procedures were concluded, the system was prepared for the synthesis process.

Using this method, in a first step, cyclotron produced $[^{11}C]CO_2$ is trapped at room temperature in the molecular sieves (see Figure 19). By heating these molecular sieves up to 250°C and by means of continuous flow of N_2, $[^{11}C]CO_2$ is released and bubbled to the reactor vessel that was prefilled with a given volume of $LiAlH_4$/THF solution, becoming trapped in this solution. Once the $[^{11}C]CO_2$ was completely trapped, THF is then fully evaporated (120°C) and HI is added into the reaction vessel to generate $[^{11}C]CH_3I$. The latter is then distilled under continuous flow of N_2 (120°C) and passed through a 180°C preheated AgOTf column for instant conversion to $[^{11}C]CH_3OTf$.

Between the reactor and the AgOTf column is placed a phosphorus pentoxide/ascarite drying column to reduce traces of humidity in the system, since H_2O easily reacts with AgOTf, generating $[^{11}C]CH_3OH$ which will affect the reaction radiochemical yield.

The $[^{11}C]CH_3OTf$ synthesised is finally delivered from the module to pre-coated loop with the chemical precursor solution.

In summary, the chemical reactions that occur in the wet method synthesis of $[^{11}C]CH_3OTf$ are shown in Figure 20.

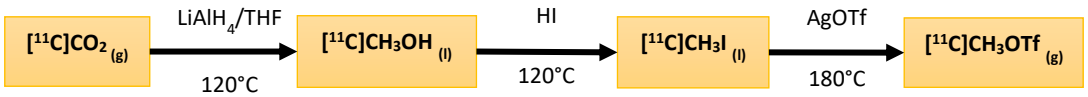

Figure 20. Chemical equations of the "wet" method synthesis of $[^{11}C]CH_3OTf$, starting from $[^{11}C]CO_2$.

After the last synthesis performed in the day, it was necessary to remove the $LiAlH_4$/THF and HI reagent vials, and do a full system cleaning using hydrochloric acid and ethanol. Finally, the system was carefully dried using N_2.

2.2.2 – Gas phase

Starting from the cyclotron produced $[^{11}C]CO_2$, $[^{11}C]CH_3I$ was synthesised by gas phase approach in the Synthra [11C]Choline commercial synthesis module. This module is a computer controlled and user programmable synthesiser of ^{11}C-labelling precursors. Synthesis of $[^{11}C]CH_3I$ and $[^{11}C]CH_3OTf$ were carried out completely automatically and monitored via the SynthraView Software (Synthra GmbH, Hamburg, Germany). This software displays real-time graphical view of temperature, pressure, activity and flow rate values regarding the several components of the systems. The schematic representation of the system is shown in Figure 21.

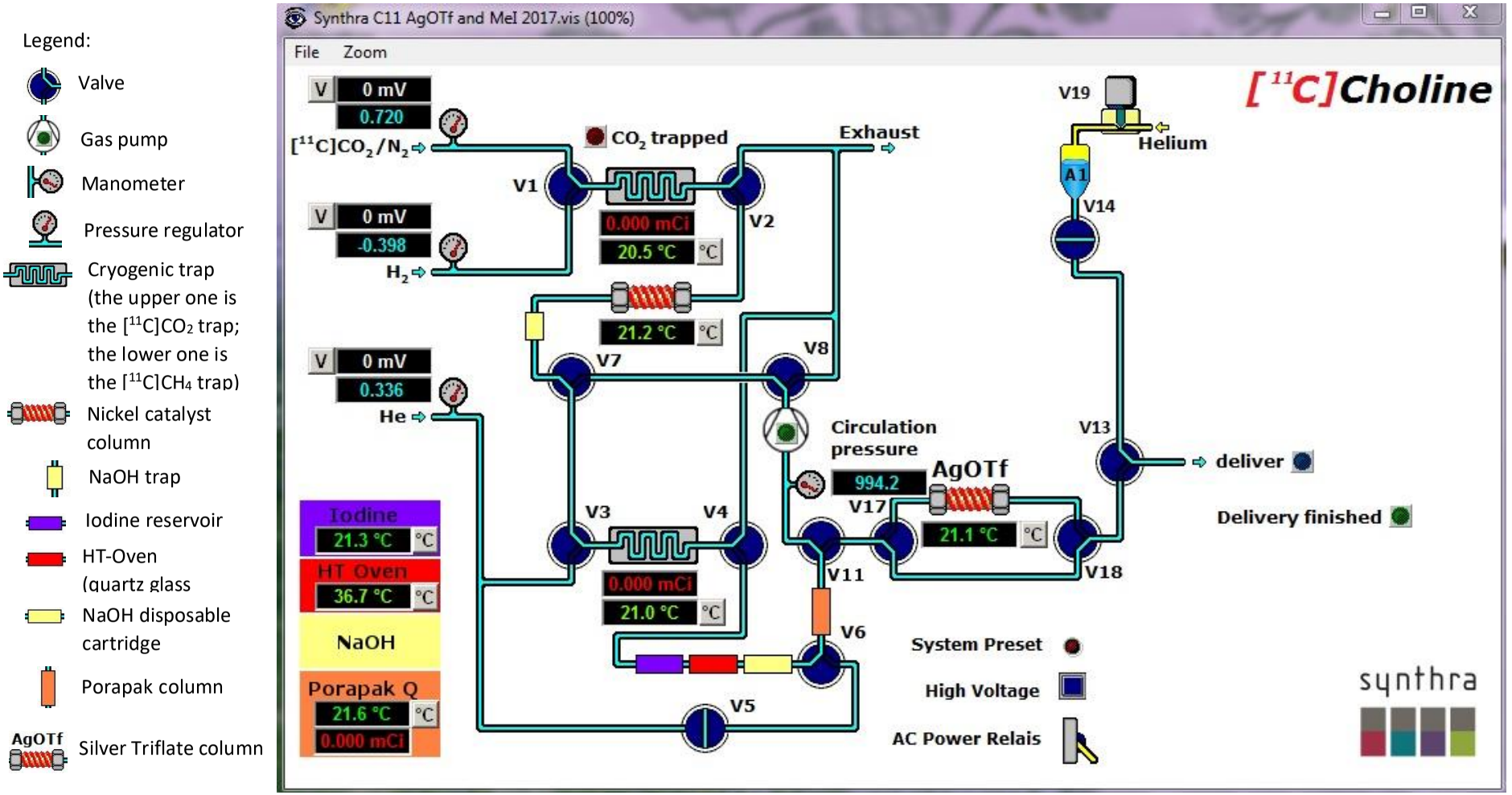

Figure 21. Graphic user interface of SynthraView Software and schematic representation of several components of the Synthra [11C]Choline module. Obtained from the SynthraView Software, with the system at resting state).

In this method, incoming $[^{11}C]CO_2$ is trapped in a CO2-trap previously cooled down with liquid nitrogen until -180°C. The gas is then purified in that trap and all unwanted components such as $[^{11}C]CO$ are transferred to the exhaust. By heating the CO_2-trap to 50°C and under H_2 flow, $[^{11}C]CO_2$ is released and converted to $[^{11}C]CH_4$ by reaction with H_2 on a nickel catalyst at 425°C. Unreacted $[^{11}C]CO_2$ and water resultant from this reduction were trapped in an intermediate NaOH trap. $[^{11}C]CH_4$ is then trapped in a CH_4-trap with liquid nitrogen, at -120°C. After purification, the $[^{11}C]CH_4$ reacts with vaporised elemental iodine in the high temperature oven (HT-oven) at 750°C to produce $[^{11}C]CH_3I$ through a closed recirculation pathway, allowing this iodination reaction to be repeated multiple times and thus maximize the reaction yield. During this recirculation process, formed $[^{11}C]CH_3I$ is trapped in the porapak trap at room temperature while unreacted iodine vapours and HI side-product are absorbed in the NaOH disposable cartridge.

Following iodination, the intermediate $[^{11}C]CH_3I$ is released by heat (200°C) from the porapak trap under helium flow and is instantaneously converted to $[^{11}C]CH_3OTf$ by passing it through a column of silver triflate heated at 190°C.

In summary, the chemical reactions that occur in the gas phase synthesis of $[^{11}C]CH_3OTf$ are shown in Figure 22.

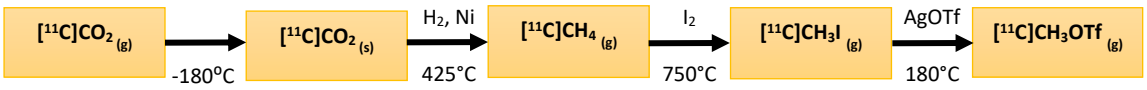

Figure 22. Chemical equations of the gas phase synthesis of $[^{11}C]CH_3OTf$, starting from $[^{11}C]CO_2$.

The liquid nitrogen is kept in a special dewar vessel that is coupled to the synthesis module. It must be filled before the beginning of the synthesis as it is placed inside the hot cell.

2.3 - Radiosynthesis of [^{11}C]PiB and [^{11}C]β-CITFE

2.3.1 - ^{11}C-methylation system

The ^{11}C-methylation system is constituted by several components and is based on the solvent captive loop method (see Figure 23). This technique requires no heating or cooling since the automated labelling process is performed at room temperature. Monitoring and control of the system is done via the Autoloop™ System Sotftware (Bioscan Inc., Washington DC, USA).

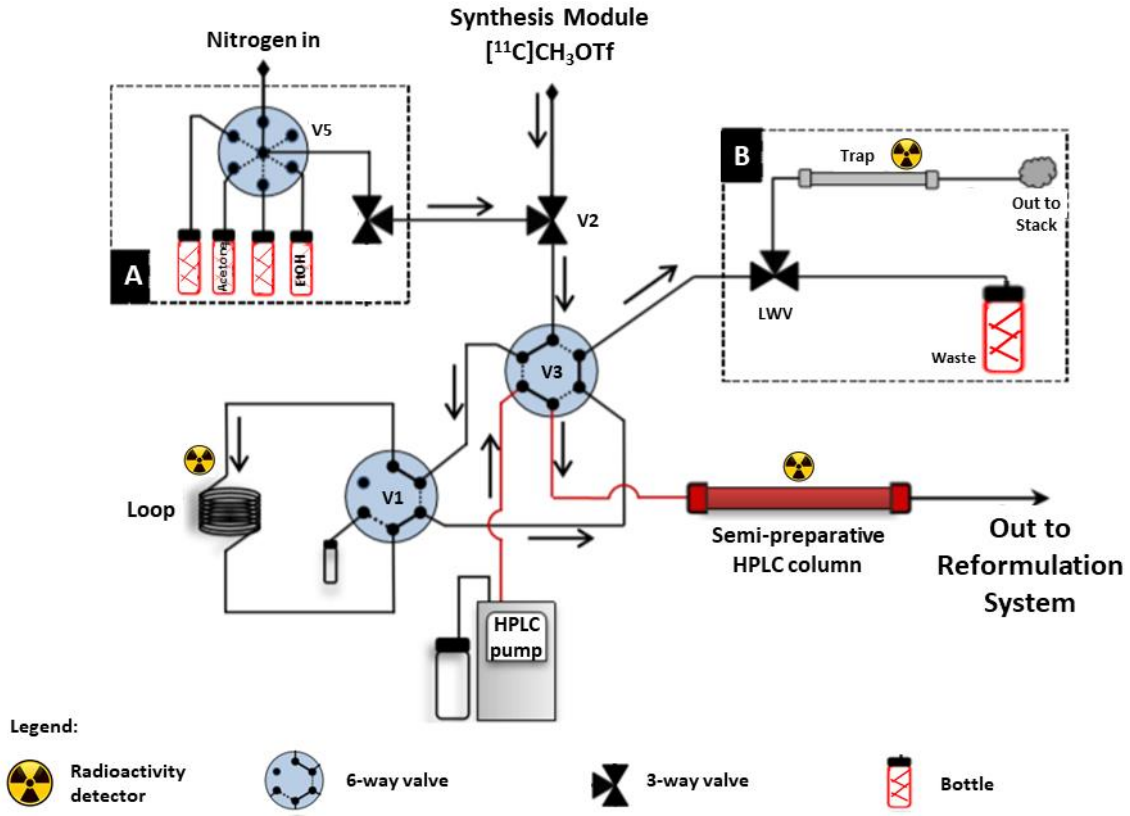

Figure 23. Schematic diagram of the loop methylation system and the connected HPLC system. A: solvent delivery module. B: waste recovery system. The cold precursor solution is injected into the loop through V1 valve. Adapted from [10].

The cold precursor solution is injected into the loop (1/16-inch outer diameter tubing, 2 ml of internal volume) through a Rheodyne model 7125i syringe-loading sample injector valve, similarly used in the QC HPLC system. Before the injection of any precursor solution, the injector valve should be purged.

A 3-way commercial valve (Neptune Research & Development, Inc., New Jersey, USA) is utilised to introduce incoming ^{11}C-methylation agent into the loop and also to deliver washing solvents and inert gas to the captive loop system. The solvent delivery module is placed outside the hot cell and controls the introduction of those solvents and inert gas. Only two out of four available bottles were filled with washing solvents (water and acetone). After each synthesis, the system was programmed to perform an automated washing cycle of water and acetone followed by N_2 drying.

The system also has a selector valve that enables whether the streaming of ^{11}C-labelling gas into the loop or the movement of the reaction products from the loop towards the semi-preparative HPLC.

2.3.2 - Preparation of the precursors' solution

PiB precursor

The 6-OH-BTA-0 (PiB) precursor purchased from Huayi (1 mg per vial) was dissolved in 170 µl of anhydrous acetone (VWR International Ltd) plus 30 µl anhydrous ACN (Sigma-Aldrich), concentration of 1 mg/200 µl . The dissolved precursor was then stirred in a vortex for 1 minute.

After use, the remaining PiB solution in this vial must be stored in the refrigerator.

CITFES precursor

CITFES precursor vial (10 mg) was dissolved in 1 ml of anhydrous acetone (concentration of 1 mg/100 µl) and then stirred in a vortex for 1 minute.

Two different approaches were tested when preparing the precursor for a synthesis to determine which yielded better results. Firstly, 100 µl of the precursor solution were transferred to an eppendorf tube. After that, 10 µl of tetrabutylammonium hydroxide solution (TBAOH) (Termofisher ACROS Organics™, Geel, Belgium) plus 40 µl of anhydrous acetone were added into the precursor solution and stirred in a vortex for 1 minute. The second experiment consisted on the use of 100 µl (1 mg) of the CITFES precursor dissolved in acetone.

The remaining precursor solution must be stored in the refrigerator after use.

2.3.3 - Labelling reaction

After dissolution and before locking the hot cell to start the radiosynthesis, a volume of 100 µl of PiB or CITFES precursor solution was slowly injected into the loop using a 100 µl Hamilton syringe (Hamilton Company, Bonaduz, Switzerland), allowing the precursor to coat the internal surface of the stainless steel loop.

Once produced, the $[^{11}C]CH_3OTf$ coming from the synthesis module was transferred to the loop by a low inert gas stream. Considering that the loop was previously coated with the chemical precursor solution, as the transfer proceeded, the radioactive gas was being trapped inside the loop and detected by a proximal radiation detector.

After $[^{11}C]CH_3OTf$ complete transfer and capture, the loop was sealed allowing the ^{11}C-methylation reaction to proceed. In this work, reaction times for PiB and CITFES were 2 and 4 minutes, respectively.

2.3.4 - Purification of [^{11}C]PiB and [^{11}C]β-CITFE

Once the reaction was complete, the reaction products were transferred to the semi-preparative HPLC column for further purification by passing a proper mobile phase and flow rate through the loop.

Regarding whether the labelled compound to purify was [^{11}C]PiB or [^{11}C]β-CITFE, several mobile phases were tested. For [^{11}C]PiB the mobile phases prepared were 0.1 M AMF aqueous solution /ACN (60/40, 55/45, 50/50 and 45/55 (V/V)) at a flow rate of 9 ml/min; concerning

[^{11}C]β-CITFE, 0.1 M AMF aqueous solution/ACN 45/55 and 40/60 (V/V) mobile phases were tested at a flow rate of 6 ml/min.

Considering the fact that [^{11}C]PiB and [^{11}C]β-CITFE retention times had previously been identified and that the HPLC column was installed in series with an ultraviolet (UV) detector (254 nm) and an appropriate radioactivity detector, it was possible to separate and collect the desired [^{11}C]PiB and [^{11}C]β-CITFE peak by triggering the switching of the diverter valve. However, and although the compound of interest was collected at this point, it still contained organic solvents from the mobile phase that must be removed due to their toxicity for animal and human use.

2.3.5 - Reformulation of [^{11}C]PiB and [^{11}C]β-CITFE final products

The final radiosynthesis step consisted in the reformulation of the radiopharmaceutical into a sterile injectable solution for preclinical or clinical use. This process was carried out in an automated reformulation module, Synthera Extension, which is controlled via the IBA Synthera-HPLC Software, using the SPE method. This user programmable module has a set of 10 pinch valves that controls liquids flow, and a syringe driver (manufactured in-house) designed for a 20 ml syringe luer eccentric tip (Terumo Medical Corporation, New Jersey, USA) coupling. This system employs a reusable support cassette where a sterile disposable kit for ^{11}C radiopharmaceuticals was placed. Five female connectors are fitted to the end part of the cassette, providing four different positions (one is reserved for the 20 ml syringe) for connection of the SPE cartridge and necessary solvent syringes (NaCl, ethanol, WFI) for the reformulation. The cassette and tubing support system used for the reformulation of [^{11}C]PiB and [^{11}C]β-CITFE in this work is shown in Figure 24.

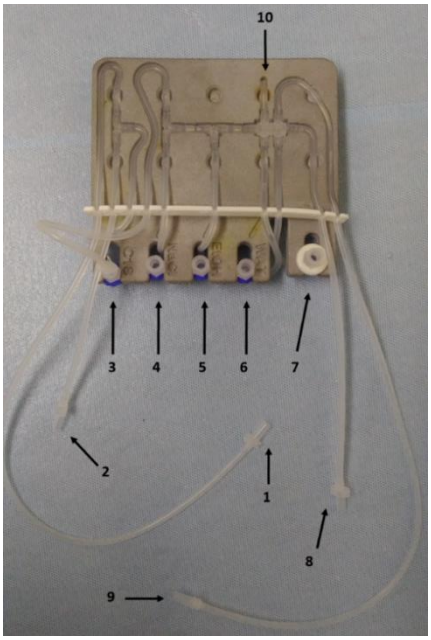

Figure 24. Support cassette for [^{11}C]PiB and [^{11}C]β-CITFE reformulation kits. 1- final product vial; 2- waste; 3- C18 light SPE cartridge; 4- 0.9% NaCl syringe; 5- ethanol syringe; 6- WFI syringe; 7- 20 ml syringe luer eccentric tip; 8- inert gas; 9- HPLC collect vial; 10- vent line.

The reformulation process applied can be described in the following steps:

1. Dilution of the collected fraction containing [^{11}C]PiB or [^{11}C]β-CITFE with 15 or 17 ml of WFI, respectively;
2. Bubbling the dilute fraction with inert gas for a few seconds to guarantee an effective mixing;
3. Passing the diluted fraction with [^{11}C]PiB or [^{11}C]β-CITFE through the SPE cartridge;
4. Rinsing the SPE cartridge with 5 ml of WFI to remove any organic solvent left from the HPLC mobile phase;
5. Drying the SPE cartridge with inert gas to remove the WFI;
6. Elution of the SPE cartridge with 1 ml of ethanol (10% of the total final product vial);
7. Dilution of the product in the final product vial with 9 ml of NaCl 0.9% to have a suitable ethanol concentration and to correct osmolarity;
8. Sterilization of the final product during steps 6. and 7. by means of a 0.2 μm sterilization filter placed before the FPV;

At the end of the reformulation, a sterile injectable radiopharmaceutical solution of 10 ml was obtained, ready for QC and posterior preclinical and clinical use.

2.4 - Quality control

QC tests are the same for both [^{11}C]PiB and [^{11}C]β-CITFE radiotracers and should be performed on each radiopharmaceutical batch. These include visual inspection, pH measurement, radiochemical and chemical purity, radionuclidic identity, molar activity, residual solvents concentration, bacterial endotoxins and sterility tests. In the absence of a specific monograph in the Pharmacopoeia relative to [^{11}C]PiB and [^{11}C]β-CITFE, quality requirements applied comply with the “Radiopharmaceutical preparations” monograph of Ph. Eur..

Firstly, the radioactive yield of the final product was measured using a dose calibrator. The radiopharmaceutical was then subjected to visual inspection to ensure that the product was clear, colourless and free of any particulate matter. The pH of the solution was measured by use of a pH meter to ensure that its value was between 4.5 and 8.5.

Radiochemical, chemical purity and molar activity were measured by an analytical HPLC equipped with an UV and radiation detector and a reverse-phase Agilent Zorbax Eclipse XDB-C18 column, 5 μm, 4.6x150 mm. For [^{11}C]PiB, the mobile phase used for the analysis was ACN/0.1 M AMF (40/60, V/V) with a flow rate of 3 ml/min whereas for [^{11}C]β-CITFE the mobile phase was ACN/0.1 M AMF (65/35, V/V) with a flow rate of 2 ml/min. For quantification of the radiochemical purity, the area of the radioactive peak corresponding to [^{11}C]PiB or [^{11}C]CITFE must represent more than 95% of the sum of all radioactive peak areas detected in the chromatogram.

Molar activity was quantified by the measurement of the area under [^{11}C]PiB UV and [^{11}C]β-CITFE UV mass peaks which were fitted to standard calibrations previously made. Currently there is not a minimum acceptable specific activity value for these two radiotracers. Chemical purity, whose limit was inferred from literature data and must correspond to more than 95%, was measured by UV absorbance of [^{11}C]PiB and [^{11}C]β-CITFE.

Organic volatile solvents (ethanol and ACN) concentration was measured by a gas chromatography system previously calibrated for the solvents in analysis. Ethanol and ACN concentrations must not exceed 2500 mg/10 ml and 4 mg/10 ml, respectively, for both [^{11}C]PiB and [^{11}C]β-CITFE.

Radionuclidic identity of ^{11}C was confirmed by measurement of the physical half-life (half-life test) on the dose calibrator. The final result must be within the interval of 19.9 to 20.9 min.

Bacterial endotoxins and sterility tests can be performed after batch release for use. [^{11}C]PiB and [^{11}C]β-CITFE bacterial endotoxins content was determined using the LAL test, performed in the Endosafe® PTS™ portable testing system (Charles River Laboratories, Massachusetts, USA). The radiopharmaceutical is considered to be contaminated if there were more than 175 endotoxins units per ml. Sterility test was performed in an external certified laboratory.

Chapter III – Results and Discussion

The earliest approach in ^{11}C radiochemistry to produce the methylation precursors [^{11}C]CH_3I and [^{11}C] CH_3OTf utilised a "wet" chemistry approach, a technique characterized by low molar activity obtained in these compounds and, consequently, in the ^{11}C-final radiopharmaceutical. The commercial "wet" chemistry system used in ICNAS-P for the routine production of ^{11}C-radiopharmaceuticals, and thus in this project, has worked from 2011 until May of 2017. From then on, the [11C]Choline gas phase module developed by Synthra GmbH was installed for that same purpose, a simpler and more recent methodology that offers higher molar activity values than those typically obtained with the "wet" method [84]. It was a goal to analyse and optimise the molar activity and EOS activity obtained for [^{11}C]PiB and [^{11}C]β-CITFE, state-of-the-art radiotracers for AD and PD, and the most requested clinical scans in ICNAS, using both "wet" and gas phase chemistry approaches.

While the developed work was performed within the busy company's routine, it also aimed to optimise the functioning of the new installed Synthra gas phase module to ensure the reproducibility and reliability of several successive synthesis per day, hence answering to the daily ^{11}C-radiopharmaceuticals requests while maintaining the highest molar activity possible. Another way to improve molar activity was by reducing the global time of the synthesis, a modification that consequently increases the radiochemical yield in the EOS. Ultimately, synthesised radiopharmaceuticals must fulfil all QC requirements for human and animal use.

Data was collected through [^{11}C]PiB and [^{11}C]β-CITFE synthesis intended for preclinical and clinical studies and also experimental tests under synthesis mimicking conditions, all performed by application of identical irradiation periods and integrated currents in the cyclotron.

1 – "Wet" Method Synthesis Module

The [^{11}C]CH_3I synthesis process and subsequent conversion to [^{11}C]CH_3OTf was carried out using the MeI-Plus™ automated module, which was optimised (prior to this project) to achieve the highest possible radiochemical yield and molar activity of the ^{11}C-methylation agent while ensuring reliability and reproducibility to respond to the needs of the preclinical and clinical practice [10, 83].

A full synthesis of the [^{11}C]CH_3OTf methylation agent was completed in approximately 11 minutes, from end of bombardment (EOB). The trapping and release of radioactivity from the molecular sieves and the following processes in the reactor vessel were monitored by radiometric detectors (see Figure 25).

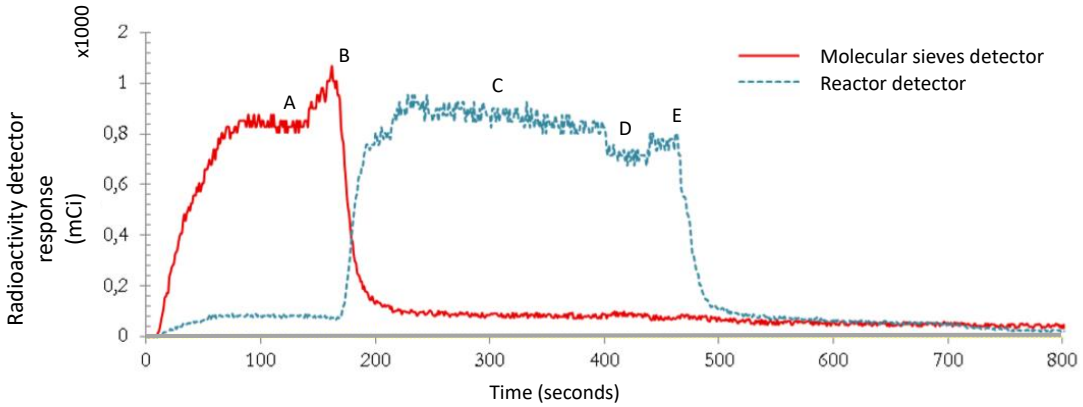

Figure 25. [^{11}C]CH_3OTf production activity profile on the MeI Plus™ "wet" method module. (A) Maximum [^{11}C]CO_2 trapping. (B) Molecular sieves heating and [^{11}C]CO_2 release. (C) Maximum [^{11}C]CO_2 trapping by reduction of $LiAlH_4$. (D) THF evaporation followed by HI reaction. (E) Maximum level of [^{11}C]CH_3I produced and beginning of its distillation. Adapted from [10].

[^{11}C]PiB activity obtained at EOS was 77.99 ± 27.69 mCi.

Regarding [^{11}C]β-CITFE, we observed major differences in the EOS activity obtained when TBAOH was added into the precursor solution opposed to when this base was not used in the preparation of the precursor for a single synthesis (explained in subsection 4.1 of this chapter). The preparation using TBAOH in the precursor solution yielded 25.98 ± 11.45 mCi at EOS. Many times, low [^{11}C]β-CITFE activities obtained at EOS implied additional efforts in the QC to release the product for injection as fast as possible. In the worst case scenario, the activity after QC and at time of injection was not sufficient activity for a patient dose (10 mCi), which implied a new irradiation and thus a new radiosynthesis. Another complication that came with low activities was the low concentration of the product solution with regard to preclinical applications and volume limitations for mice injections that might be passed over.

However, when the cold precursor solution injected for reaction consisted simply in CITFES dissolved in anhydrous acetone, we obtained 55.56 ± 9.80 mCi at EOS (see Figure 26).

[^{11}C]PiB and the optimised [^{11}C]β-CITFE final activities were sufficient for QC and preparation of patient doses, which is 15 mCi for [^{11}C]PiB and 10 mCi for [^{11}C]β-CITFE according to the standard protocols in ICNAS-P. In addition to this, these activity values resulted in product concentrations adequate for preclinical doses.

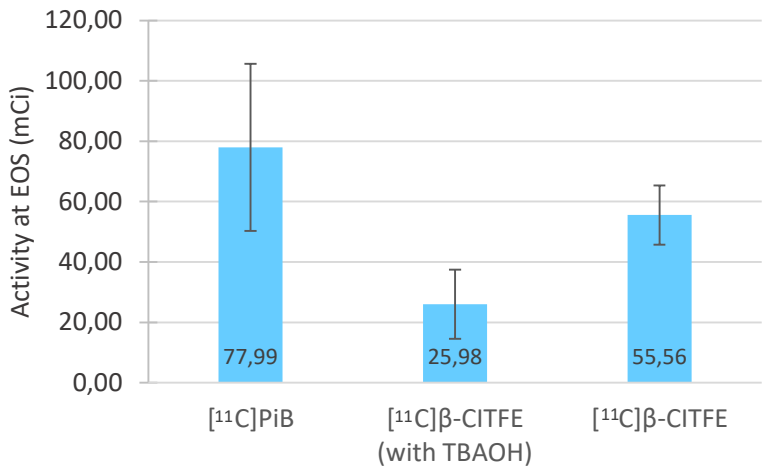

Figure 26. Activities obtained at EOS for [^{11}C]PiB, [^{11}C]β-CITFE when the cold precursor was prepared with TBAOH, and [^{11}C]β-CITFE, using the "wet" method module.

We strongly believe that the lower final activities of [^{11}C]β-CITFE observed at EOS using TBAOH in the preparation of its precursor are due, especially, to an increased quantity of water present in the ^{11}C-methylation reaction environment. The reaction between CITFES, a carboxylic acid, and a strong base, such as TBAOH, leads to the formation of a carboxylic acid salt and water. This way, the precursor solution injected in the loop has water in its composition straightaway.

Considering that water readily reacts in contact with [^{11}C]CH_3OTf due to the extremely high affinity between these two molecules, high quantities of radiochemical impurity [^{11}C]CH_3OH are produced during the in loop ^{11}C-methylation of [^{11}C]β-CITFE, thereby affecting negatively the reaction radiochemical yield. In fact, HPLC chromatogram exhibited an approximately 10-fold higher radiation signal from [^{11}C]CH_3OTf when comparing to that detected from [^{11}C]β-CITFE, a demonstration of how great the affinity between water and [^{11}C]CH_3OTf is. So, by eliminating TBAOH, the primary source of water in the reaction environment is eliminated as well, higher quantity of [^{11}C]CH_3OTf is available for CITFES labelling, thereby resulting in an increased radiochemical yield as we observed when [^{11}C]β-CITFE was methylated solely in the presence of anhydrous acetone.

Molar activity values obtained for [^{11}C]PiB and [^{11}C]β-CITFE were 37.73 ± 20.29 GBq/µmol and 18.48 ± 14.75 GBq/µmol, respectively (see Figure 27).

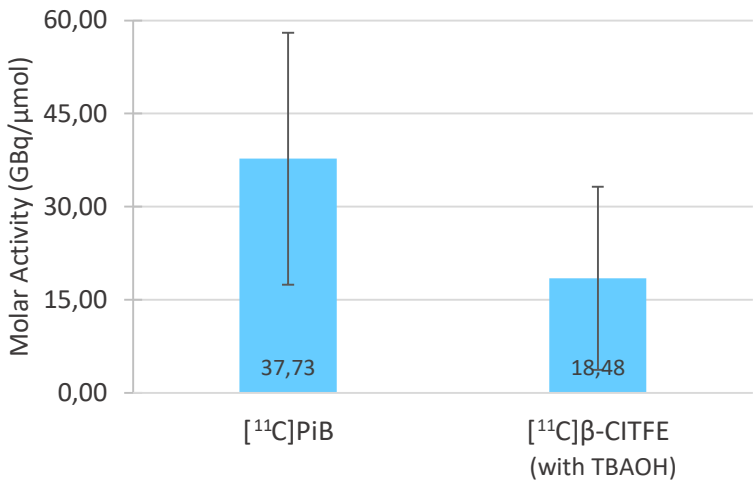

Figure 27. Molar activities obtained for [^{11}C]PiB, [^{11}C]β-CITFE when the precursor was prepared with TBAOH, using the "wet" method module.

2 – Gas Phase Synthesis Module

Considering that the cyclotron target, irradiation conditions, gases and transfer lines were optimised in order to avoid stable carbon contamination and provide the highest [^{11}C]CO_2 activity possible, it became important to reduce all other contamination factors, especially during the synthesis of the methylation precursor, in the synthesis module.

Since the gas phase synthesis module was a brand new system installed in the radiochemistry laboratory to be included within routine ^{11}C-radiopharmaceutical production, maintenance procedures were strictly necessary to be established to keep the machine working at full potential and with high reliability, avoiding synthesis failures and thus unnecessary costs for the company and inconveniences for the patients.

A full [^{11}C] CH_3OTf synthesis process and its delivery to the solvent captive loop was done in approximately 14 minutes. Trapping and releasing of the radioactivity in and between the different components in the system were monitored by radiometric detectors (see Figure 28).

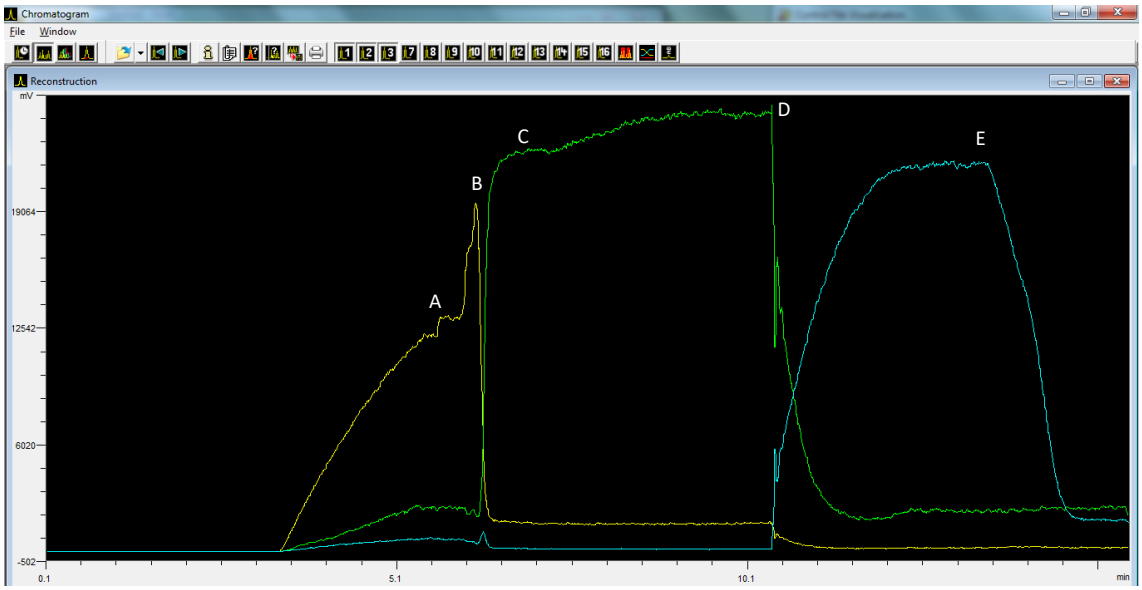

Figure 28. [^{11}C]CH_3OTf production activity profile on the Synthra [11C]Choline gas phase module. Yellow line: CO_2-trap detector. Green line: CH_4-trap. Blue line: porapak detector. (A) Maximum [^{11}C]CO_2 trapping on the CO_2-trap. (B) [^{11}C]CO_2 release. (C) Maximum [^{11}C]CH_4 trapping on the CH_4-trap. (D) [^{11}C]CH_4 release, conversion to [^{11}C]CH_3I and [^{11}C]CH_3I trapping in the porapak, during multiple gas recirculations. (E) Maximum level of [^{11}C]CH_3I produced and beginning of its release.

2.1 - Leak test

As this synthesis is carried out through gas phase approach, it is required that the whole system remains tight, otherwise the synthesis fails due to leakage of the radioactive gases. Therefore it becomes essential to test if the system is tight whenever there is any physical intervention in the system, especially, but also before each synthesis.

In order to test the tightness of the system, we set a helium flow to 100 ml/min and valves V3, V4, V6, V11 and V8 were turned so that the helium flowed through the manometer and through a closed system. This way, it was expected the pressure to rise until it reached a maximum and stable value. At this point, the helium flow should be approximately 2 ml/min or below, and the pressure in the closed system should be about 3500 mbar.

The system must be depressurized after testing by turning the V8 valve to the exhaust.

Whenever the helium cylinder bottle that supplies the synthesiser is replaced, care must be taken when regulating the flow provided to the module. When performing the leak test, which thus implies the pressurization of the system to its maximum, a pressure range between 3000 and 3500 mbar in the closed system is ideal and safe since higher pressure values can represent a risk to the equipment.

2.2 – Iodine oven temperature

For the synthesis of [^{11}C]CH_3I, it is necessary for the oven of the iodine reservoir to heat up, so that the solid iodine can vaporize and react with [^{11}C]CH_4 at high temperature in the quartz

glass tube to form $[^{11}C]CH_3I$. Instead of the original 110°C set in the manufacturer programme, the iodine reservoir oven can be heated up to 95°C without compromising the optimal conversion of $[^{11}C]CH_4$ to $[^{11}C]CH_3I$ as we did not observe differences in the $[^{11}C]CH_3I$ activity trapped in the porapak column.

With this change, less iodine is consumed in each synthesis representing not only an economic saving in the purchase of this expensive reagent, but also a less frequent need to refill the iodine reservoir by the operator, which can be an advantage in a busy production routine.

2.3 - Routine maintenance

As a consequence of the normal use of the machine, maintenances that require opening the system must be performed. These interventions can cause atmospheric air to get inside the tubing system and chemical components. Therefore purging the module tubing lines is important to eliminate this source of stable ^{12}C, the main responsible for a decrease in the molar activity of the synthesised methylation agent, and also some humidity naturally present in the atmospheric air. As explained before, the extreme reactivity of $[^{11}C]CH_3OTf$ with water leads to the formation of the radiochemical impurity $[^{11}C]CH_3OH$ which significantly decreases the radiochemical yield of the ^{11}C-methylation afterwards.

For these reasons, even if the system did not require any intervention that implied its opening, before each synthesis, the system was flushed and dried with inert gas (H_2 or He) as a preventive procedure to remove particles and gases from prior synthesis present in the lines.

In a daily use of the module, as it is in this work and in the routine of ICNAS-P, doing a more exhaustive and complete conditioning process once a month is a good reference. However, depending on the results obtained during the successive synthesis, a reason why it is really important to keep track of the synthesiser chemical and physical behaviour and consequently the molar activity and radiochemical activity of the products obtained in the EOS, this reference might be shifted, as will be discussed. The conditioning consisted of:

- heating up the CO_2-trap to 200°C and the nickel-oven to 425°C with a 5000 mV H_2 flow for a minimum of 30 minutes, with the output tubing of the NaOH column (after the nickel-catalyst) opened;

- heating up the CH_4-trap to 200°C, the HT-oven to 750°C and the Porapak to 200°C with a 5000 mV He flow for a minimum of 30 minutes, with the circuit opened through valve V8 to the exhaust.

Whenever it was necessary to open the system to add solid iodine into its reservoir, the vacuum pump was additionally used when purging the lines in order to maximize the removal of air within the small spheres of iodine and inside the reservoir itself. The same procedure using the vacuum pump was applied every time the NaOH disposable cartridge was changed.

Over time, crystallized iodine accumulates in the inner surface of the NaOH disposable cartridge holder adapter fitted on the output of the quartz glass tube. This deposition happens during productions due to the abrupt temperature difference between the quartz glass (750°C)

and the adapter, which is at room temperature. After this point, residual iodine vapours that do not crystallize and HI side-product are absorbed in the NaOH disposable cartridge. We observed, as synthesis were successively done, that the ever-increasing amount of crystallized iodine caused a reduction in the overall flow rate in the recirculation pathway by simple obstruction, thereby affecting the yield of the $[^{11}C]CH_4$ iodination. Thus, it is crucial to frequently do a visual inspection of the accumulation of iodine in this adapter and clean it (acetone is a good solvent) to ensure that the circulation is optimised, and so is the conversion of $[^{11}C]CH_4$ to $[^{11}C]CH_3I$ (see Figure 29). After cleaning, and before placing it back onto the machine, the adapter must be dried in order to avoid the introduction of water into the system.

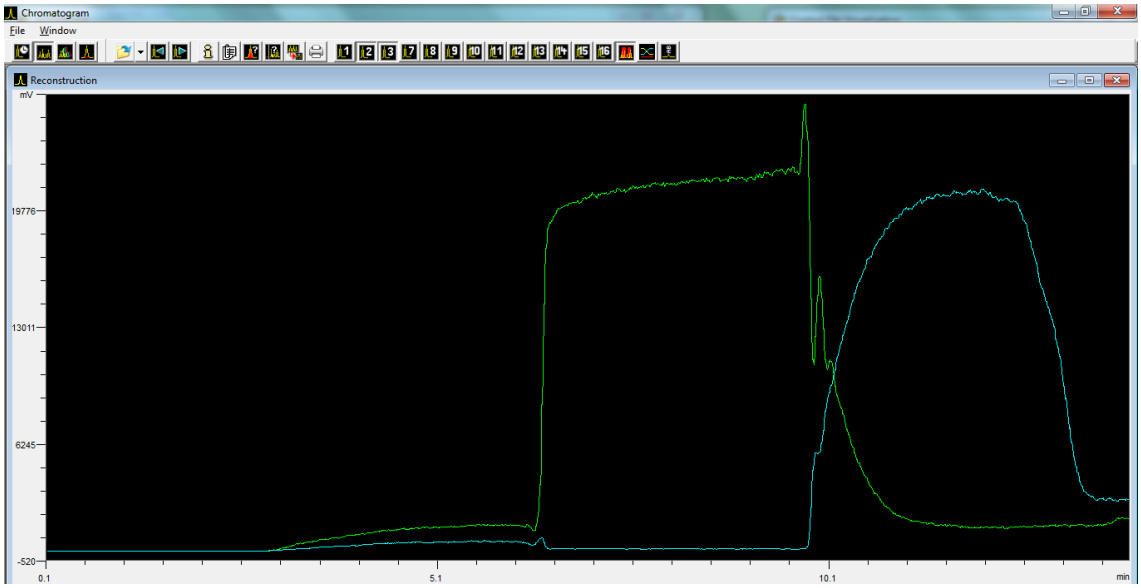

Figure 29. Example of a fast circulation of the activity in the recirculation pathway and efficient $[^{11}C]CH_3I$ production and retention in the porapak. The maximum level of $[^{11}C]CH_3I$ produced occurs approximately 2 minutes after the beginning of the iodination reaction. Green line: CH_4-trap radiometric detector. Blue line: porapak radiometric detector.

Despite cleaning the NaOH disposable cartridge holder adapter to remove the crystallized iodine, there were times where we still came across slowed down, nearly obstructed circulation, suggesting that the recirculation pathway should be blocked at some other component (see Figure 30). In fact, iodine can also crystallize over time in the iodine reservoir, in the entrance of the quartz glass tube, for the temperature issues mentioned before, or due to an overload of iodine in the reservoir. To avoid the latter point, we understood that is preferable to add less solid iodine each time so that the iodine amount in the reservoir has some safe void distance below the entrance of the quartz glass. We established checking the iodine level once a week as a good reference for the typical routine in ICNAS-P. However, according to the number of syntheses done, it might be prudent to check this level more often.

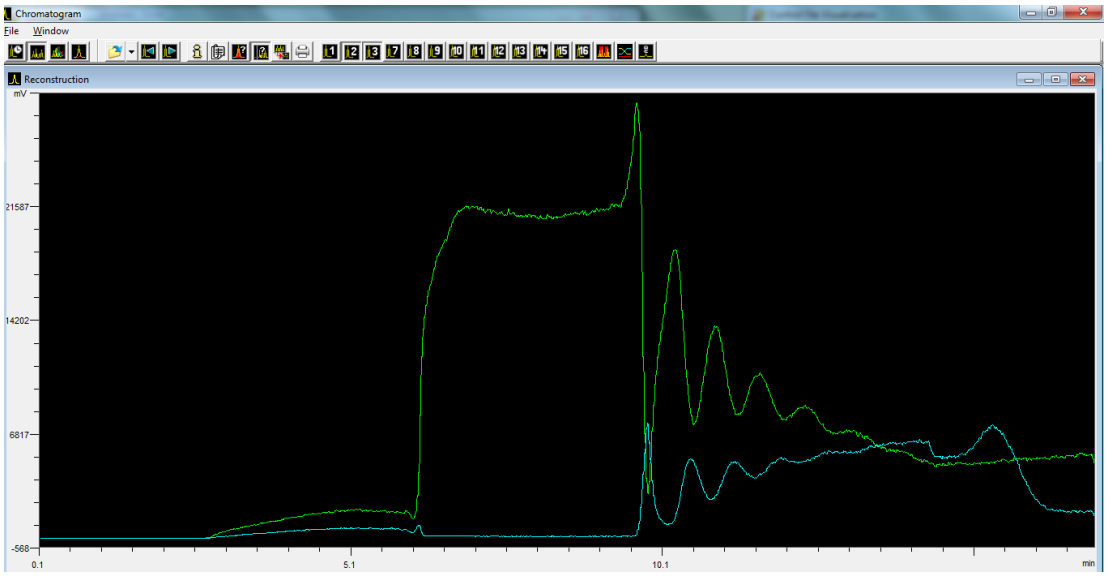

Figure 30. Example of a significant obstruction. Each peak is one round through the recirculation pathway. The conversion yield of $[^{11}C]CH_4$ to $[^{11}C]CH_3I$ is really low due to the limited opportunities for iodination reactions resultant from the extremely slow circulation. Green line: CH_4-trap radiometric detector. Blue line: porapak radiometric detector.

When the obstruction was caused by the natural iodine deposition over time in the entrance of the quartz glass, blockage in this position was fixed by heating up the high temperature oven of the quartz glass to 780°C (800°C is the maximum for the machine, so temperature can be increased to this value, if 780°C proves not to be enough) while setting a He flow of 5000 mV through valve V8 to the exhaust, for a minimum of one hour (again, time duration of this procedure can be changed according to the degree of the obstruction). The execution of this process requires a lot of attention from the operator though, because, considering the high amount of iodine that is blown out due to the high temperature and the long duration of the high flow, the NaOH disposable cartridge will quickly saturate with iodine vapours potentially requiring its change during this process in order to avoid contamination of any of the downstream valves and components. For this reason, the iodine saturation of this cartridge should not exceed two thirds of its height. As iodine is largely consumed in this process, it might be necessary to check and add solid iodine into the reservoir afterwards.

In the case of an overload of iodine in the reservoir, changing the quartz glass tube has shown to be the most effective approach to fix this problem.

During the synthesis of the methylation precursor, we once observed full loss of radioactivity between the CO_2-trap and the CH_4-trap which therefore resulted in a synthesis failure. Between these two components, besides the nickel catalyst column where $[^{11}C]CO_2$ is converted to $[^{11}C]CH_4$, is placed a column filled with NaOH beads whose function consists in retaining water, the other reaction product of the reduction of $[^{11}C]CO_2$ with H_2. As synthesis are done and added up, the ever-increasing retained water causes a gradual hardening of the NaOH beads, leading eventually to a full obstruction of the gas flow. To prevent such problem, we established a flow test that should be performed before each synthesis to ensure that H_2 is flowing with no interference. To do so, we set a H_2 flow to 100 ml/min and we switched valves

V1, V2, V7, V3 and V4 so that it flowed from its supply inlet to the exhaust. According to the flow rate value provided by the software, we can infer if there is any degree of obstruction.

Over time, even if there is no evident obstruction in the NaOH column, the NaOH beads should be changed monthly as a preventive procedure. As NaOH readily absorbs water from the atmospheric air, handling and refilling the previously well dried column with this chemical must be performed quickly, hence minimizing immediate contamination.

2.4 – Activity at EOS and molar activity

During the optimisation of the gas phase process, [^{11}C]β-CITFE synthesis were done through methylations using only acetone as a solvent, since this preparation showed to improve the labelling reaction yield.

[^{11}C]PiB and [^{11}C]β-CITFE activities obtained at EOS were 81.24 ± 29.83 mCi and 90.66 ± 41.47 mCi (see Figure 31). These final activities were largely sufficient to serve for the required patient dose, according to the standard procedures in ICNAS-P. Additionally, these activity values resulted in solutions whose concentrations were suitable and sufficient for mice microdoses.

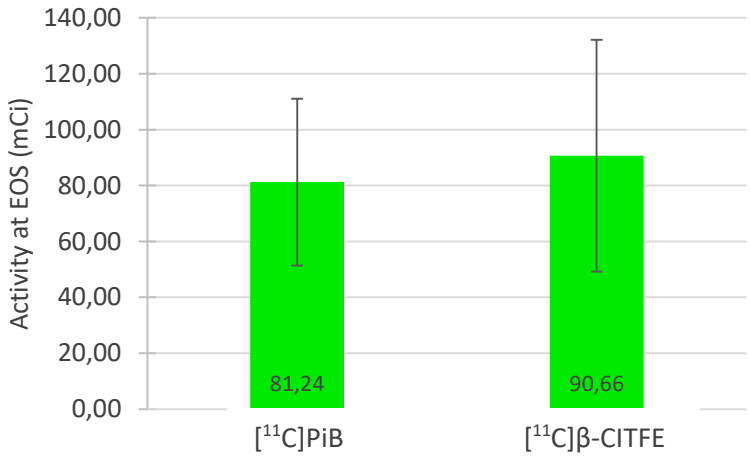

Figure 31. Activities obtained at EOS for [^{11}C]PiB and [^{11}C]β-CITFE, using the gas phase module.

On the other hand, molar activity values obtained for [^{11}C]PiB and [^{11}C]β-CITFE were 128.65 ± 56.73 GBq/µmol and 93.39 ± 48.83 GBq/µmol, respectively (see Figure 32).

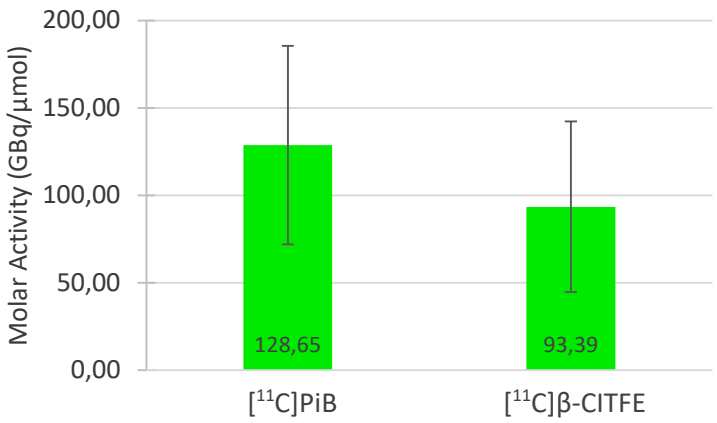

Figure 32. Molar activities obtained for [^{11}C]PiB and [^{11}C]β-CITFE, using the gas phase module.

Daily routine procedures such as the leak test, flow tests and system purge/drying demonstrated to be important practices to maintain high reliability of successive synthesis in terms of high radiochemical yield and high molar activity of the ^{11}C-methylation precursor. Additionally, in-process control and tracking during the continuous use of the synthesiser proved to be crucial to keep the machine working at full potential and avoid synthesis failures and, more than that, to evaluate and decide which and when more exhaustive maintenances should be executed.

Actually, the radiation trapping profile of the [^{11}C]CH_3I in the porapak column is the most relevant indicator of obstructions in the recirculation pathway that can derive either from crystallized iodine in the entrance of the quartz glass or in the NaOH disposable cartridge holder adapter or even in both. As the circulation becomes slower in the loop, the more minimized the [^{11}C]CH_4 iodination will be because the opportunities for repeated reaction with new iodine vapours will be less.

To solve this problem, high temperature in the high temperature oven of the quartz glass tube was applied according to the procedure previously described. Considering that this is a relatively time consuming process, we took this time to simultaneously condition the rest of the system components.

Through the data of 162 consecutive [^{11}C]PiB synthesis and tests, starting from the first [^{11}C]PiB synthesis ever done using the gas phase module in ICNAS-P, we can analyse how the established high temperature and high flow system conditionings have impacted the final activity and molar activity obtained for this radiotracer(see Figure 33). From all these synthesis, several molar activity values could not be calculated due to the impossibility to use the UV light to measure the product concentration.

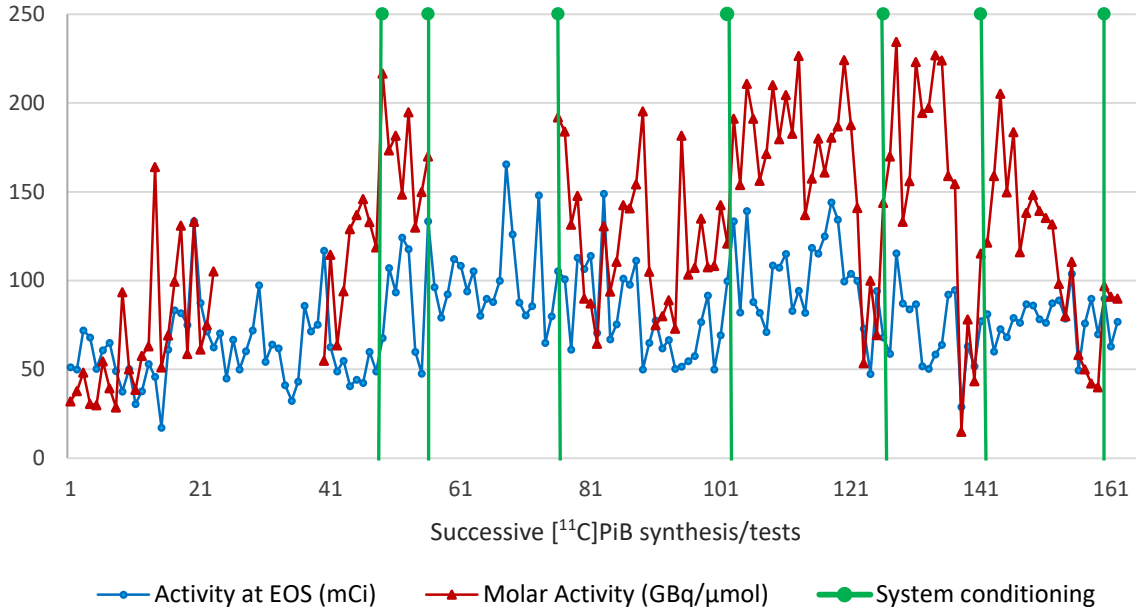

Figure 33. Schematic representation of activity at EOS and molar activity values along 162 consecutive [^{11}C]PiB synthesis/tests and timing of system conditioning during this period.

After the first conditioning, which was motivated by a nearly total obstruction of the recirculation pathway, average values of EOS activities quite improved from then on. Not surprisingly, conversion of [^{11}C]CH_4 to [^{11}C]CH_3I was optimised by the faster circulation and thus higher opportunities for reaction. Consequently, the activity of [^{11}C]CH_3OTf and, therefore, the activity of the final ^{11}C-radiopharmaceutical should be increased. With these conditionings, we were able to obtain very decent activity values within this period of time.

Concerning molar activity, when high temperature and high flow conditionings were performed on the system, we expected an increase in this physical property since these interventions allowed a more effective removal of atmospheric air, and therefore carrier ^{12}C, from the reactive components of the system. In fact, within the data available, all conditionings have had an immediate and impactful effect in the final [^{11}C]PiB molar activity.

As for [^{11}C]PiB and as we expected, [^{11}C]β-CITFE molar activities and activities at EOS also showed an immediate increase after system conditioning.

During the normal use of the module, when the retention of [^{11}C]CH_3I in the Porapak column consistently suggested the presence of obstruction, we removed, as a first approach to the problem, the NaOH disposable cartridge holder adapter to examine if there was any accumulation of crystallized iodine that could explain the slowed down gas circulation. If this accumulation was not verified, high temperature and high flow conditioning of the quartz glass was then done. Over time, if the gas circulation and the conversion of [^{11}C]CH_4 to [^{11}C]CH_3I was carried out within the normal speed rate, we performed the monthly referenced conditioning described in the subsection 2.3 of this section, which hence allowed us to keep the synthesiser working at full potential and in a fairly consistent way. Many times, this shorter and less intensive

conditioning was enough to maintain the gas circulation during the conversion of $[^{11}C]CH_4$ to $[^{11}C]CH_3I$ optimised and thus consistently provide high molar activities and activities at EOB.

Evidently, system opening and consequent exposure to humidity and atmospheric air for a considerable period of time as well as the cleaning of any component (column, valve) also justified its conditioning, according to the part of the system that was intervened. The change of any chemical component also required its conditioning (in this case, it is only necessary to condition the column with the new chemical added).

The high standard deviation observed in the data showed in Figure 33 comes from the fact they were collected successively, meaning that some low molar activity and EOS activity values correspond to occasions that the synthesiser was less functional. Additionally, the synthesis of the ^{11}C-methylation precursor is integrated in a complex sequential chemical and engineering process, i.e., since the radionuclide production in the cyclotron until the synthesis of the final ^{11}C-radiopharmaceutical, there are several particular factors (bombardment, reaction, purification and reformulation of the final product) that can greatly affect its molar activity and activity at EOS if a complication pops up in any of these phases. Additionally, complications during the synthesis usually make this process longer since time will be consumed to identify, evaluate and fix the problem, if possible. Taking into account the short ^{11}C physical half-live, the final activity at EOS and the molar activity will consequently be lower in these cases.

Experience along a comprehensive and constant monitoring of the machine proved to be the best way to detect alterations within the system as early as possible and thus assess when it was beneficial to perform some kind of preventive maintenance. By keeping the system optimised, we were able to deliver higher and more consistent activities at EOS and molar activities for $[^{11}C]$PiB and $[^{11}C]$β-CITFE, reducing the probability of poor quality or even failed synthesis.

Amongst the data of the 162 consecutive $[^{11}C]$PiB productions presented in this word, there were only 2 synthesis failures due to the gas phase module. The first corresponded to a full obstruction of the NaOH column and the other to a nearly total obstruction of the recirculation pathway that yielded insufficient $[^{11}C]CH_3I$ for further $[^{11}C]$PiB synthesis, both situations explained previously. Still, these two failures were crucial in the optimisation of the use of this machine since they enabled us to understand and create the explained preventive routine maintenance in this thesis.

3 – “Wet” Method Versus Gas Phase Synthesis Modules

In this project, we had the amazing opportunity to work with the two routinely applicable automated techniques for producing $[^{11}C]CH_3I$ and $[^{11}C]CH_3OTf$ in the clinical setting: the “wet” chemistry approach and the gas phase approach. This has allowed us to acquire a comprehensive overview concerning the chemical and process engineering aspects of these production systems and their incorporation into the routine of a radiopharmaceutical production company like ICNAS-P.

3.1 – Routine procedures

Considering that MeI Plus™ ("wet" method) and Synthra's (gas phase) modules consist of two completely distinct systems, especially in terms of the chemicals used for $[^{11}C]CH_3I$ synthesis and the mechanical apparatus, it is evident that both modules require different care, maintenance, cleaning, preparation and synthesis procedures.

Since the "wet" chemistry module makes use of very reactive chemicals ($LiAlH_4$, THF and the strong HI) in the liquid phase, keeping the lines, valves, and the reactor cleaned, dried and under inert atmosphere was mandatory to prevent the equipment from deterioration and also to avoid contaminations during the synthesis of the methylation precursor, important factors to maintain the system consistent and reliable while delivering the highest radiochemical yield and molar activity possible.

Therefore, this module required, in the beginning of each day, a full system cleaning and an effective drying afterwards. This process was then proceeded by loading the reagents vial (solution of $LiAlH_4$ and THF previously prepared, and HI) onto the system and a second system cleaning. After this, flow tests were done to verify that all valves were working correctly and that the system was not obstructed between the module and the loop. In summary, this preparation consumed no less than 50 minutes, every day.

Other procedures, such as molecular sieves conditioning (20 minutes ideally) and their cooling to room temperature (15 minutes), were additionally required when preparing the MeI Plus module for a synthesis. After each synthesis, the MeI Plus™ module was programmed to do an automatic system cleaning (7 minutes). This way, 45 minutes would be needed as a recovery time between successive synthesis, in ideal functioning conditions (excluding interventions or additional maintenances). However, as reagents are consumed during synthesis, it might be necessary to refill the vials with more volume, which implied loading the vials onto the system, again, and cleaning it right after.

Finally, after the last synthesis of the day and before switching the machine off, the remaining reagents were unloaded and the system was fully cleaned, requiring an additional 45 minutes.

For producing $[^{11}C]$PiB and $[^{11}C]$β-CITFE, $[^{11}C]CH_3OTf$ is the precursor needed to be synthesised. However, methylation reactions using $[^{11}C]CH_3I$, as it is in the case of other ^{11}C-radiopharmaceuticals produced in ICNAS-P, required the operator to manually change the tubing circuit in the MeI Plus™ module in order to use this compound (direct $[^{11}C]CH_3I$ distillation to the loop) or $[^{11}C]CH_3OTf$ ($[^{11}C]CH_3I$ passes through the AgOTf column, converts to $[^{11}C]CH_3OTf$ and only then is distilled to the loop) as methylation agent. In addition to this, to produce $[^{11}C]CH_3OTf$, before starting the synthesis, the operator must also set the temperature of the AgOtf column to 180°C, otherwise conversion of $[^{11}C]CH_3I$ to $[^{11}C]CH_3OTf$ would not happen as it would remain at room temperature, and reset it to room temperature after the synthesis. It should be noted that if the tubing connected to the AgOTf column had to be opened, this component should not be at high temperature to avoid the retention of water from the atmospheric air.

On the other hand, working with the gas phase synthesiser has revealed itself as a much more user-friendly approach and easier in terms of preparation and use. Regarding the mentioned concerns on the production of $[^{11}C]CH_3OTf$, Synthras's module has two distinct circuits (see Figure 18) and corresponding software programmes depending on whether $[^{11}C]CH_3I$ or $[^{11}C]CH_3OTf$ is supposed to be synthesised and delivered for the methylation reaction. In this case, the operator just needed to select the appropriate programme, minimizing intervention and thus possible human errors, and eliminating exposure of the system to atmospheric air.

The gas phase module did not require any specific preparation for its functioning. All the preparation needed concerns the synthesis itself and included purge of the tubing system, leak test, flow test through the NaOH column and HT-oven heating up to 750°C, which did not take longer than 20 minutes (see Table 4). Sufficient volume of liquid nitrogen must be ensured for the synthesis. As soon as the synthesis programme ended, the module was ready for a new synthesis. Yet, to enable efficient trapping, the porapak column should be at room temperature when starting the new synthesis.

Table 4. Preparation and cleaning times required by MeI Plus™ "wet" method module and Synthra's gas-phase module.

	"Wet" method	Gas phase
Module preparation	50 min	Not needed
Synthesis preparation	35 min	20 min
Time between EOB and $[^{11}C]CH_3I$/$[^{11}C]CH_3OTf$ synthesis and delivery	11 min	14 min
Post-synthesis cleaning	7 min	Not needed
End of the day cleaning	45 min	Not needed

All things considered, the "wet" chemistry module implied intense and time-consuming preparation and cleaning. In the case of a busy production schedule as it is throughout this work, with daily ^{11}C-radiopharmaceuticals requests, these necessary procedures can potentially limit the number of $[^{11}C]CH_3I$ and $[^{11}C]CH_3OTf$ synthesis possible per day. Additionally, the use of aggressive chemicals easily damaged the valves, causing unexpected synthesis failures as they could block or even stop working all of a sudden. Alongside the high human intervention on the preparation and normal functioning of the MeI Plus™ comes a higher risk of mistakes that may affect the final outcome in terms of radiochemical yield and molar activity, and eventually result in synthesis failures. This demanded full attention and care when working with this synthesiser.

Even though Synthra [11C]Choline gas phase module operates by use of several different chemicals and multiple heating components, each requiring precise temperature control, this synthesiser has a great engineering design with easy to use control software.

Considering the two most frequently replaced reagents in the gas phase module, the solid iodine and the NaOH disposable cartridge, at least 10 sequential productions can be performed before replacing any of these reagents. Including its very high reliability and the fast

preparation required for a synthesis run, Synthra [11C]Choline gas phase synthesiser shown to be a suitable system to fit into the demands of ICNAS-P busy routine.

3.2 – Activity at EOS

Although that, according to literature, the "wet" method provides higher radiochemical yields, mainly due to a shorter synthesis time and also to the lower losses of activity plus higher chemical yields since reactions take place in the same reactor (except the conversion of $[^{11}C]CH_3I$ to $[^{11}C]CH_3OTf$, but this conversion rate is almost 100%), comparing the synthesis of $[^{11}C]$PiB and $[^{11}C]$β-CITFE using the "wet" and gas phase approaches in our work, we observe that the gas phase method delivered higher activities at EOS for both radiopharmaceuticals (see Figure 34) [85].

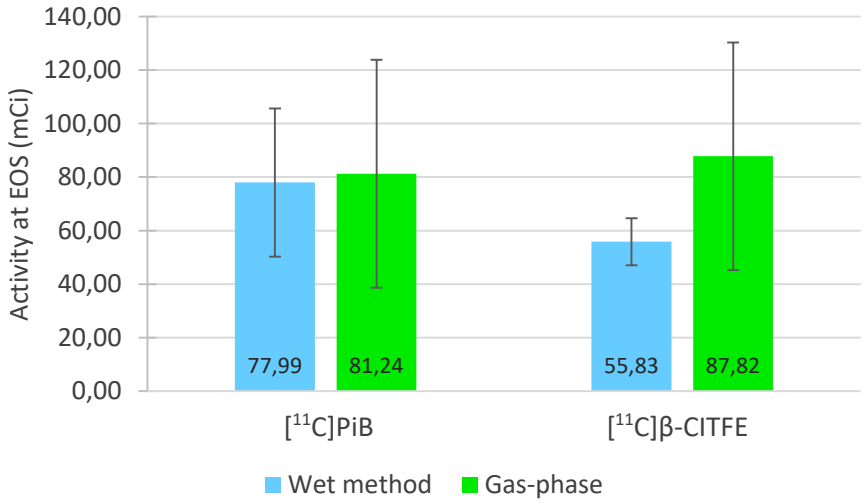

Figure 34. Activities obtained at EOS for $[^{11}C]$PiB and $[^{11}C]$β-CITFE, using the "wet" method module and gas phase module.

We believe that superior engineering and technological apparatus characteristic of gas phase systems can actually justify the higher activities obtained using this system.

3.3 – Molar Activity

Comparing the molar activities obtained using the "wet" and gas phase synthesisers, we found a 3.4 and 5 fold increase in the gas phase production of $[^{11}C]$PiB and $[^{11}C]$β-CITFE, respectively (see Figure 35). This major improvement observed in our work is in accordance with the general consensus within the PET radiochemistry community that the gas phase approach to produce ^{11}C-methylation agents is superior to the classic "wet" method [84].

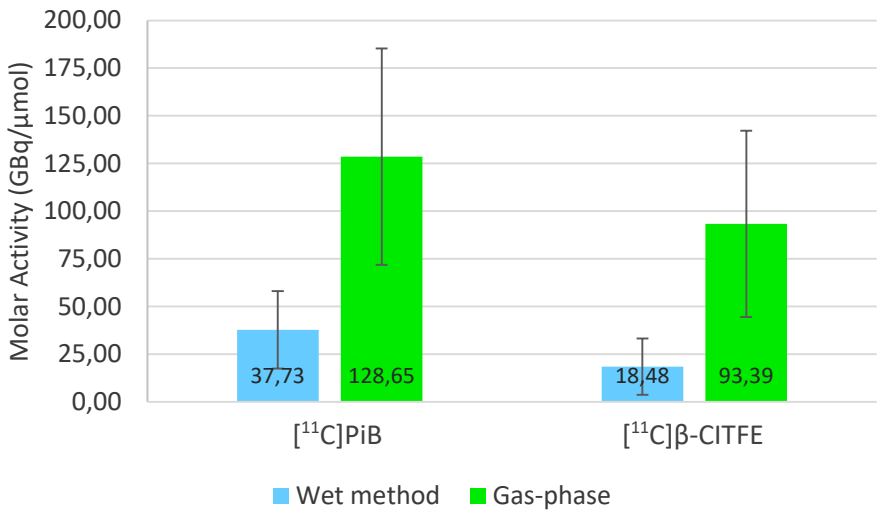

Figure 35. Molar activities obtained at EOS for [^{11}C]PiB and [^{11}C]β-CITFE, using the "wet" method module and gas phase module.

Sources of carrier ^{12}C are extremely dependent on the particular configuration and equipment involved in the production process of each particular site, whereby it is important to analyse and understand the individual contribution of every possible source to the final molar activity in order to get comparable results. As consistently concluded in numerous previous works on this matter, the main contributions to the isotopic dilution of ^{11}C with stable ^{12}C come from the cyclotron target during the actual proton bombardment and from the post-processing of [^{11}C]CO_2 in the synthesis module [85].

Regarding the cyclotron production of ^{11}C, a process already optimised in ICNAS-P, target material, target gas purity and transfer lines were the same either when the "wet" or the gas phase synthesisers were working, whereas total time of bombardment and applied beam current throughout the productions were similar. Thus, any atmospheric CO_2 contamination within the irradiation process or transfer lines would impact in approximately identical extent the molar activity of the produced [^{11}C]CO_2 in both synthesis approaches.

Interestingly though, when two ^{11}C-radiotracer synthesis were done in the same day using the gas phase module, we observed in all cases that molar activity quite increased on the second synthesis. This improvement, which can be attributed to a conditioning effect in the target, has also been seen in experiments reported in the literature, using an aluminium target [33]. This shows how greatly the [^{11}C]CO_2 production process in the cyclotron can affect the molar activity of the final product. As for the "wet" method, this was also observed, however not significantly and only in a few cases, possibly because the major source of contamination happens during the post-processing of [^{11}C]CO_2 in the synthesis module.

Considering the consistency applied in the cyclotron production of ^{11}C throughout this work, the great molar activity improvement seen when the [^{11}C]CH_3OTf production was changed from the "wet" to the gas phase module was actually due to the simpler chemistry approach of the gas phase synthesiser and the avoidance of the use of $LiAlH_4$. This reagent, used in the "wet" method for the reduction of [^{11}C]CO_2, is the primary source of ^{12}C since it can equally absorb CO_2 when exposed to atmospheric air, during the preparation of the $LiAlH_4$/THF solution. Therefore,

radioactive and stable CO_2 coexist during the synthesis process, leading to a drastic decrease of the molar activity of [^{11}C]CH_3OTf and, consequently, of the final ^{11}C-radiotracer. Despite the meticulous care when preparing the $LiAlH_4$/THF solution, molecular sieves conditioning and all the cleaning and drying procedures done in the "wet" method module, presence and incorporation of reasonable high quantities of [^{12}C]CO_2 proved to be inevitable, which was later reflected in the low molar activities obtained for [^{11}C]PiB and [^{11}C]β-CITFE. Additional CO_2 contamination could also be caused by leaks in the system since contamination can come at any step of the synthesis process, before the treatment with hydroid acid.

The difficulties we faced in eliminating the various sources of carrier ^{12}C were shared amongst "wet" chemistry system users during many years. Indeed, the gas phase approach emerged in the past as an alternative method to provide solutions to these problems. The elimination of $LiAlH_4$ in the process represented a successful effort that soon allowed the increase of attainable [^{11}C]CH_3I and [^{11}C]CH_3OTf molar activities, a huge improvement we were able to confirm with our work [84]. However, when ^{11}C was obtained in the form of [^{11}C]CO_2, as it was in our work, this molecule still had to be reduced with a catalyst to produce [^{11}C]CH_4 meaning that we still had to face problems associated to the introduction of carrier ^{12}C into the system. System purge and conditioning of the CO_2-trap and nickel catalyst column have shown to be good procedures to minimize contaminations though and thus provide higher molar activity values of the methylation agent and the final ^{11}C-radiopharmaceutical.

Yet, using the gas phase method, molar activity values could be even higher if we were able to produce [^{11}C]CH_4 in-target. Aside from a simpler and shorter synthesis circuit since the incoming [^{11}C]CH_4 is directly trapped from the cyclotron and ready to be introduced into the recirculation loop for iodination to produce [^{11}C]CH_3I, a 6-17 fold increase of molar activity was reported in the literature in the preparation of some ^{11}C-radiotracers by switching the use of cyclotron produced [^{11}C]CO_2 to [^{11}C]CH_4. By excluding [^{11}C]CO_2 from the whole process, the high concentration of atmospheric CO_2 (365 ppm) no longer represents a source of contamination whereas the influence of environmental CH_4 (1.75 ppm) can be disregarded, resulting consequently in higher molar activity [33].

4 – Synthesis Optimisation of [^{11}C]PiB and [^{11}C]β-CITFE

Apart from the cyclotron, the optimisation of the gas phase module, in which the actual chemical conversion of the primary precursor to the methylation agent takes place, is a must when dealing with the short lived radionuclide ^{11}C. Careful handling and maintenance significantly impact the molar activity of the [^{11}C]CH_3OTf produced, and thus the final ^{11}C-radiopharmaceutical, and extend the lifetime of the module while maintaining both reliability and reproducibility.

However, the production of the methylation agent represents just one part of the necessary procedures to complete a successful synthesis of a ^{11}C-radiopharmaceutical. After this step, radiolabelling reaction can occur in the captive solvent loop. This is followed by HPLC purification in which the radiotracer of interest is separated and collected. Finally, reformulation of the radiotracer is done in a manner suitable for intravenous injection.

Looking at the extension of the sequential and complex processes involved in the synthesis of a ^{11}C-radiopharmaceutical and considering that, after the gas phase module processes, time is the only cause of further decrease in molar activity, we aimed for potential optimisations in order to shorten the time required for these specific processes for [^{11}C]PiB and [^{11}C]β-CITFE and thus increase the molar activity and also the radiochemical yield at EOS. Actually, for ^{11}C, reducing the total synthesis time by just 3 minutes will result in a 10% increase in the radiochemical yield [85]. Beyond time optimisation, we also tested additional simple chemical modifications regarding the preparation of the CITFES precursor and the reformulation process, respectively, in an attempt to increase the radiochemical yield at EOS.

In optimised conditions, using the gas phase approach, full productions of [^{11}C]PiB and [^{11}C]β-CITFE were completed in approximately 28.5 and 29.5 minutes, respectively.

4.1 – Precursor preparation

The solvents and reagents used to dissolve and prepare the precursor may affect the yield of the methylation reaction as different interactions and thus by-products can result from it. As [^{11}C]β-CITFE final activities at EOS were usually really low by the time we started this project, often causing struggles and additional efforts to guarantee sufficient activity for the patient dose (10 mCi), we tested a different preparation compared to the established at that point.

Firstly, the lyophilized CITFES precursor (10 mg) was dissolved in 1 ml of acetone. For a single [^{11}C]β-CITFE synthesis, i.e. for a patient dose, the established preparation of the CITFES precursor consisted in the addition of 10 µl of TBAOH plus 40 µl of acetone to 100 µl (1 mg) of the precursor solution. After stirring in the vortex, 100 µl of this solution was then injected into the captive solvent loop. Considering that CITFES is a carboxylic acid, the addition of the strong base TBAOH will result in the formation of a carboxylic acid salt and water.

To avoid the introduction of water into the reaction environment, and thus the formation of the radiochemical impurity [^{11}C]CH_3OH, we tested the direct utilization and loop injection of 100 µl (1 mg) of the CITFES solution for reaction. The major increase observed in the [^{11}C]β-CITFE activity at EOS is shown and explained in the section 1 of this chapter. Because of this radioactivity yield optimisation and after ensuring the product quality for human injection, we have hereafter adopted this approach regarding the preparation of CITFES precursor for [^{11}C]β-CITFE synthesis in ICNAS-P.

4.2 – Chromatographic purification

Considering the short ^{11}C half-life of 20.4 minutes, the radiotracer synthesis must be performed as quickly as possible. This process can be particularly optimised during the purification of [^{11}C]PiB and [^{11}C]β-CITFE as a shortening in the separation time of the methylation reaction products will increase the radioactivity of the radiotracer available.

Reverse phase chromatography is a technique utilised to separate solute molecules depending on their hydrophobic binding interaction with the mobile phase and the stationary phase of the HPLC column. In this chromatographic technique, the more hydrophobic molecules are more strongly retained in the stationary phase, where they remain longer until they start to partition out to the mobile phase again, leading to an effective separation of the solute molecules. Since the composition of the mobile phase is one of the factors that affect the retention of the solutes between the two phases, adding more ACN (less polar component) to the mobile phase will decrease its polarity and thus the analyte retention time. With this simple modification, the chromatographic run is optimised by shortening the time necessary for this step.

While performing the chromatography, an adequate time difference between each retention time must be ensured so that there is no overlap between distinct reaction products as it can irreversibly affect the radiochemical and/or chemical purity of the final product.

4.2.1 - [^{11}C]PiB purification

For the purification of [^{11}C]PiB, four mobile phases containing 0.1 M AMF aqueous solution/ACN were prepared under different solvent proportions: 60/40, 55/45, 50/50 and 45/55 (V/V) and all chromatographic runs were carried with a flow rate of 9 mL/min. Retention time of the product peak, [^{11}C]PiB chemical and radiochemical purity obtained by testing of each mobile phase are summarized in Table 5.

Table 5. Influence of the mobile phase composition on the retention time of [^{11}C]PiB in the HPLC purification run, on chemical purity and radiochemical purity.

AMF/ACN (V/V)	60/40	55/45	50/50	45/55
Retention time (min)	7.25 ± 0.50	5.72 ± 0.10	3.98 ± 0.28	3.25 ± 0.10
Chemical purity (%)	99.15 ± 0.66	90.94 ± 2.32	85.33 ± 5.90	83.5 ± 7.97
Radiochemical purity (%)	97.49 ± 0.99	95.40 ± 0.46	96.39 ± 1.12	98.45 ± 0.52

According to what was previously explained, as the mobile phases contained more ACN, we confirmed that the retention times of [^{11}C]PiB (and the other reaction products) were shorter, hence allowing a faster purification of the compound of interest and consequently a higher radiochemical yield. However, at the same time, the chemical purity of [^{11}C]PiB was also decreased, compromising the quality of the product.

The distance, and thus retention times, between PiB precursor and [^{11}C]PiB peaks were getting shorter as the mobile phase contained more ACN, leading to an increasing overlap of these two peaks. For this reason, the collection of [^{11}C]PiB happened to contain increasing amount of PiB precursor, as we were able to observe through UV absorption in analytical HPLC. Since PiB precursor is not radioactive, its collection along [^{11}C]PiB did not affect the radiochemical purity.

To comply with the [^{11}C]PiB chemical purity limit of at least 95%, we maintained the 0.1M AMF aqueous solution/ACN (60/40) mobile phase for the reverse phase chromatography.

4.2.2 - [^{11}C]β-CITFE purification

Purification of [^{11}C]β-CITFE was performed using two different mobile phase containing 0.1 M AMF aqueous solution/ACN with the proportions of 45/55 and 40/60, and using an isocratic flow of 8 ml/min.

Table 6. Influence of the mobile phase composition on the retention time of [^{11}C]β-CITFE in the HPLC purification run, on chemical purity and radiochemical purity.

AMF/ACN (V/V)	45/55	40/60
Retention time (min)	6.77 ± 0.45	5.32 ± 0.23
Chemical purity (%)	99.71 ± 0.27	99.67 ± 0.30
Radiochemical purity (%)	98.14 ± 0.66	98.68 ± 0.75

As expected, the retention times of [^{11}C]β-CITFE were shorter when the proportion of ACN was higher. With this optimised mobile phase, we were able to reduce the purification of the product in 1.45 minutes while guaranteeing a proper separation of [^{11}C]β-CITFE and other reaction products. The final product presented high purity and high radiochemical purity, complying with the standards for intravenous administration.

4.3 – Quality control

The final sterile ^{11}C-radiotracer vial was recovered in a lead container and was then transferred to the QC laboratory to assess the compliance with both radiation and pharmaceutical standards not only to ensure intravenous safety but also to evaluate its biological efficiency since the radiopharmaceutical *in vivo* behaviour, and so the success of the PET scan, is dependent on high levels of radionuclidic, radiochemical and chemical purity.

Both [^{11}C]PiB and [^{11}C]β-CITFE final solutions presented themselves as clear, colourless and free of particulate matter, in all of the synthesis done throughout this project. After measurement of the EOS activity in a dose calibrator, a small sample was taken for QC tests. The average pH of the [^{11}C]PiB and [^{11}C]β-CITFE injectable solutions were 5.56 ± 0.72 and 5.78 ± 0.81.

Having the half-life as a characteristic physical property of each radioisotope, radionuclide identity can be assessed using the dose calibrator to measure the half-life of the radionuclide present in the product solution (20.4 minutes for ^{11}C). A deviation from the acceptable limit (19.9 to 20.9 minutes) can indicate the presence of other radioisotopes that can potentially disturb the image quality beyond the unnecessary irradiation to the patient. However, all [^{11}C]PiB and [^{11}C]β-CITFE synthesis showed a half-life of 20.34 ± 0.21 minutes.

The concentration of residual solvents present in [^{11}C]PiB and [^{11}C]β-CITFE injectable solution was quantified by gas chromatography. Since these solutions are formulated with 10% ethanol and ACN is one of the solvents of the HPLC mobile phase, these impurities were inevitably present in the injectable solution. In [^{11}C]PiB solution, ethanol and ACN concentrations were of 798.25 ± 265.33 mg/10 ml and 1.02 ± 0.41 mg/ 10 ml. With regard to [^{11}C]β-CITFE, ethanol and ACN concentrations were of 876.14 ± 146.85 mg/10 ml and 1.22 ± 0.53 mg/10 ml.

Radiochemical purity is defined as the percentage of the radioactive isotope that is presented in the desired chemical form and is quantified in the analytical HPLC using a radiometric detector. For [^{11}C]PiB and [^{11}C]β-CITFE, this property must be higher than 95%, which means that at least 95% of ^{11}C radionuclide must be attached to these molecules. In the diagnostic field, biodistribution of radioactive impurities can obscure the region of interest and thus interfere with the interpretation of the PET image and moreover cause undesirable pharmacologic effects[86]. With the established optimised conditions for the synthesis of [^{11}C]PiB and [^{11}C]β-CITFE, as well as in other tests done for this work, radiochemical purity was always above the 95% limit (see Table 5 and 6, and Figure 36 and 37).

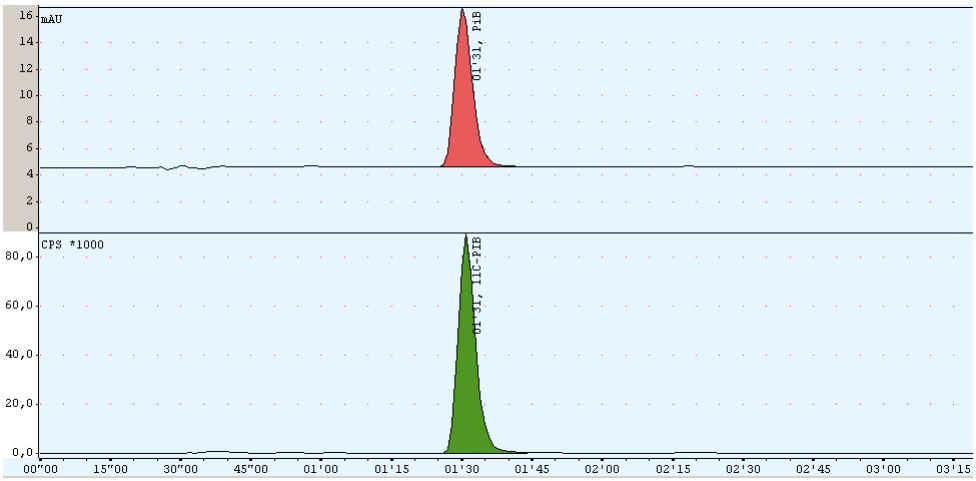

Figure 36. Analytical HPLC of [^{11}C]PiB. The red peak corresponds to the UV absorbance of [^{11}C]PiB while the green peak corresponds the activity of [^{11}C]PiB.

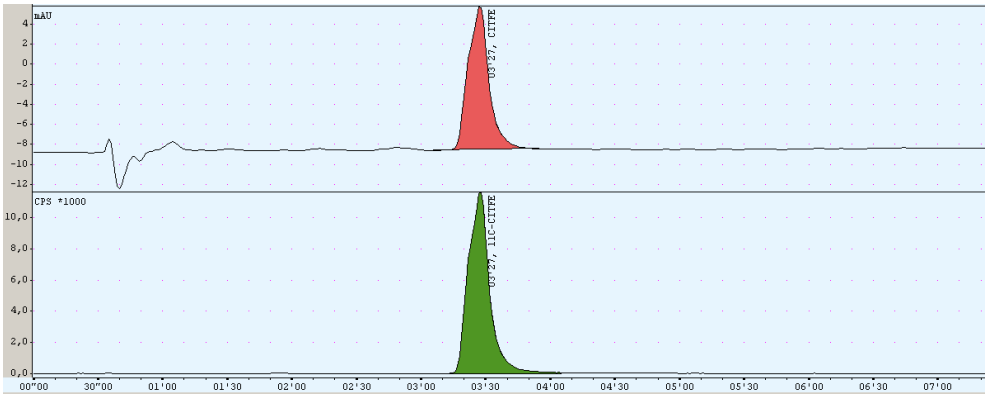

Figure 37. Analytical HPLC of [^{11}C]β-CITFE. The red peak corresponds to the UV absorbance of [^{11}C]PiB while the green peak corresponds the activity of [^{11}C]β-CITFE.

On the other hand, chemical purity is referred to the proportion of the product that is in the specified chemical form and is measured by UV absorbance in the analytical HPLC (see Figure 36 and 37). It should be typically above 95%, a limit inferred from data from literature. At the same time, this analysis also allows the identification and quantification of other individual chemical impurities in the radiopharmaceutical solution. Generally, these impurities are only problematic if they are toxic to the patient, if they cause undesired biochemical interactions or modify the physiological process under study.

All [^{11}C]PiB and [^{11}C]β-CITFE final solutions revealed a level of radiochemical purity above 95.02% and 97.03%, respectively, complying with the standard limit. However, during this work, we have tested different HPLC mobile phases that, despite not affecting the radiochemical purity, significantly did affect [^{11}C]PiB chemical purity. The larger collection of PiB precursor, as the ACN content increased in mobile phase, was noted in the analytic HPLC as the proportion of this impurity consistently increased, failing the proposed QC standard for chemical purity. All synthesis regarding [^{11}C]β-CITFE synthesis provided chemical purity higher than 95% as well as all [^{11}C]PiB synthesis done with the 0.1 M AMF aqueous solution/ACN (60/40) mobile phase, in the reverse phase purification.

Taking into consideration the activity of the radiotracer at EOS, the total volume of the solution, and the molar mass of the compound, molar activity was measured using equation (2) and by integration the area of the product UV mass peak that was fitted to a standard calibration curve previously generated through different concentrations of cold PiB and CITFES precursors.

$$Molar\ activity\ (GBq/\mu mol) = \frac{\frac{A\ (GBq)}{V\ (ml)}}{C\ \left(\frac{ng}{ml}\right)} x\ M\ (ng/\mu mol) \quad (2)$$

Posterior to the administration of [^{11}C]PiB and [^{11}C]β-CITFE, bacterial endotoxins content in the radiotracer solution was analysed using the LAL test. All samples demonstrated a concentration less than 17.5 EU/ml, complying with the quality standards.

In conclusion, the whole process from the release of [^{11}C]CO_2 by the cyclotron until radiopharmaceutical administration, including QC, is performed in 40-45 minutes. It should be noted that even if there is a lot of activity available in the EOS and after QC, the administration of the radiopharmaceutical should not be delayed much longer, as it will happen at the expense of the loss of molar activity.

Chapter IV – Conclusion

The development of PET and its use as a powerful diagnostic technique in nuclear medicine is largely dependent on radiochemistry and synthesis technology achievements. ^{11}C is the most convenient PET radionuclide for labelling of biologically active compounds since radioactive ^{11}C-molecules are indistinguishable from their stable form in metabolic processes, and also due to its short half-life of 20.4 minutes, providing the advantage to perform repeated scans, each associated with favourable dosimetry [87]. The introduction of [^{11}C]CH_3I is taken as a milestone in the history of ^{11}C-tracers development. With this, reactions and radiochemistry techniques alongside automated engineering solutions for the synthesis of these precursors became an area of intense research and development to deliver reliable and reproducible synthesis methodologies to ultimately provide high activity and high molar activity ^{11}C-radiopharmaceuticals.

^{11}C-synthesis modules should comply with a set of specific properties in order to fulfil the demands of an active production routine as it is in a radiopharmaceutical company like ICNAS-P. Consequently, the most suitable synthesisers must allow the possibility of automation of all processes, the reproducibility of robust processes and reliability of the machine, high radiochemical yield and high molar activity methylation precursors, the production of multiple synthesis per day, reduced preparation and maintenance efforts [85].

The radiosynthesis process of [^{11}C]PiB and [^{11}C]β-CITFE, using the MeI Plus™ "wet" method module, which was operated until 2017 in ICNAS-P, provided molar activity values of 37.73 ± 20.29 GBq/µmol and 18.48 ± 14.75 GBq/µmol, respectively. Low molar activities obtained along with extensive time-consuming cleaning and preparation procedures required by this module shown to be major drawbacks of this system.

In the meantime, the Synthra [11C]Choline gas phase module in ICNAS-P brought greatly enhanced molar activity values for [^{11}C]PiB and [^{11}C]β-CITFE radiotracers: 128.65 ± 56.73 GBq/µmol and 93.39 ± 48.83 GBq/µmol, respectively. However, the mere purchase and use of a commercial gas phase system will not assure maximum molar activities by itself. We experienced and detected potential problems with this methodology which might contribute to inconsistent yields and occasional synthesis failure. Therefore, we agree that constant monitoring and routine system maintenance are key procedures to maintain a highly reliable machine, working at full potential, able to deliver high activity and high molar activity methylation precursors.

Generally known within the radiochemical community and confirmed with this work, the superiority of this methodology in terms of chemistry and engineering makes the gas phase the method of choice when radiotracers with high molar activity are required, particularly in brain PET studies where receptor ligands are present in limited quantities. These aspects were

confirmed *in vivo* by human clinical PET studies where healthy individuals were confronted with patients whose history and/or symptomatology refers to suspected AD ([^{11}C]PiB PET scan), and PD ([^{11}C]β-CITFE PET scan). Using [^{11}C]PiB for the diagnosis of AD, it was observed an increased uptake in the characteristic regions of this dementia (temporal, parietal and frontal cortex) and very low uptake in control cases (see Figure 38). In PET scans for the diagnosis of PD using [^{11}C]β-CITFE, normal uptake in the basal ganglia was observed in healthy individuals opposed to the decreased uptake detected in these regions in PD patients (see Figure 39).

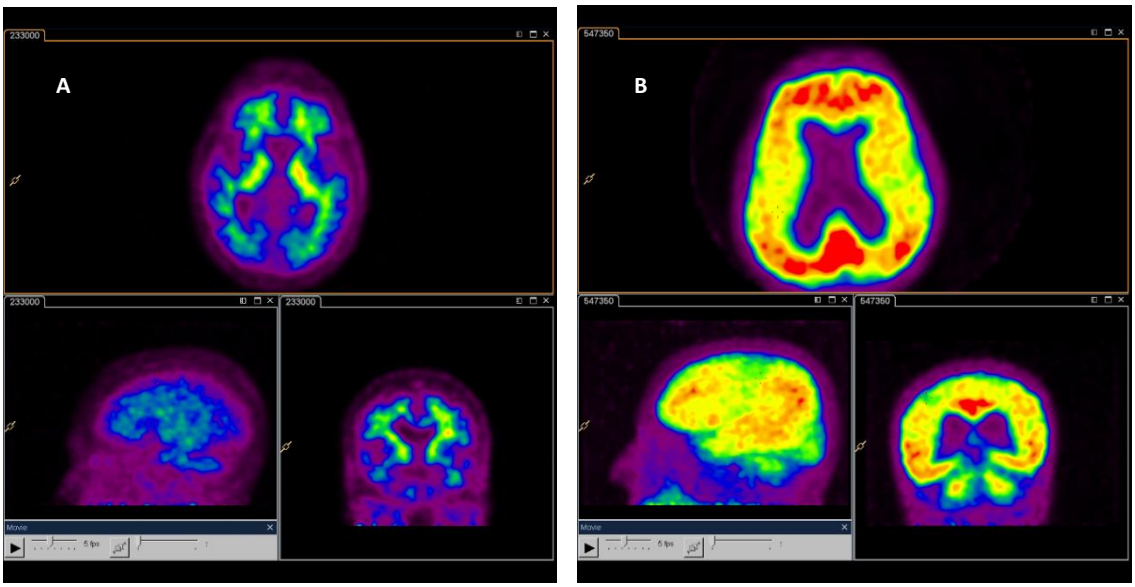

Figure 38. [^{11}C]PiB Aβ binding to the brain of a healthy control (A) and an AD patient (B). PET images of (A) show normal, white matter uptake while (B) shows high frontal, temporal and parietal cortex uptake resulting from extensive Aβ accumulation. Red indicates high, green medium and blue low [^{11}C]PiB retention. Images courtesy of ICNAS.

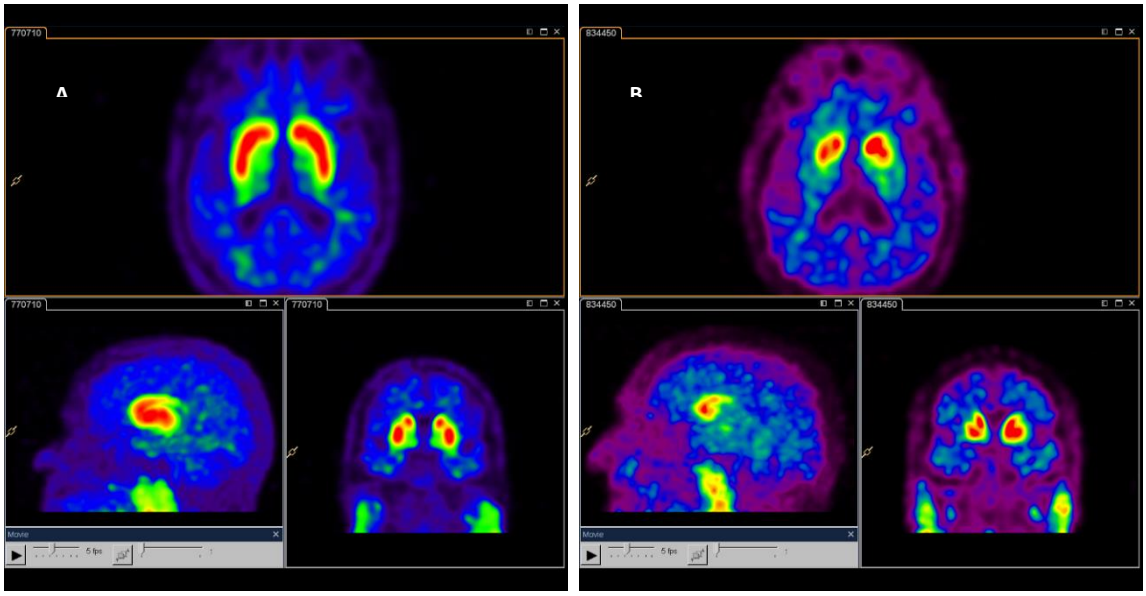

Figure 39. [^{11}C]β-CITFE DAT binding to the brain of a healthy control (A) and a PD patient (B). PET images of (A) show high basal ganglia uptake reflecting normal dopaminergic integrity. (B) shows decreased basal ganglia uptake due to the dopaminergic neuronal loss. Red indicates high, green medium and blue low [^{11}C]β-CITFE retention. Images courtesy of ICNAS.

In this context, this project is pertinent as it assists with actually relevant radiopharmaceuticals that meet the need of preclinical and clinical molecular imaging in ICNAS. Besides this fact, and bearing in mind that ICNAS is the only facility in Portugal that produces [^{11}C]PiB and [^{11}C]β-CITFE, this work is expected to make an impact on the diagnosis and clinical management of AD and PD in our country and provide an important tool for basic and clinical research and development in this area.

The ultimate application of this work, i.e., the delivery of high quality [^{11}C]PiB and [^{11}C]β-CITFE, state-of-the-art radiopharmaceuticals for the diagnosis of AD and PD, respectively, is particularly valuable and impactful in the management of these NDs in Portugal, since ICNAS-P, together with ICNAS, is the only facility in the whole country that has the full equipment necessary for the synthesis of ^{11}C-radiopharmaceuticals. With the availability of these radiotracers, which thus provide physicians the confidence for decision making at an early stage of the development of these ND and enables informed clinical diagnosis and clinical management, individual patients will be tremendously benefited as well as the healthcare system in general.

Chapter V – Future Perspectives

Being the gas phase module the first part of a sequential process intended for the synthesis of several ^{11}C-tracers, besides [^{11}C]PiB and [^{11}C]β-CITFE, the performed optimisations are also applicable for the preparation of other ^{11}C-radiopharmaceuticals produced in ICNAS-P for clinical and preclinical studies, such as [^{11}C]Flumazenil, [^{11}C]PK11195, [^{11}C]Methionine and [^{11}C]Raclopride, and may assist for new ^{11}C-based radiotracers in the future.

With the aim of improve the molar activity of ^{11}C-radiopharmaceuticals, there is the interesting challenge of synthesising [^{11}C]CH_3I and [^{11}C]CH_3OTf methylation precursors from the in-target production of [^{11}C]CH_4. The exclusion of [^{11}C]CO_2 from the process excludes in its turn the contamination problem of atmospheric CO_2 on gases, target chambers and other sources, hence leading to higher molar activity. This possibility has prompted modern gas phase modules to allow system modifications so that users can adapt the machine according to their preference/logistic possibilities.

Another exciting possibility resulting from the high radiochemical yields obtained at EOS for both [^{11}C]PiB and [^{11}C]β-CITFE, sufficient for two patient doses, lies in the performance of two simultaneous PET scans, using two suitable PET scanners, using a single production. Besides the saving costs for the company, and evident double income, more PET requests can be answered in a shorter period of time.

References

[1] L. Zhu, K. Ploessl, and H. F. Kung, “PET/SPECT imaging agents for neurodegenerative diseases,” *Chem Soc Rev.*, vol. 43, no. 19, pp. 6683–6691, 2015.

[2] Y.-S. Lee, “Radiopharmaceuticals for Molecular Imaging,” *Open Nucl. Med. J.*, vol. 2, no. 1, pp. 178–185, 2014.

[3] F. C. Wong and E. E. Kim, “A review of molecular imaging studies reaching the clinical stage,” *Eur. J. Radiol.*, vol. 70, no. 2, pp. 205–211, 2009.

[4] I. G. Surgery *et al.*, *Application of Plasma to Humans (Blood Coagulation and Regenerative Medicine)*. 2019.

[5] P. Price, “PET as a potential tool for imaging molecular mechanisms of oncology in man,” *Trends Mol. Med.*, vol. 7, no. 10, pp. 442–446, 2001.

[6] P. W. Miller, N. J. Long, R. Vilar, and A. D. Gee, “Synthesis of 11C, 18F, 15O, and 13N radiolabels for positron emission tomography,” *Angew. Chemie - Int. Ed.*, vol. 47, no. 47, pp. 8998–9033, 2008.

[7] D. J. Schlyer, “PET tracers and radiochemistry,” *Ann. Acad. Med. Singapore*, vol. 33, no. 2, pp. 146–154, 2004.

[8] G. B. Saha, *Fundamentals of Nuclear Pharmacy, Fifth Edition*. 2003.

[9] J. Kurth, M. Sakretz, S. Teipel, and B. Joachim Krause, “Molecular imaging of dementia,” *Geriatr. Ment. Heal. Care*, vol. 1, no. 3, pp. 56–62, 2013.

[10] V. H. Alves, A. J. Abrunhosa, and M. Castelo-Branco, “Optimisation of synthesis, purification and reformulation of (R)-[N-Methyl-11C]PK11195 for in vivo PET imaging studies,” *3rd Port. Bioeng. Meet. ENBENG 2013 - B. Proc.*, 2013.

[11] N. Gupta, P. M. Price, and E. O. Aboagye, “PET for in vivo pharmacokinetic and pharmacodynamic measurements,” *Eur. J. Cancer*, vol. 38, no. 16, pp. 2094–2107, 2002.

[12] D. W. Townsend, “Combined PET/CT: the historical perspective,” *Semin. Ultrasound. CT. MR*, vol. 29, no. 4, pp. 232–5, 2008.

[13] International Atomic Energy Agency, “Cyclotron Produced Radionuclides: Principles and Practice,” *October*, no. 465, p. 230, 2009.

[14] EANM, “The Radiopharmacy A Technologist’s Guide,” pp. 22–23, 2016.

[15] W. Wadsak and M. Mitterhauser, “Basics and principles of radiopharmaceuticals for PET/CT,” *Eur. J. Radiol.*, vol. 73, no. 3, pp. 461–469, 2010.

[16] V. Gómez-Vallejo, “Development of New Strategies for the Synthesis of Radiotracers Labeled with Short-Lived Isotopes: Application to 11C and 13N.,” p. 81, 2010.

[17] M. J. Welch and C. S. Redvanly, *Handbook of Radiopharmaceuticals: Radiochemistry and*

Applications. Wiley, 2003.

[18] H. H. Coenen *et al.*, "Consensus nomenclature rules for radiopharmaceutical chemistry — Setting the record straight," *Nucl. Med. Biol.*, vol. 55, pp. v–xi, 2017.

[19] International Atomic Energy Agency, "Operational guidance on hospital radiopharmacy: a safe and effective approach," 2008.

[20] S. M. Shaw and R. D. Ice, "Nuclear pharmacy, part I: Emergence of the specialty of nuclear pharmacy," *J. Nucl. Med. Technol.*, vol. 28, no. 1, pp. 8–11, 2000.

[21] S. Guhlke, A. M. Verbruggen, and S. Vallabhajosula, "Radiochemistry and radiopharmacy," *Clin. Nucl. Med.*, pp. 34–76, 2007.

[22] M. Szlosek-Pinaud, M. Allard, E. Fouquet, and D. James, "State of Art in 11C Labelled Radiotracers Synthesis," *Curr. Med. Chem.*, vol. 15, no. 3, pp. 235–277, 2008.

[23] G. Antoni, "Development of carbon-11 labelled PET tracers - Radiochemical and technological challenges in a historic perspective," *J. Label. Compd. Radiopharm.*, vol. 58, no. 3, pp. 65–72, 2015.

[24] N. A. Gomzina, O. F. Kuznetsova, and D. D. Vaulina, "Methylation as a method for synthesis of radiopharmaceuticals for positron emission tomography," *Russ. Chem. Bull.*, vol. 64, no. 7, pp. 1536–1546, 2015.

[25] K. Serdons, A. Verbruggen, and G. M. Bormans, "Developing new molecular imaging probes for PET," *Methods*, vol. 48, no. 2, pp. 104–111, 2009.

[26] P. J. H. Scott, "Methods for the incorporation of carbon-11 to generate radiopharmaceuticals for PET imaging," *Angew. Chemie - Int. Ed.*, vol. 48, no. 33, pp. 6001–6004, 2009.

[27] A. P. Wolf and C. S. Redvanly, "Carbon-ll and Radiopharmaceuticals *," vol. 28, no. May 1976, pp. 29–48, 1977.

[28] F. Wuest, M. Berndt, and T. Kniess, "Carbon-11 labeling chemistry based upon [11C]methyl iodide.," *Ernst Schering Res. Found. Workshop*, no. 62, pp. 183–213, 2007.

[29] V. Gómez-Vallejo and J. Llop, "Specific activity of [11C]CH3I synthesized by the 'wet' method: Main sources of non-radioactive carbon," *Appl. Radiat. Isot.*, vol. 67, no. 1, pp. 111–114, 2009.

[30] D. M. Jewett, "A simple synthesis of [11C]methyl triflate," *Int. J. Radiat. Appl. Instrumentation. Part*, vol. 43, no. 11, pp. 1383–1385, 1992.

[31] A. A. Wilson, A. Garcia, L. Jin, and S. Houle, "Radiotracer synthesis from [11C]-iodomethane: A remarkably simple captive solvent method," *Nucl. Med. Biol.*, vol. 27, no. 6, pp. 529–532, 2000.

[32] A. A. Wilson, A. Garcia, S. Houle, and N. Vasdev, "Utility of commercial radiosynthetic modules in captive solvent [11C]-methylation reactions," *J. Label. Compd. Radiopharm.*, vol. 52, no. 11, pp. 490–492, 2009.

[33] V. Gmez-Vallejo, V. Gaja, J. Koziorowski, and J. Llop, "Specific Activity of 11C-Labelled Radiotracers: A Big Challenge for PET Chemists," *Positron Emiss. Tomogr. - Curr. Clin. Res. Asp.*, 2012.

[34] C. Kuntner and D. Stout, "Quantitative preclinical PET imaging: Opportunities and challenges," *Front. Phys.*, vol. 2, no. February, pp. 1–12, 2014.

[35] M. R. Zhang and K. Suzuki, “Sources of carbon which decrease the specific activity of [11C]CH 3I synthesized by the single pass I 2 method,” *Appl. Radiat. Isot.*, vol. 62, no. 3, pp. 447–450, 2005.

[36] D. A. Wolk and W. E. Klunk, “Update on amyloid imaging: From healthy aging to Alzheimer’s disease,” *Curr. Neurol. Neurosci. Rep.*, vol. 9, no. 5, pp. 345–352, 2009.

[37] R. K. J. Brown, N. I. Bohnen, K. K. Wong, S. Minoshima, and K. A. Frey, “Brain PET in suspected dementia: Patterns of altered FDG metabolism,” *Radiographics*, vol. 34, no. 3, pp. 684–701, 2014.

[38] M. Benadiba, G. Luurtsema, L. Wichert-Ana, C. A. Buchpigel, and G. B. Filho, “New molecular targets for PET and SPECT imaging in neurodegenerative diseases,” *Rev. Bras. Psiquiatr.*, vol. 34, no. SUPPL2, pp. 125–148, 2012.

[39] O. Isacson, H. Seo, L. Lin, D. Albeck, and A. C. Granholm, “Alzheimer’s disease and Down’s syndrome: Roles of APP, trophic factors and ACh,” *Trends in Neurosciences*. 2002.

[40] S. Vallabhajosula, “Positron emission tomography radiopharmaceuticals for imaging brain beta-amyloid,” *Semin. Nucl. Med.*, vol. 41, no. 4, pp. 283–299, 2011.

[41] Alzheimer’s Disease International, “World Alzheimer Report 2019: Attitudes to dementia.,” 2019.

[42] I. Santana, F. Farinha, S. Freitas, V. Rodrigues, and Á. Carvalho, “Epidemiologia da demência e da doença de Alzheimer em Portugal: Estimativas da prevalência e dos encargos financeiros com a medicação,” *Acta Med. Port.*, vol. 28, no. 2, pp. 182–188, 2015.

[43] M. Strassnig and M. Ganguli, “About a peculiar disease of the cerebral cortex: Alzheimer’s original case revisited.,” *Psychiatry (Edgmont).*, vol. 2, no. 9, pp. 30–3, 2005.

[44] D. Perl, “Neuropathology of Alzheimer’s Disease,” *Mt. Sinai Jounal Med.*, vol. 77, no. 1, pp. 32–42, 2010.

[45] V. L. Villemagne, “Amyloid imaging: Past, present and future perspectives,” *Ageing Res. Rev.*, vol. 30, pp. 95–106, 2016.

[46] V. L. Villemagne *et al.*, “Aβ-amyloid and Tau Imaging in Dementia,” *Semin. Nucl. Med.*, vol. 47, no. 1, pp. 75–88, 2017.

[47] D. J. Selkoe and J. Hardy, “The amyloid hypothesis of Alzheimer’s disease at 25 years,” *EMBO Mol. Med.*, vol. 8, no. 6, pp. 595–608, 2016.

[48] J. Hardy and D. Selkoe, “The amyloid hypothesis of Alzheimer’s disease: progress and problems on the road to therapeutics,” *Science (80-.).*, vol. 297, no. 5580, pp. 353–356, 2002.

[49] A. Leuzy *et al.*, “Tau PET imaging in neurodegenerative tauopathies—still a challenge,” *Mol. Psychiatry*, vol. 24, no. 8, pp. 1112–1134, 2019.

[50] S. S. Yoon and S. A. Jo, “Mechanisms of amyloid-β peptide clearance: Potential therapeutic targets for Alzheimer’s disease,” *Biomol. Ther.*, vol. 20, no. 3, pp. 245–255, 2012.

[51] A. Serrano-Pozo, M. P. Frosch, E. Masliah, and B. T. Hyman, “Neuropathological alterations in Alzheimer disease,” *Cold Spring Harb. Perspect. Med.*, vol. 1, no. 1, pp. 1–23, 2011.

[52] A. G. Vlassenko, T. L. S. Benzinger, and J. C. Morris, “PET amyloid-beta imaging in preclinical Alzheimer’s disease,” *Biochim. Biophys. Acta - Mol. Basis Dis.*, vol. 1822, no. 3, pp. 370–379, 2012.

[53] C. A. Mathis, B. J. Lopresti, and W. E. Klunk, “Impact of amyloid imaging on drug development in Alzheimer’s disease,” *Nucl. Med. Biol.*, vol. 34, no. 7, pp. 809–822, 2007.

[54] E. Braak, K. Griffing, K. Arai, J. Bohl, H. Bratzke, and H. Braak, “Neuropathology of Alzheimer’s disease: What is new since A. Alzheimer?,” *Eur. Arch. Psychiatry Clin. Neurosci.*, vol. 249, no. SUPPL. 3, pp. 14–22, 1999.

[55] C. Ballard, S. Gauthier, A. Corbett, C. Brayne, D. Aarsland, and E. Jones, “Alzheimer’s disease,” *Lancet*, vol. 377, no. 9770, pp. 1019–1031, 2011.

[56] A. T. Rao, A. J. Degnan, and L. M. Levy, “Genetics of Alzheimer disease,” *Am. J. Neuroradiol.*, vol. 35, no. 3, pp. 457–458, 2014.

[57] R. W. Mahley, K. H. Weisgraber, and Y. Huang, “Apolipoprotein E4: a causative factor and therapeutic target in neuropathology, including Alzheimer’s disease,” *Proc. Natl. Acad. Sci. U. S. A.*, vol. 103, no. 15, pp. 5644–5651, 2006.

[58] Y. F. Shea, L. W. Chu, A. O. K. Chan, J. Ha, Y. Li, and Y. Q. Song, “A systematic review of familial Alzheimer’s disease: Differences in presentation of clinical features among three mutated genes and potential ethnic differences,” *J. Formos. Med. Assoc.*, vol. 115, no. 2, pp. 67–75, 2016.

[59] L. C. de Souza, M. Sarazin, A. L. Teixeira-Junior, P. Caramelli, A. E. dos Santos, and B. Dubois, “Biomarcadores da doença de Alzheimer,” *Arq. Neuropsiquiatr.*, vol. 72, no. 3, pp. 227–231, 2014.

[60] P. Buchhave *et al.*, “Longitudinal study of CSF biomarkers in patients with Alzheimer’s disease,” *PLoS One*, vol. 4, no. 7, pp. 2–6, 2009.

[61] W. Jagust, “Positron emission tomography and magnetic resonance imaging in the diagnosis and prediction of dementia,” *Alzheimer’s Dement.*, vol. 2, no. 1, pp. 36–42, 2006.

[62] C. Marcus, E. Mena, and R. M. Subramaniam, “Brain PET in the diagnosis of Alzheimer’s disease,” *Clin. Nucl. Med.*, vol. 39, no. 10, pp. e413–e426, 2014.

[63] C. R. Jack *et al.*, “Serial PIB and MRI in normal, mild cognitive impairment and Alzheimers disease: Implications for sequence of pathological events in Alzheimers disease,” *Brain*, vol. 132, no. 5, pp. 1355–1365, 2009.

[64] H. Engler *et al.*, “Two-year follow-up of amyloid deposition in patients with Alzheimer’s disease,” *Brain*, vol. 129, no. 11, pp. 2856–2866, 2006.

[65] W. E. Klunk *et al.*, “The binding of 2-(4’-methylaminophenyl)benzothiazole to postmortem brain homogenates is dominated by the amyloid component,” *J. Neurosci.*, vol. 23, no. 6, pp. 2086–2092, 2003.

[66] W. E. Klunk *et al.*, “Imaging Brain Amyloid in Alzheimer’s Disease with Pittsburgh Compound-B,” *Ann. Neurol.*, vol. 55, no. 3, pp. 306–319, 2004.

[67] R. Laforce and G. D. Rabinovici, “Amyloid imaging in the differential diagnosis of dementia: Review and potential clinical applications,” *Alzheimer’s Res. Ther.*, vol. 3, no. 6, 2011.

[68] E. Ray Dorsey *et al.*, “Global, regional, and national burden of Parkinson’s disease, 1990–2016: a systematic analysis for the Global Burden of Disease Study 2016,” *Lancet Neurol.*, vol. 17, no. 11, pp. 939–953, 2018.

[69] S. Caproni and C. Colosimo, “Diagnosis and Differential Diagnosis of Parkinson Disease,” *Clin. Geriatr. Med.*, vol. 36, no. 1, pp. 13–24, 2020.

[70] H. Nyström, *Parkinson’s disease: the prodromal phase and consequences with respect to working life*. 2016.

[71] R. B. Postuma *et al.*, “MDS clinical diagnostic criteria for Parkinson’s disease,” *Mov. Disord.*, vol. 30, no. 12, pp. 1591–1601, 2015.

[72] A. M. Bonnet and J. L. Houeto, “Pathophysiology of Parkinson’s disease,” *Biomed. Pharmacother.*, vol. 53, no. 3, pp. 117–121, 1999.

[73] K. Marek and D. Jennings, “Can we image premotor Parkinson disease?,” *Neurology*, vol. 72, no. 7 SUPPL. 2, 2009.

[74] K. R. Chaudhuri and N. Titova, “Societal Burden and Persisting Unmet Needs of Parkinson’s Disease,” *Eur. Neurol. Rev.*, vol. 14, no. 1, p. 28, 2019.

[75] J. M. Ellis and M. J. Fell, “Current approaches to the treatment of Parkinson’s Disease,” *Bioorganic Med. Chem. Lett.*, vol. 27, no. 18, pp. 4247–4255, 2017.

[76] D. J. Brooks, “Molecular imaging of dopamine transporters,” *Ageing Res. Rev.*, vol. 30, pp. 114–121, 2016.

[77] G. Pagano, F. Niccolini, and M. Politis, “Imaging in Parkinson’s disease,” *Clin. Med. J. R. Coll. Physicians London*, vol. 16, no. 4, pp. 371–375, 2016.

[78] D. R. Williams and I. Litvan, “Parkinsonian syndromes,” *Contin. Lifelong Learn. Neurol.*, vol. 19, no. 5, pp. 1189–1212, 2013.

[79] L. Farde, N. Ginovart, C. Halldin, Y. H. Chou, H. Olsson, and C. G. Swahn, “A PET study of [11C]β-CIT-FE binding to the dopamine transporter in the monkey and human brain,” *Int. J. Neuropsychopharmacol.*, vol. 3, no. 3, pp. 203–214, 2000.

[80] S. Chalon *et al.*, “The story of the dopamine transporter PET tracer [18F]LBT-999: From conception to clinical use,” *Front. Med.*, vol. 6, no. APR, pp. 1–5, 2019.

[81] J. T. Kuikka *et al.*, “Iodine-123 labelled N-(2-fluoroethyl)-2β-carbomethoxy-3β-(4-iodophenyl)nortropane for dopamine transporter imaging in the living human brain,” *Eur. J. Nucl. Med.*, vol. 22, no. 7, pp. 682–686, 1995.

[82] Z. Y. Liu, F. T. Liu, C. T. Zuo, J. B. Koprich, and J. Wang, “Update on Molecular Imaging in Parkinson’s Disease,” *Neurosci. Bull.*, vol. 34, no. 2, pp. 330–340, 2018.

[83] G. S. Clemente, “Synthesis optimization of [11C]pittsburgh compound b by the captive solvent method,” Instituto Politécnico de Lisboa, 2013.

[84] B. Mock, “Automated C-11 Methyl Iodide/Triflate Production: Current State of the Art,” *Curr. Org. Chem.*, vol. 17, no. 19, pp. 2119–2126, 2013.

[85] J. S. Lewis, A. D. Windhorst, and B. M. Zeglis, *Radiopharmaceutical chemistry*. Springer Nature Switzerland AG, 2019.

[86] P. Maltby, “Radiopharmacy quality control,” *Eur. Assoc. Nucl. Med.*, vol. CTE, 2009.

[87] K. Kilian and A. Pękal, “Synthesis of Endogenous Compounds Labeled with 11 C for Positron Emission Tomography,” in *Proceedings of the II Symposium on Positron Emission Tomography*, 2015, vol. 127, no. May.